catalysts

MDPI

Review

A Review on Green Hydrogen Valorization by Heterogeneous Catalytic Hydrogenation of Captured CO_2 into Value-Added Products

Rafael Estevez, Laura Aguado-Deblas, Felipa M. Bautista, Francisco J. López-Tenllado, Antonio A. Romero and Diego Luna *

Departamento de Química Orgánica, Universidad de Córdoba, Campus de Rabanales, Ed. Marie Curie, 14014 Córdoba, Spain
* Correspondence: diego.luna@uco.es; Tel.: +34-957212065

Abstract: The catalytic hydrogenation of captured CO_2 by different industrial processes allows obtaining liquid biofuels and some chemical products that not only present the interest of being obtained from a very low-cost raw material (CO_2) that indeed constitutes an environmental pollution problem but also constitute an energy vector, which can facilitate the storage and transport of very diverse renewable energies. Thus, the combined use of green H_2 and captured CO_2 to obtain chemical products and biofuels has become attractive for different processes such as power-to-liquids (P2L) and power-to-gas (P2G), which use any renewable power to convert carbon dioxide and water into value-added, synthetic renewable E-fuels and renewable platform molecules, also contributing in an important way to CO_2 mitigation. In this regard, there has been an extraordinary increase in the study of supported metal catalysts capable of converting CO_2 into synthetic natural gas, according to the Sabatier reaction, or in dimethyl ether, as in power-to-gas processes, as well as in liquid hydrocarbons by the Fischer-Tropsch process, and especially in producing methanol by P2L processes. As a result, the current review aims to provide an overall picture of the most recent research, focusing on the last five years, when research in this field has increased dramatically.

Keywords: CO_2 hydrogenation; power-to-gas; power-to-liquid; green methanol; methanation reaction; Fischer-Tropsch process; E-fuels; synthetic fuels

Citation: Estevez, R.; Aguado-Deblas, L.; Bautista, F.M.; López-Tenllado, F.J.; Romero, A.A.; Luna, D. A Review on Green Hydrogen Valorization by Heterogeneous Catalytic Hydrogenation of Captured CO_2 into Value-Added Products. *Catalysts* **2022**, *12*, 1555. https://doi.org/10.3390/catal12121555

Academic Editors: Mónica Viciano, Sergio Sopeña de Frutos and Carolina Blanco

Received: 26 October 2022
Accepted: 25 November 2022
Published: 1 December 2022

1. Introduction

Nowadays, there is a serious concern about the danger caused by the high GHG (greenhouse gas emissions) produced by our way of life, and in particular by the anthropogenic emissions of carbon dioxide (CO_2). Thus, if current trends continue, the planets temperature could rise dangerously, accelerating the climate change and resulting in an increase in the level of the oceans and their acidification. This scenario is already having a very negative impact on the ecosystems of the planet, as well as having a deep negative influence on the economic and social development of many countries all over the world [1]. To reduce the impact of this atmospheric pollutant, an important effort is being made, embodied in different international treaties, to carry out the substitution of fossil fuels with different renewable energy sources [2]. Considering that CO_2 alone accounts for around 77% of total greenhouse gases and that natural removal of CO_2 through forests and oceans is not enough to remove the excessive amount of CO_2 present in the atmosphere, other CO_2 mitigation strategies are required. Thus, in addition to renewable energies such as hydropower, wind, and solar energy, which are being considered as alternatives for fossil fuel mitigation, the use of various technologies for the Carbon Capture and Storage (CCS) of CO_2 [3], as well as its subsequent transformation into useful chemicals [4], is being considered, because CO_2 is a nontoxic chemical that is widely used as a C1 building block in the synthesis of highly important chemicals (Figure 1) [5,6].

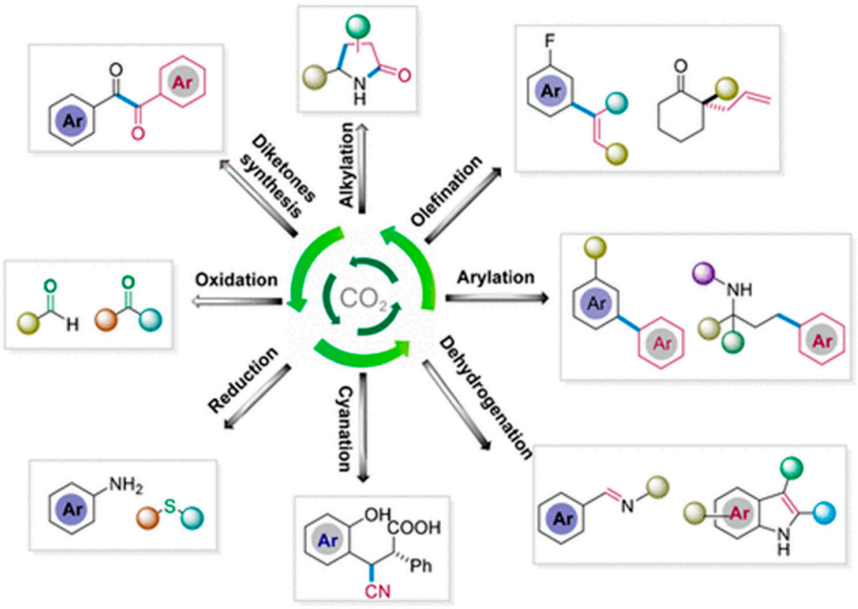

Figure 1. CO_2-Promoted Reactions for the Synthesis of Fine Chemicals and Pharmaceuticals. Reproduced with permission from the author [6]. Copyright © 2021, American Chemical Society.

In addition, CO_2 is being used not only in chemical transformation but also in mineralization and biological processes, such as those of an autotrophic biota and some microorganisms such as algae, cyanobacteria, and chemoautotrophic bacteria that have CO_2 fixing mechanisms [7], following routes such as thermochemical, electrochemical, and photocatalytic conversion, with different levels of maturity and performance [8,9].

Hence, catalytic conversion of CO_2 into chemicals and fuels is a "two birds, one stone" approach to fighting climate change, contributing also to solving the energy and green supply deficits in the modern world, as shown in Figure 2 [10].

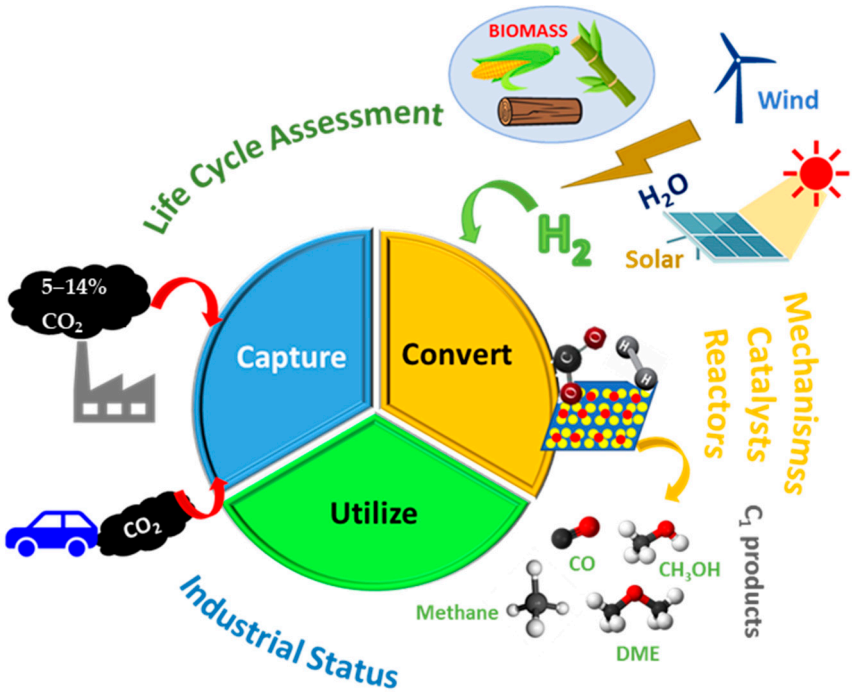

Figure 2. Selective circular process demonstrating the "two birds, one stone" advantage of chemical transformation of captured CO_2 into fuels or chemical commodities over other technologies for simple capture and storage.

In this way, as a complementary strategy to the capture and storage of CO_2, it is also necessary to consider the capture, storage, and utilization (CCS/U) of CO_2 as a feedstock for the synthesis of different fine chemical products, such as urea, methanol, formic acid, dimethyl ether, dimethyl or diethyl carbonates, and many others [5,11–13].

Therefore, it is completely pertinent to evaluate the technical possibilities to hydrogenate the CO_2 after its capture as one of the most promising ways to transform it into fine chemicals or biofuels. According to data in Table 1, considering blue hydrogen's low emissions level, blue and green hydrogen could be used together to begin the transition to net zero emissions, which is planned for 2050. As can be seen, the blue hydrogen could constitute an intermediate for use in the CO_2 hydrogenation processes, also considering that, at this time, the European Union Commission has labeled as sustainable some energy raw materials, such as nuclear and natural gas [14].

Table 1. A comparative summary of hydrogen production processes and hydrogen color codes.

Hydrogen	Brown	Grey	Blue	Green
Feedstock	Coal	Natural Gas	Natural Gas	Renewable electricity
Carbon Capture	Gasification No CCS	Steam methane reforming No CCS	Advanced gas reforming CCS	Electrolysis
GHG: Emissions ($tonCO_2/tonH_2$)	Highest 19	High emissions 11	Low emissions 0.2	Potential for zero GHG emissions
Estimated Cost (per kg H_2)	$1.2–$2.1	$1–$2.1	$1.5–$2.9	$3–$7.5

CCS: carbon capture and storage; GHG: greenhouse gas; tCO_2/tH_2—ton of carbon dioxide per ton of hydrogen.

In addition, it must be taken into account that the production costs of both types of hydrogen will continue to decline over the next few decades, favoring the CCS/U process, as can be seen in Figure 3 [15].

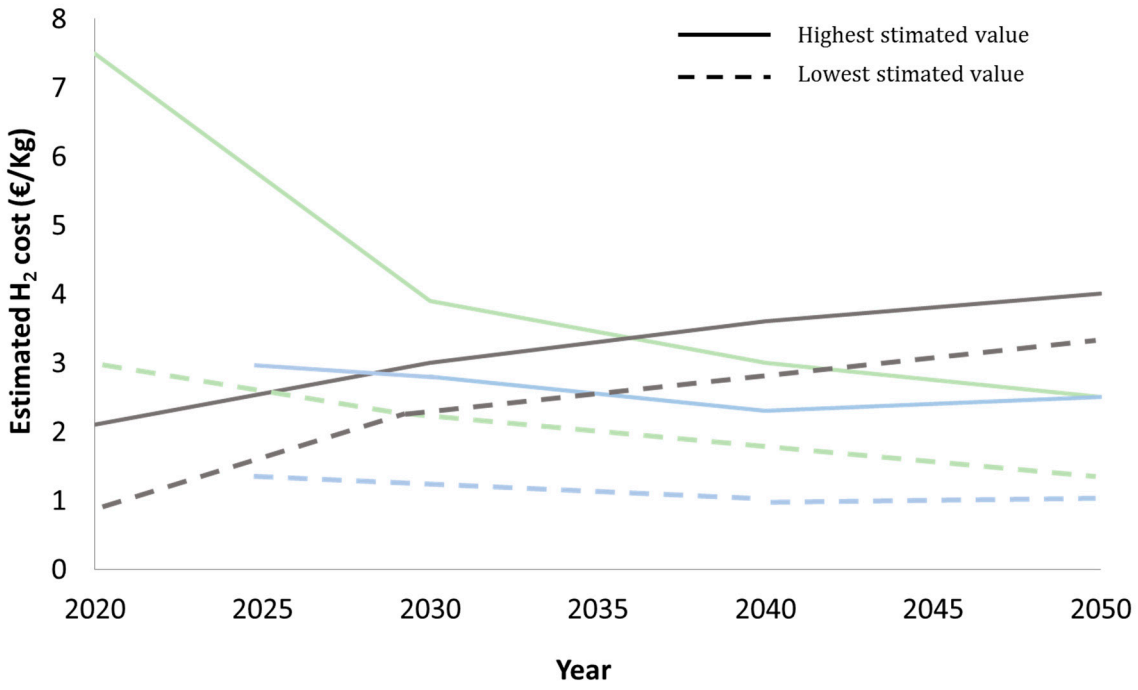

Figure 3. A comparative summary of estimated hydrogen production costs in the next two decades. (Green lines: green hydrogen; blue lines: blue hydrogen; grey lines: grey hydrogen).

Furthermore, it is necessary to consider the necessary complementarity between both types of hydrogen over a long period of time to guarantee a stable supply of this raw

material over time for any CO_2 hydrogenation process carried out on an industrial scale. Besides, green hydrogen is greatly influenced by climatic factors, mainly wind intensity and solar radiation, so a supply of hydrogen obtained by a technology controlled by a safe raw material, such as natural gas, that generates very low CO_2 emissions is foreseeable [16].

On the other hand, the massive production of electricity, obtained by renewable technologies, can be used as another strategy that could complement the decarbonization process. However, this requires an effective and economically viable method that allows its storage, given the extreme dependence of these technologies on the climate. In this sense, the transformation of CO_2 and water by either power-to-liquids (P2L) and/or power-to-gas (P2G) processes, employing this Renew Energy, has recently gained much attention as an efficient way for CO_2 mitigation and obtaining value-added synthetic crude and/or synthetic natural gas [17]. Hence, combining the use of CO_2 and renewable H_2, obtained by water electrolysis, to produce chemicals and biofuels seems to be the most promising way for a larger H_2 utilization as an energy vector, providing, for instance, methane or methanol, as well as other light oxygenated hydrocarbons for fuel cell (FC) applications in electric engines [18]. In this way, a closed loop between Renew Energy sources and CO_2 reuse can be obtained, coupled with the benefits of clean energy sources and fossil fuels. The main drawback of these processes is that they are not economically competitive yet in comparison with processes carried out with conventional hydrogen (blue or gray), which is obtained from fossil fuels, with the consequent CO_2 emissions [19,20].

Up to date, there are still several applications more economically described for CO_2 capture and utilization than catalytic hydrogenation processes, such as methane recovery from hydrates [21], the production of biofuel and biomaterials by bacteria for the production of value-added products such as biodiesel, bioplastics, extracellular polymeric substances, biosurfactants, and other related biomaterials [22], or CO_2 utilization in agricultural greenhouses. However, the CCS methods are recognized as the most useful procedures to reduce CO_2 emissions while using fossil fuels in power generation [23]. Furthermore, the economic cost of producing green hydrogen is expected to fall rapidly, allowing the activation of various catalytic hydrogenation procedures on an industrial scale capable of significantly reducing GHG emissions. Thus, several studies are being conducted to develop innovative hydrogen generation systems by using low-carbon energy like wind and solar, which could enable the wide use, effective storage, and full market penetration of green hydrogen [24].

In this regard, either natural gas steam-methane reforming (SMR) or blue hydrogen could be considered a viable partner for accelerating hydrogen penetration in CO_2 capture, storage, and utilization (CCSU) [25].

Thus, catalytic hydrogenation processes close the cycle that allows the recovery of green hydrogen, obtained in very different amounts depending on seasonal fluctuations in renewable energy production. In addition, through these catalytic hydrogenation processes, a portfolio of useful chemicals and renewable fuels can be obtained, such as methane, methanol, ethanol [26], cyclic carbonates [27,28], or higher hydrocarbons such as aromatics [29,30], etc. Figure 4 [31].

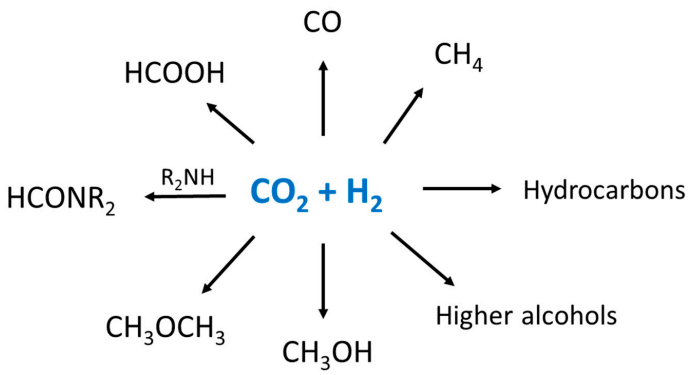

Figure 4. Catalytic CO_2 hydrogenation pathways to obtain fine chemicals and renewable fuels.

Among these processes, methanol obtained by hydrogenation of CO_2 using electrocatalytically generated green hydrogen presents a great interest for the development of a complete strategy for the application of renewable energies since it can be used to convert and store the excess of electrical energy into chemical energy, contributing to smooth the natural fluctuation in the Renew Energy supply [32].

In fact, as can be seen in Figure 5, about 48% of the total methanol demand is for chemical intermediate uses, whereas the remaining 52% is for energy uses. The predominant use of methanol, at 29%, is in the production of formaldehyde, followed by its use in alternative fuels, such as gasoline blending, DME, and biodiesel, which make up 21% of the total demand.

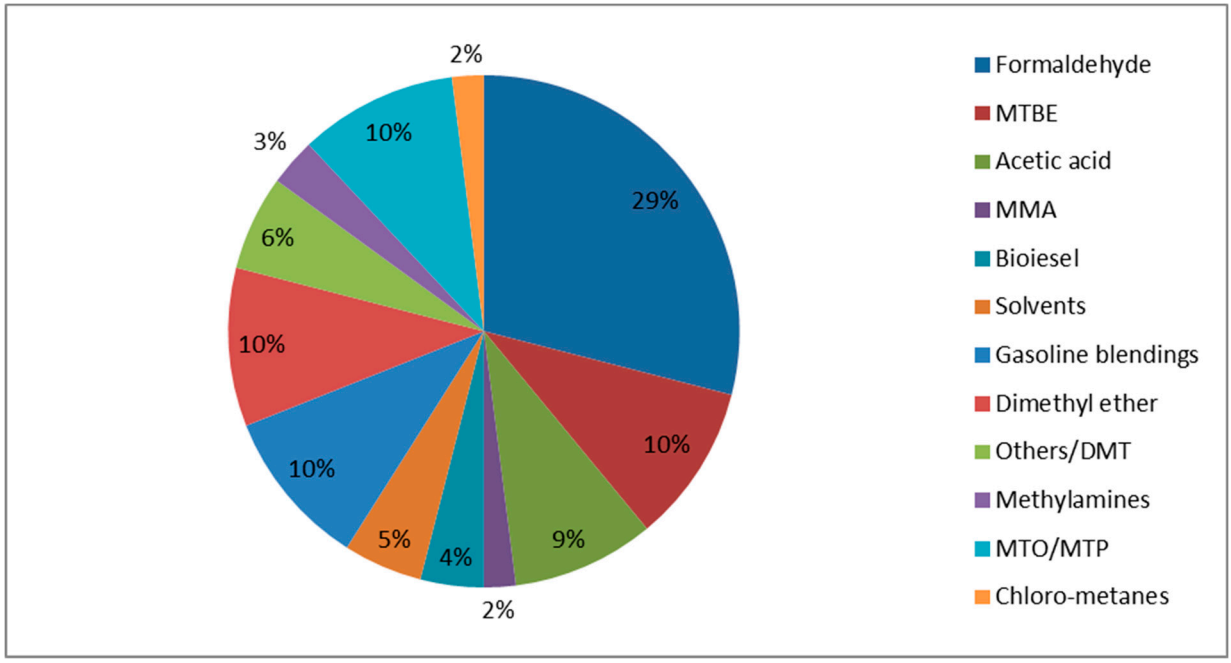

Figure 5. Currently, methanol is the main fuel used.

Therefore, methanol could become a central compound in the worldwide energy landscape.

Summarizing, in the near future, the utilization of CO_2 and H_2 obtained by water electrolysis to produce P2L and P2G is one of the most promising strategies for CO_2 mitigation. However, due to economic limitations, CCS methods are recognized as the most useful procedures to reduce CO_2 emissions. In this sense, catalytic hydrogenation of CO_2 to obtain different products with added-value presents great interest. This review provides an overview of the various CO_2 heterogeneous catalytic hydrogenation reactions that can be used for the storage and transport, with a focus on the so-called liquid and gaseous organic hydrogen carriers, that is, the processes known as power-to-gas (P2G) and power-to-liquids (P2L).

2. Catalytic Hydrogenation of CO_2 to Renewable Methane

The catalytic hydrogenation of CO_2 to methane and water is a thermochemical process described over a hundred years ago and is known as the Sabatier reaction, or CO_2 methanation (Equation (1)) [33]. This is carried out catalytically at high temperatures (300–400 °C) and pressures (30 bar) in the presence of a suitable catalyst [34], although low-catalytic low temperature methanation has been studied in recent years [35]. By using green hydrogen, synthetic natural gas (SNG) is obtained, which can be used directly or stored for later use, allowing the transfer of electrical energy to a useful renewable fuel.

$$CO_2 + 4H_2 \rightarrow CH_4 + 2H_2O,\ \Delta H^0{}_{298K} = -165\ kJ/mol \quad (1)$$

The reaction is thermodynamically favored ($\Delta G_{298K} = -113.2$ kJ/mol), but it involves an eight-electron process to reduce the fully oxidized carbon to methane, with important kinetic limitations, so that a catalyst is required in order to achieve high selectivity and conversion. Thus, catalysts based on noble- and transition-metal materials (Ru, Rh, Pd, and Ni) supported on metal oxides (Al_2O_3, CeO_2, ZrO_2, TiO_2, SiO_2, La_2O_3) are usually applied for the CO_2 methanation process [36–39]. Therefore, even though Ru is the most active metal, its high cost limits the large-scale application of Ru-based catalysts. In contrast, Ni-based systems are the most widely investigated for industrial purposes, as they combine a reasonable high selectivity for methane with lower costs [40,41].

Nevertheless, sintering of Ni nanoparticles and carbon deposition on the support surfaces of catalysts usually lead to their deactivation [42]. The carbon deposition phenomenon occurs either through CO disproportionation reactions (Equation (2)), or via CH_4 decomposition (Equation (3)), ref. [43]:

$$2CO \rightarrow C + CO_2, \Delta H^0_{298K} = -173 \text{ kJ mol}^{-1} \quad (2)$$

$$CH_4 \rightarrow C + 2\,H_2, \Delta H^0_{298K} = 75 \text{ kJ mol}^{-1} \quad (3)$$

Thus, an incessant number of investigations currently aim at achieving the CO_2 conversion to methane via hydrogenation, using deposited Ni on very different supports and applying it with very different methodologies, since the tandem Ni/support exhibit a higher performance/cost ratio. To optimize the efficiency of these supported Ni catalysts, various inorganic materials, including Al_2O_3, SiO_2, TiO_2, CeO_2, and ZrO_2, that favor the dispersion of Ni particles and enhance their activity and stability, have been studied. In this respect, the sintering of Ni particles supported on Al_2O_3 can be inhibited to some extent, so that Al_2O_3 seems to be superior to the other supports [42,44–48].

On the other hand, in order to optimize these Ni/Al_2O_3 systems, extensive studies about the influence of operating conditions on carbon deposition, with special emphasis on the effects of the operating temperature, reaction time, and H_2/CO ratio, are being carried out, given that all are significant factors in the morphology and amount of carbon deposits, because until now it has not been possible to satisfactorily eliminate this carbon deposition in the Ni/Al_2O_3 catalysts [44,45,49–52]. Furthermore, there is a substantial amount of research being conducted on other factors that may influence both the catalytic performance and the intensity of carbon deposition during successive reactions with reused, supported Ni catalysts. Figure 6 collects a number of parameters influencing the catalyst design to improve the low-temperature catalytic performance of supported Ni catalysts toward the CO_2 methanation process [53].

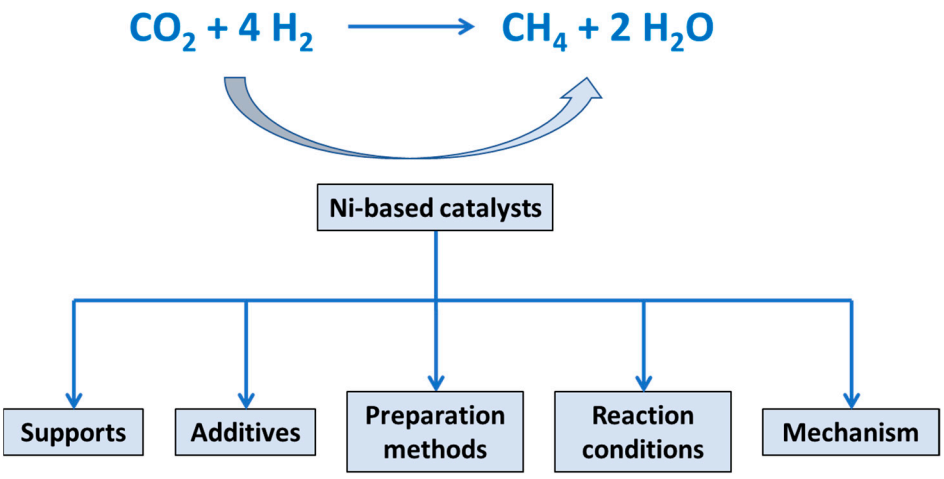

Figure 6. Main parameters influencing the catalyst design to improve the catalytic performance of supported Ni catalysts in the CO_2 methanation process. Adapted from ref. [54].

On the other hand, mixtures of inorganic solids as supports, in many cases together with Al_2O_3, as well as other metals as co-catalysts with Ni, such as Co, La, Ru, and many others, have also been studied [46,55–59]. In this regard, the bimetallic systems Ni and Ru have shown promising results [60,61], outperforming the reaction over monometallic Ru or Ni catalysts. Thus, the formation of Ni-Ru alloys or the synergy between two adjacent metallic phases open the door to new high-performance and low-cost methanation catalysts [62,63], as illustrated in Figure 7.

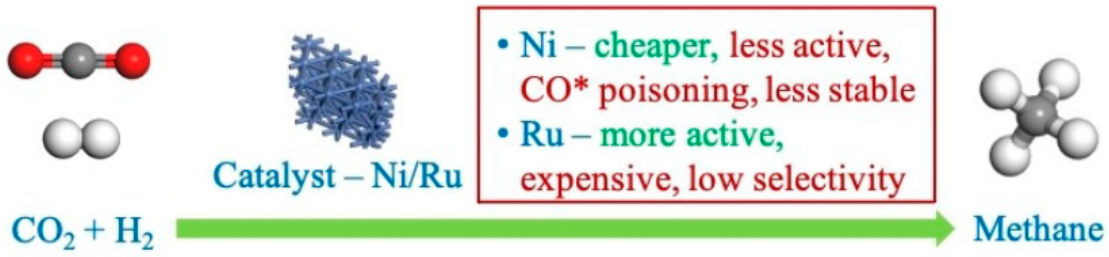

Figure 7. Differential aspects between supported Ni and Ru metals in developing a more active, stable, and selective catalyst for the CO_2 methanation reaction. Adapted from ref. [63]. Copyright 2021 John Wiley and Sons.

The determining steps in the reaction, using Ni and Ru catalysts, are the HCO* dissociation to CH* and O* and the CH_3* hydrogenation to CH_4, respectively. Hence, as the selectivity of the reaction on Ni is higher than that on Ru, the activity attained on Ru catalysts is higher. Therefore, it can be concluded that the combination of both metals allows for a characteristic synergistic activity, in which Ru drastically improves the reducibility of Ni catalysts, also improving the Ni metallic dispersion and providing additional methanation sites [62]. In addition, it is an important finding that the addition of certain promoters, such as CeO_2, La_2O_3, Sm_2O_3, Y_2O_3, and ZrO_2 is clearly beneficial, not only because the corresponding metal-oxide promoted catalysts exhibited higher catalytic performance than Ni/Al_2O_3, but also because the stability along the successive uses is clearly increased [64]. CO_2 methanation has recently been achieved on Mg-promoted Fe catalysts, where Mg/Fe_2O_3 catalysts exhibiting the highest yield of 32% (400 °C) in CH_4 production, under practical operation conditions (8 bar, 10,000 h^{-1}) [65]. Thus, the competitive advantage presented by the low price of these materials in comparison with those usually used, Ni and Ru, should be highlighted.

Considering the huge amount of work regarding CO_2 methanation, a review of different catalysts usually investigated in carbon dioxide methanation by using different noble and non-noble metals supported on different materials is collected in Table 2.

Table 2. A comparative summary of different metal-supported catalysts studied in the carbon dioxide methanation process.

Metal	Promoter	Catalyst Support	Conversion (%)	T (°C)	P (atm) *	Ref.
Ni	CeO_2	γ-Al_2O_3	>60	300	0–10	[34]
Ru	—	TiO_2	>60	210–300	1.0	[66]
Ru	—	Al_2O_3, CeO_2, MnO_x, ZnO	25–80	400	1.5	[67]
Ni	—	CeO_2, Al_2O_3, Y_2O_3	60–80	250−500	1.0	[42]
Ni	TiO_2	Al_2O_3	40	550	3.0	[43]
Ni	Mn	TiO_2	95	350	—	[68]
Ni, Ni-Co	—	Al_2O_3	90	350–400	1.0	[44]
Ni	—	CeO_2-ZrO_2	55–99.8	200–350	—	[49]
Ni	—	ZrO_2	72	300	—	[69]

Table 2. *Cont.*

Metal	Promoter	Catalyst Support	Conversion (%)	T (°C)	P (atm) *	Ref.
Ni	—	Al_2O_3	5–75	350–450	1.0	[45]
Ni	Ce	SiC	80–95	600	10–15	[47]
Ni	La	Mg-Al	61	250	1.0	[50]
Ni	La	γ-Al_2O_3	4–14	377–400	1.0	[46]
Ni-Ru	—	CaO-Al_2O_3	84	380–550	1.0	[70]
Ni	CeO_2	Al_2O_3-ZrO_2-TiO_2	83	300–400	5.0	[51]
Ni-ZrO_2	—	Carb. Nanotubes	10–50	200–500	1.0	[52]
Ni	—	γ-Al_2O_3	66–92	250–350	—	[71]
Ni/Al_2O_3	—	3D-copper	3–45	300–500	1.0	[72]
Ni	—	Al_2O_3, CeO_2, CeO_2-ZrO_2	60–80	200–450	1.0	[73]
Ni/GDC	—	Ceramic monolith, Open-cell foam	70–52	300–600	1.0	[74]
Ni	—	Attapulgite	60–80	200–600	1.0	[75]
Ni	—	Al_2O_3, CeO_2, ZrO_2	70–90	200–600	1.9	[76]
Ni	Sm_2O_3, Pr_2O_3, MgO	CeO_2	55	200−500	1.0	[77]
Ni	—	CeO_2 nanocatalyst	84	220	1.0	[78]
Ni	—	CeO_2	81	250	1.0	[79]
Ni	La	Hydrotalcite-Al_2O_3	60–80	225–425	1.0	[55]
Ni	—	Sepiolite, Todorokite	70–100	250–450	1.0	[80]
Ni	—	ZSM-5@MCM-41	80	400	1.0	[81]
Ni	La	MgO, Al_2O_3	60–80	200–400	1.0	[82]
Ni-Ru	—	Al_2O_3	70–85	200–500	1.0	[60]
Ni	—	Al_2O_3	30	400	15.8	[48]
Ni	Mg, Ca, Sr, Ba	Al_2O_3	40–60	200–600	1.0	[56]
Ni	—	Al_2O_3, CeO_2	60–80	200–500	1.0	[83]
Ni	—	Al_2O_3-ZrO_2	60–77	160–460	1.0	[57]
Ni-Ru	—	Al_2O_3	40–85	250–550	1.0	[61]
Ni-Ru	—	MgO-Al_2O_3	40–65	650–550	1.0	[84]
Ni	Pt, Ru, Rh	CeO_2, $CeZrO_4$, CeO_2/SiO_2	65–70	200–400	1.0	[85]
Ni-Ru		CeO_2-ZrO_2	50–80	200–450	1.0	[86]
Ni-Ru		$MgAl_2O_4$	55–70	200–400	1.0	[87]
Ni	CeO_2, La_2O_3, Sm_2O_3, Y_2O_3, ZrO_2	Al_2O_3	75–95	200–300	5.0	[64]

* Atm = 1, indicates atmospheric pressure, in flow process.

As can be seen, very good CO_2 conversion values have been obtained, as the 99.8% value reported by Ashok et al. over a Ni supported on CeO_2-ZrO_2 [49]. In addition to the importance of CO_2 methanation by itself, the possibility of integrating the water electrolysis and CO_2 methanation is a highly effective way to store the excess of renewable electricity produced by whichever renewable sources, such as wind and photovoltaic power generation, are intermittent due to weather conditions [88]. Therefore, storage of the electric excess is closely related to the power-to-gas (P2G) systems, so they are promising technologies to achieve this purpose. Thus, the transformation of green energy into synthetic natural gas (SNG) is carried out, which, as it comes from CO_2 obtained by capture and storage (CCS), exhibits a renewable character. Besides, the generated SNG can be stored or directly injected into the existing natural gas network.

Figure 8 shows the integrated co-electrolysis and syngas methanation for the direct production of synthetic natural gas from CO_2 and H_2O using a hydrotalcite-derived 20%Ni-2%Fe/(Mg, Al)O_x catalyst and a commercial methanation catalyst (Ni/Al_2O_3) [89].

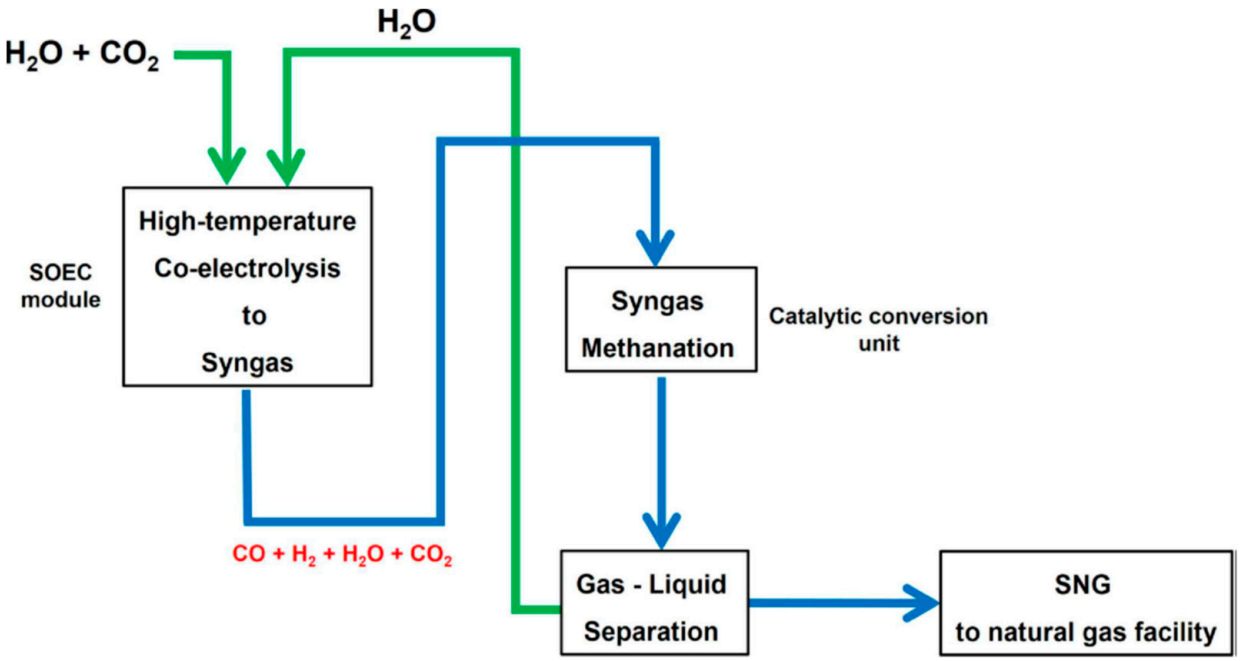

Figure 8. Integrated P2G process for synthetic natural gas (SNG) production from CO_2 and H_2O. Adapted from ref. [89]. Copyright 2021 John Wiley and Sons.

Likewise, a general plant scheme to transform CO_2 and water into synthetic natural gas is shown in Figure 9 [90]. Thus, in a circular power to gas process, renewable hydrogen, or green hydrogen, produced by water electrolysis powered by renewable electricity, such as solar or wind, will be critical to achieving net-zero emissions, and major advances in electrolyzer technologies are being developed in this regard [91–99]. However, the efficiency of the plant processes, regardless of the technological methodology or the experimental conditions used, strongly depends on the efficiency of metal-supported catalysts, Table 2.

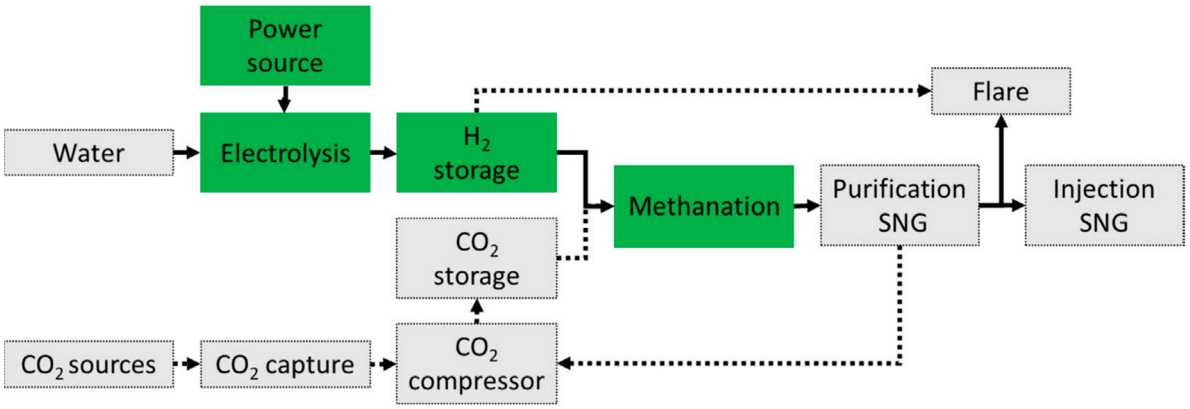

Figure 9. Power-to-Gas (PtG) plant scheme as implemented for the production of synthetic natural gas from CO_2 and green H_2. Reproduced from ref. [90], open access, Copyright 2020 Elsevier.

3. Catalytic Hydrogenation of CO_2 in Power-to-Liquid (P2L) Processes

Various liquid organic hydrogen carriers (LOHCs) compounds, such as hydrocarbons or high molecular weight alcohols, can be obtained through catalytic hydrogenation of CO_2, but the most prominent power-to-liquid (P2L) processes at this time are methanol synthesis, DME production [100], and Fischer-Tropsch fuels [101].

3.1. Catalytic Hydrogenation of CO_2 to Renewable Methanol

Methanol is supposed to have potential not only as a hydrogen-alternative energy vector (i.e., direct use as a fuel), but also as a hydrogen storage material. In addition, given that methanol is already synthesized on a large scale, there is the possibility of using existing infrastructure and production plants [102]. Accordingly, methanol is the simplest C1 liquid product that can be obtained from CO_2 (Figure 10). Therefore, methanol can be considered a key component of the anthropogenic carbon cycle in the framework of a "Methanol Economy" [103–105]. Indeed, the versatility of methanol, currently used to obtain multiple chemical products such as formaldehyde, acetic acid, methyl tertiary-butyl ether (MTBE), dimethyl ether (DME), or even olefins, as well as the possibility of its use as renewable fuel, while also taking advantage of the existing infrastructures for the transport and distribution of fuels, is what justifies the so-called "Methanol Economy" [106]. Thus, even though most of the methanol is currently produced from natural-gas-derived syngas, its alternative production using CO_2, water, and renewable electricity could present an opportunity to advance toward carbon neutrality [107].

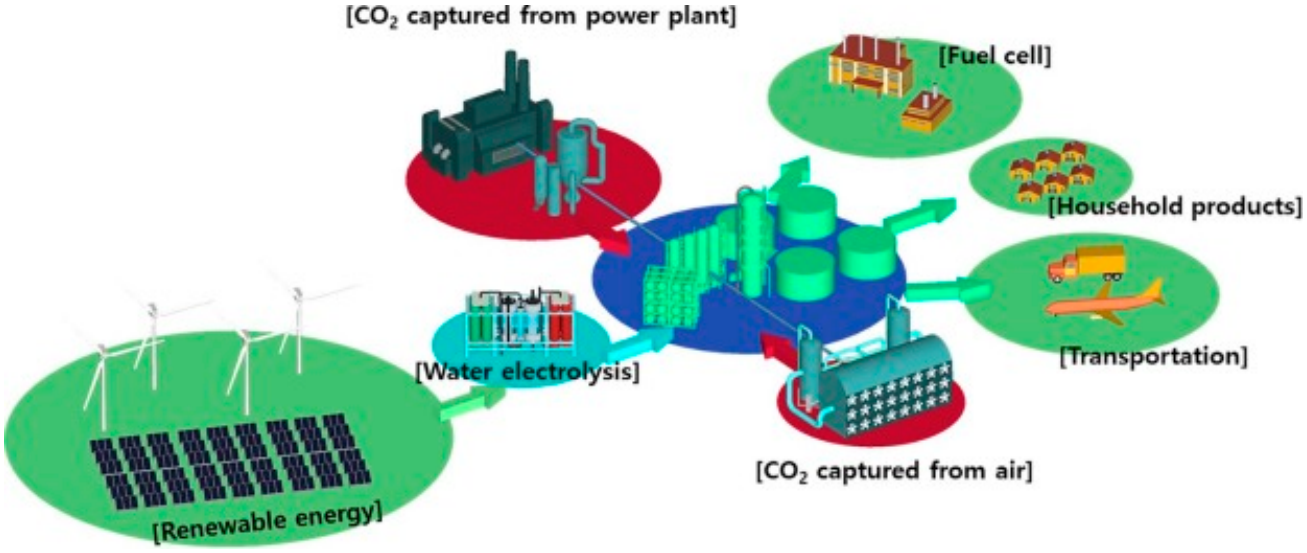

Figure 10. Overview of the Power-to-Liquid (P2L) scheme for renewable green methanol synthesis using CO_2 hydrogenation technology with green H_2 [104].

Regarding the different possibilities to obtain methanol from captured CO_2, such as electrochemical, photochemical, photoelectrochemical, and catalytic conversion, it is the heterogeneous catalysis that attracts the most attention.

The heterogeneously catalyzed reaction of hydrogen with carbon monoxide and carbon dioxide (syngas) to obtain methanol was described nearly 100 years ago, and the standard catalyst $Cu/ZnO/Al_2O_3$, currently applied in the methanol industrial synthesis reaction, has been used for the last 50 years [108,109]. This industrial reaction is currently taking place over $Cu\text{-}ZnO/Al_2O_3$ catalysts at pressures of 5 and 100 atm and temperatures in the 220–300 °C interval. Despite the fact that the reaction is exothermic, the conversion of CO_2 to methanol is kinetically limited, only obtaining a methanol conversion of around 15–25%. Thus, methanol is produced from synthesis gas (syngas) on an industrial scale, which is obtained from the steam reforming of fossil methane with a certain CO/H_2 ratio called metgas, which also contains about 3% by volume of CO_2. When this metgas is treated with H_2 at high pressures and moderate temperatures in the presence of conventional catalysts, $Cu/ZnO/Al_2O_3$, methanol is obtained (Equation (4)) [108]:

$$CO_2 + 3H_2 \leftrightharpoons CH_3OH + H_2O \; \Delta H = -49.16 \; kJmol^{-1} \quad (4)$$

However, by starting with pure CO_2 and H_2, rather than a mixture of CO, CO_2, and H_2 as in the syngas procedure, the chemical process is simplified, so the reaction and purification processes in conventional methanol-producing industrial plants could also be simplified. That is because, despite the direct synthesis of methanol from CO_2 is less exothermic (Equation (5)) and it is also accompanied by the reverse water–gas-shift (RWGS) as a secondary reaction (Equation (6)), the high exothermic character of the methanol formation from syngas (Equation (4)) necessitates the use of a very complex reactor capable of providing efficient cooling for the heat generated. Conversely, the thermal control inside the reactor during the methanol synthesis from CO_2 is easier due to the lower heat profile of this process.

$$CO_2 + 3H_2 \leftrightharpoons CH_3OH + H_2O\ \Delta H = -49.16\ kJmol^{-1} \quad (5)$$

$$CO_2 + H_2 \leftrightharpoons CO + H_2O\ \Delta H = 41.22\ kJmol^{-1} \quad (6)$$

Another advantage of this process is that the only reaction impurities are essentially limited to water and dissolved CO_2 in the crude methanol. In this way, it is possible to diminish the cost and improve the efficiency of the process in comparison with the process of methanol production from syngas. Another important issue is the overall cost of the two processes, given that today, syngas is cheaper than green hydrogen and captured CO_2. For this reason, great efforts are being made to obtain green hydrogen on an industrial scale or other low-carbon hydrogen production methods, such as aqua hydrogen or blue hydrogen (obtained via new technologies from fossil fuels but with a lower carbon footprint).

Given that there is a general motivation regarding the use of captured CO_2 for the methanol synthesis as a liquid-to-power process, a great effort is being devoted to improving the current Cu-based catalysts employed to get more active, selective, and stable heterogeneous catalysts [110]. On the other hand, new noble metal-supported catalysts, able to increase the efficiency of this process for direct CO_2 hydrogenation to obtain bio methanol are being researched [111,112].

3.1.1. Hydrogenation CO_2 to Methanol using Cu-Based Catalysts

Once the convenience of advancing the catalytic processes of direct hydrogenation of CO_2 to obtain methanol was accepted, the first candidates were copper-based catalysts due to both their low cost and their good efficiency for methanol synthesis from synthesis gas, or Syngas [113,114]. However, some disadvantages, such as the formation of CO as a byproduct of the reverse water−gas shift (RWGS) reaction (Equation (6)), and the sintering of copper particles, which are responsible for catalyst deactivation after several reuses, determine the need to get better catalytic systems [115]. That is why numerous studies are currently being carried out in an attempt to improve the catalytic behavior of Cu, for which the role of various supports and/or additives that work as promoters is being investigated. The supports mainly consist of several metal oxides, such as Al_2O_3, SiO_2, ZnO, ZrO_2, CeO_2, TiO_2, or In_2O_3. The main role of these supports and promoters is to alter the electronic and geometric properties of active centers, thereby altering the metal-support interactions. Thus, various authors demonstrate that the yield to methanol is determined by active sites modulated by metal-support interaction as well as the influence of promoters [116]. This electronic interaction between supports and catalytically active metals is manifested through its influence on the energy levels of the frontier orbitals of the corresponding metal. The closer they are to the corresponding HOMO-LUMO of the CO_2 and H_2 molecules, the greater the catalytic efficiency of the reaction.

Thus, in a relatively short period of time, numerous studies have appeared on the performance of Cu catalysts by examining the effects of the composition of the support and the influence of the method of catalyst synthesis (Table 3), the influence of several additives used as promotors (Table 4), as well as other factors of interest in the final behavior of the catalyst, including the use of CuO instead of Cu metal as a catalytically active species (Table 5). In Tables 3–5, the comparative performance of different Cu-supported catalyst

systems in the carbon dioxide hydrogenation to methanol reaction is collected. In general, the catalytic performance of the catalysts was tested in a fixed-bed stainless-steel tubular reactor at different pressures and temperatures. Furthermore, the conversion and selectivity to methanol limits values obtained are collected. In this regard, an extensive review of supported Cu catalysts studied is presented, focusing on the last five years and highlighting the special importance that the CO_2 hydrogenation catalytic process has gained.

Table 3. Comparative performance of different Cu supported catalysts in the carbon dioxide hydrogenation to methanol reaction obtained by using different solid supports and/or different synthesis.

Catalyst Support	Conversion (%)	S_{CH3OH} (%)	T (°C)	P (Atm)	Ref.
ZnO/Al_2O_3	60–90	50–80	210–250	60	[109]
ZnO/ZrO_2	50–80	65–85	220	30	[117] [a]
ZnO/ZrO_2	20–60	30–90	200–300	1–40	[113] [b]
Al_2O_3	50–70	50–65	180−300	1–360	[114] [a]
ZnO	2–9	45–95	220–300	30	[118]
Al_2O_3/MgO	0–25	20–30	150–250	10	[119]
ZrO_2/CeO_2	3–10	40–82	220−260	30	[120] [c]
SiO_2	5	79	190−250	30	[121]
ZrO_2/ZnO	30–70	30–70	190–250	10–30	[122]
Na-ZSM-5/ZnOx	2–12	25–100	200–300	30	[123]
CuO/ZrO_2	5–15	15–70	230	10	[124]
Al_2O_3/MgO	20–35	5–35	200–400	20	[125]
Al_2O_3/ZnO	5–35	5–70	200–400	20	[126]
SiO_2/TiIV Surf.	4–18	49–85	230	25.0	[127]
SiO_2/ZnII Surf	1–5	48–86	230	50.0	[128]
ZnO/ZrO_2/Mg-Al (LDH)	1–7	50–100	200–300	30.0	[129]
ZnO/MnO/SBA-15 silica	4–8	100	180	40.0	[130]
ZnO	9–13	65–80	240	30.0	[131]
ZnO/SiO_2	90–100	65–100	250	40.0	[132]
ZrO_2	2–7	30–70	350	10.0	[133]
ZnO/Attapulgite	12–18	7–25	320	6.0	[134]
ZnGa/LDH nanosheet	17–20	30–50	270	50.0	[135]
Sr-Perovskite	1–16	36–63	200–280	20–50	[136]
$Ce_xZr_yO_z$	5–16	45–95	200–300	30	[137]
ZrO_x	13.1	78.8	260	45	[138] [c]
ZrO_2	1.0–5.0	68–75	220	30	[139]
ZnO	1.0–25.0	10–90	200–300	20	[140]
ZnO/Faujasite	2.0	27–35	240−260	15	[141] [a,c]
ZnO/CeO_2	1.0–3.5	20–70	250	30	[142] [c]
ZnO/ZrO_2/C-nanofibers	8–14	78–92	180	30	[143]
ZnO/Al_2O_3	10–28	33–85	240	40	[144]
ZnO/SiO_2	8–14	50–59	220	30	[145]
AlCeO	2–24	12–95	200–280	30	[146]
AlCeO	6–22	25–97	200–280	30	[147]
ZnO	1–14	1–60	150–300	1.0	[148]
CeO_2	1–7	20–90	240–300	20	[149]
$Al_2O_3/ZrO_2/ZnO$	<7.0	43–59	230	30	[150]
ZnO/ZrO_2	19.6	50	280	50	[151]
ZnO/ZrO_2	9–15	87–98	250	50	[152]
Al_2O_3	50	-	325	1.25	[153]

[a] This study mainly deals with the effects of the CO_2 hydrogenation reaction mechanism. [b] The catalysts' ability to be reused is determined. [c] Special attention is paid to the existence of strong metal-support interaction effects (SMSI).

Table 4. Influence of the use of different additives on the performance of the carbon dioxide hydrogenation to methanol reaction using different Cu-supported catalysts.

Promoter	Catalyst Support	Conversion (%)	S_{CH3OH} (%)	T (°C)	P (Atm)	Ref.
Pr_2O_3	ZnO	80–100	75–100	200–260	30	[115]
In_2O_3	ZrO_2	1–6	60–90	210–290	10–250	[153]
CeO_2	Al_2O_3	16–23	59–94	220–280	40	[147]
LaOx	Silica SBA-15	45–85	45–81	220–280	30	[154]
W	CeO_2	13	87	250	35	[155]
Pd	$Ce_{0.3}Zr_{0.7}O_2$	15–25	90–95	250	50	[156] [a]
Sm_2O_3	ZrO_2	8–14	50–80	230	10	[157]
Al + Ga	ZnO	16–18	99	250	30	[158]
Al	ZnO	1–17	99	250	30	[159] [b]
Zn	Graphene	18–20	50–80	250	15.0	[160]
Hydrotalcite	ZnO-Al_2O_3	6	64–73	250	15–30	[161]
ZnO-ZrO_2	Hydrotalcite	3–6	35–65	250	25.0	[162]
Zn, Ga	SiO2	0.5–5.0	10–80	220–280	8.0	[163]
Pd	SiO2	6.6–3.7	12–30	300	41	[164]
Pd	$Ce_xZr_{1-x}O_2$	13–20	10–25	250–300	30–60	[156]
Ni	CeO_2-nanotube	2–18	75–86	220–300	20–40	[165]
ZnO	Al_2O_3	10–20	50–100	160–250	10–25	[137] [a]
MgO	ZnO	4–16	25–100	200–300	30	[166]
MgO, CaO, SrO, BaO, ZnO	Al_2O_3	2–9	10–100	200–400	20	[167]

[a] This study focuses on the effects of the CO_2 hydrogenation reaction mechanism. [b] The catalysts' ability to be reused is determined.

Table 5. Comparative performance in the carbon dioxide hydrogenation to methanol reaction, of different CuO supported catalysts, using different solid as supports, different synthesis methods or different additives.

Promoter	Catalyst Support	Conversion (%)	S_{CH3OH} (%)	T (°C)	P (Atm)	Ref.
	ZrO_2	5–15	15–70	230	10	[124]
ZnO/ZrO_2	SBA-15 silica	10–25	20–35	250	30	[168]
ZnO/ZrO_2	Mg-Al (LDH)	1–7	50–100	200–300	30.0	[129]
In_2O_3	CuO	5–12	50–90	220–280	5–30	[169]
	CuO/ZrO_2	2–12	20–70	230	10.0	[170]
	$CuO/CeO_2/TiO_2$	1.5–6.5	28–52	190–235	30	[171]
$MoO_3/WO_3/Cr_2O_3$	$CuO/ZnO/ZrO_2$	18–20	40–48	240	40	[172]
	$CuO/ZnO/Al_2O_3$	10–16	>99	250	50	[173]
Ag	CuO/ZrO_2	4–8	25–45	270	10	[174]
	$CuO/Ce_{0.4}Zr_{0.6}O_2$	7–13	72–96	220–280	30	[175]
	CuO/ZnO	38	70	270	50	[176]
	$CuO/ZnO/CeO_2$	14–20	95–98	240	1.0	[177] [a]
	$Cu/Zn/Ce/TiO_x$	4–7	25–45	275	30	[178]
	$CuO/ZnO/TiO_2/Zr$	3–25	15–85	200–280	30	[179]
$CuO/ZnO/CeO_2$	TiO_2 nanotubes	10–20	25–80	220–300	30	[180]
	$CuO/ZnO/ZrO_2$	9–17	40–54	300–600	30	[181]
Graphene oxide	$CuO/ZnO/ZrO_2$	2–25	10–76	200–280	20	[182]
Carbon	CuO/ZnO	8–24	18–60	230–290	30	[183]
WO_3	CuO-ZnO-ZrO_2	5–20	42–64	240	30	[184]
ZrO_2/Al_2O_3	CuO/ZnO	20–25	40–95	200−260	27.6	[185]
In_2O_3, Pd	$CuO/ZnO/Al_2O_3$	7–16	99–100	250	50	[186]
La_2O_3	$CuO/ZnO/Al_2O_3$	1–18	5–100	160–260	1.0	[187]
SiO_2	$CuO/ZnO/ZrO_2$	2–5	10–70	200–280	20	[188]
	$CuO/ZnO/ZrO_2$	4–15	45–85	240	30	[189]
	$CuO/CeO_2/ZrO_2$	5–20	2–8	200–260	30	[190] [b]
Ag	CuO/ZrO_2	1–7	30–70	230	10	[191]
Zeolite	$CuO/ZnO/ZrO_2$	5–20	5–12	260	30	[192]
CuO-ZnO	Al_2O_3, SiO_2	2–14	46–59	250, 270	30, 50	[193]
	$Ce_{1-x}Zr_xO_2$	2–15	10–95	200–300	30	[194]
$La_xSr_{1-x}CuO$	Perovskite	1–16	4–55	250–300	30	[195]
ZrO_2, MnO_2	CuO-ZnO/SBA-15	8–9	10–25	250	30	[196]
CuO/ZnO	Oyster Shells	1–2	50–70	250	30	[197]
Pd	$CuO/ZnO/Al_2O_3$	1–10	10–90	180–240	50	[198]
La, Ti or Y	$CuZnIn/MZrO_x$	2–6	40–80	225	20	[199]
La, Ce, or Sm	$CuZnO/Zn\text{-}AlO_x$	25	54	250	40	[200]

[a] The reusability of the catalysts is determined. [b] This study mainly deals with the effects of the CO_2 hydrogenation reaction mechanism.

The influence of copper form, according to its size, i.e., bulk, nanoparticle, and cluster, has been deeply studied. In general, copper nanoparticles would enable higher activity due to having an overall higher Cu surface exposure, although more energy is generally required to increase the reaction kinetics. Regarding copper clusters, small clusters of small metallic particles tend to perform better at higher dispersion. For instance, the Cu_4 clusters exhibited a lower activation barrier to CO_2 hydrogenation than bulk Cu(111) [201].

Promoters are added to the catalyst to achieve three possible outcomes: increasing the number of available active sites, maintaining the Cu surface stability, particularly by increasing the Cu dispersion, and increasing electron transfer to the active sites, all of which can improve the catalyst activity. For their part, support materials are used to immobilize Cu particles in order to increase active site dispersion and maintain high thermal stability. Active metal–support interaction can promote a high synergy, increasing the reaction activity, particularly if the support can adsorb and transfer the reactants to the active sites without taking part in the reaction itself [116]. As can be seen in Tables 4 and 5, a great number of additives, supports, and promoters have been tested. The results obtained with this huge number of Cu catalysts studied usually fall within those usually described for the Cu-ZnO/Al_2O_3 catalysts used in the catalyzed reaction of hydrogen with carbon monoxide and carbon dioxide (syngas) to obtain methanol in the industrial synthesis reaction. This special reactivity of this industrial catalyst for methanol synthesis is attributed to the effects

of strong metal-support interactions (SMSI) that allow a favorable synergy between Cu and the Zn atoms. This means that it is feasible to optimize the choice of catalysts, considering other parameters of technical and economic importance, such as the cost of the catalyst and the possibility of its reuse in successive reactions.

However, despite the fact that using waste CO_2 should decrease the methanol production cost, the significantly low price of this CO_2 gas means that this process remains a challenge, mainly caused by the lack of an efficient catalyst that can perform this reaction in a successful way in terms of kinetics and methanol selectivity. For this reason, it is an objective of extreme priority to advance in the development of new catalysts with good activity and high selectivity for methanol synthesis through CO_2 hydrogenation.

Despite the fact that to date, Cu-based catalysts are the most important catalysts for the conversion of syngas to methanol due to their excellent reactivity and low cost, they exhibit serious shortcomings when CO_2 replaces CO because CO_2 is more inert than CO, leading to lower CO_2 conversion. Besides, the water produced during this reaction results in the sintering of catalytically active copper sites. For this reason, numerous investigations are being directed to the search for efficient catalysts in this process using non-Cu-based heterogeneous catalysts such as noble or rare metals or mixed oxide catalysts represented by M-ZrOx (M = Zn, Ga, and Cd) solid solution catalysts, which present high methanol selectivity and catalytic activity as well as excellent stability to improve the catalytic activity, selectivity, and durability of catalysts in CO_2 hydrogenation [202].

3.1.2. CO_2 Hydrogenation to Methanol by Noble or Rare Metal-Based Catalysts

Despite their limited availability and high cost, many supported noble metal-based catalysts (Pd, Pt, Au, and Ag) can achieve high methanol selectivity and catalytic activity even at low temperatures with excellent stability. Hence, a large amount of research has been conducted in recent years to optimize the catalytic behavior of systems based on noble metals for the CO_2 hydrogenation to methanol. In this sense, various factors can influence the final catalytic behavior, such as the composition of the support, the synthesis method, or the influence of various additives used as promoters (Table 6). In this respect, the catalytic behaviour of bimetalic catalysts has also piqued the interest of researchers. In this respect, the most interesting results are collected in Tables 6 and 7.

Table 6. A comparative summary of different noble metals and rare earth supported catalysts studied in the carbon dioxide hydrogenation process to produce methanol.

Noble Metal	Promoter	Catalyst Support	Conversion (%)	S_{CH3OH} (%)	T (°C)	P (Atm)	Ref.
Au		In_2O_3	5–13	60–100	250–300	50	[203] [a]
Ir		In_2O_3	18	70	300	50	[204]
Pd	Ga	SiO_2	1–5	81	230	25	[205]
Pd		CeO_2	2–18	4–100	200–280	10–250	[206]
Pd	Al	ZnO	2–14	15–70	250	30	[207]
Pd		In_2O_3	3	100	280	50	[208]
Pt		In_2O_3	37	63	30.0	1.0	[209]
Pd		In_2O_3/SBA-15	13	83	260	50	[210]
Ni_5Ga_3		SiO_2	3–35	11–16	200–300	1.0	[211]
Ni		Ga_2O_3	0.5–1	10–100	160–300	5.0	[212]
Re		TiO_2	1–2	82	150	50	[213]
Ti		$MoOx/TiO_2$	80	70	150	50	[214]
ReO_x		TiO_2	18	98	200		[215]
Co		SiO_2	2–14	10–80	260–320	20	[216]
Ag		In_2O_3	5–30	75–100	200–275	50	[217]
Au		ZrO_2	5–9	40–70	140–220	30	[218]
Au		MxOy [b]	5–45	10–95	200–350	1.0	[219]
Au		In_2O_3-ZrO_2	2–15	65–100	200–300	50	[220]
Au		CuO/CeO_2	4–10	30	200–300	30	[221]
Au		CeO_2	1∓2	5–45	240	5∓50	[222]
Ru		In_2O_3	1–30	70–97	200–300	50	[223]
Au		ZrO_2	4–6	48–75	240	40	[224]

Table 6. *Cont.*

Noble Metal	Promoter	Catalyst Support	Conversion (%)	S_{CH3OH} (%)	T (°C)	P (Atm)	Ref.
Au		$ZnO-ZrO_2$	4.5–6	82–95	320	55	[225]
Rh		In_2O_3	1–17	56–100	250–300	50	[226]
Rh		In_2O_3–ZrO_2	1–18	65–100	250–300	50	[227]
Pt		In_2O_3	1–15	54–100	225–300	50	[228] [a]
Pd		In_2O_3	1–20	70–100	200–300	50	[229]
Ni		In_2O_3	1–18	60–100	200–300	50	[230]
Au		In_2O_3	2–14	70–100	225–300	50	[203] [a]
Rh		In_2O_3	4–10	60–80	270–320	50	[231] [a]
Ni	ZrO_2	In_2O_3	1–18	43–100	200–300	50	[232]
Ni		In_2O_3	6–15	30–80	280	50	[233]
Pd		In_2O_3	10	72	295	30	[234] [a]
Pd		SiO_2	—	64–71	200	30	[235]
Pd	Ga_2O_3	SiO_2	10	17–65	220–250	30	[236]
Pd		$ZnZrO_x$	4–35	5–90	200–400	50	[237]
Pd		CeO_2	2–10	40–78	200–260	50	[238]
Pd		SiO_2	1–20	1–28	220–280	8.0	[239]

[a] Special attention is paid to the existence of strong metal-support interaction effects (SMSI). [b] MXOy: Al_2O_3, TiO_2, Fe_2O_3, CeO_2, and ZnO.

Table 7. A comparative summary of different bimetallic-supported catalysts studied in the carbon dioxide hydrogenation process to obtain methanol.

Metal	Catalyst Support	Conversion (%)	S_{CH3OH} (%)	T (°C)	P (Atm)	Ref.
Ni/In/Al	SiO_2	1.6–3.8	1–12	210–290	1.0	[240] [a]
Ni/In	SiO_2-SBA-15	1–17	1–90	300	5−50	[241]
Co/In	In_2O_3	19	69	300	50	[242]
In/Pd	SiO_2	2–5	61	300	40	[243]
Rh/In	Al_2O_3	1–10	5–90	270	45	[244] [a]
Pd/Zn	CeO_2	8–17	65–98	220–270	20	[245]
Ca/Pd/Zn	ZrO_2	2–10	97–100	220–270	20–30	[246] [a]
In/Ru	SiO_2	1–5	20–85	200−240	34	[247]
Ni/Ga	SiO_2, CeO_2, ZrO_2	1–6	5–30	180–270	1–30	[248] [a]
Pd/Cu	SiO_2	1.6–2.8	18–27	300	30–50	[249]
Pd/Cu	M_xO_y [b]	7–16	28–34	300	40	[250] [a]
Pd/Cu	SiO_2	3–7	12–40	300	40	[251]
Pd/Cu	SiO_2	3–6	12–40	300	40	[252]
Cu/Ni	Graphene	7.87	98.7	225	40	[253]
Pd/Cu/Zn	SiC	1–11	10–100	150–300	1.0	[254]
Cu/Ni	Mordenite	100	30–60	220	30	[255]
Ru/Mo	Ru−Mo Phosphide	0.5–4.5	5–75	180–220	65–72	[256]
Rh/Co	nanospheres	100	96	150	24	[257]
Pd/Zn/Al	ZnO, Al_2O_3	0.5–4.0	15–70	250	30	[207]
Ni/Sn	$InZrO_2$	1–5	55–100	225–275	25	[258]
Pd/Cu	TiO_2-MO_2 [c]	7–16	25–40	250	40	[259]
Ni/Ga	Hydrotalcite	2–3.5	60–100	200–300	30	[72]
Pd/Cu	CeO_2	2–17	24–84	190–270	30	[260] [a]
Cu/Zn	Coord. polymer	13–20	25–59	220–260	40	[261]
Cu/Zn	UiO-66 (Zr) MOF	12–22	28–54	220–300	30	[262]
Cu/ZnO	Al_2O_3	5–11	64–87	220–260	30	[263] [a]
Ag/Cu	Mordenite	—-	48–61	230	30	[264]
Cu/Zn	UiO-66 (Zr) MOF	25–30	15–24	230	50	[265]
Cu/Pd	SiO_2	2–32	1–4	220–360	40	[266] [a]
Pd/In	Unsupported nanoparticles	<3.0	25–90	190–270	50	[267]

[a] Special attention is paid to the existence of strong metal support interaction (SMSI), and/or geometric and/or electronic effects. [b] MXOy: TiO_2, ZrO_2, CeO_2, Al_2O_3, SiO_2. [c] TiO_2-MO_2: TiO_2-CeO_2 and TiO_2-ZrO_2.

As can be seen, a wide screening of heterogeneous catalysts containing noble or rare metals (e.g., Pd, Pt, Au, Rh, Ru, Ir, and Re based catalysts), as well as bimetallic systems have been studied. In general, the results obtained have revealed their excellent catalytic activity, stability, and resistance compared with Cu-based catalysts. In this regard, special

attention has been paid to the effects of metal content exhibit on the activation degree for the hydrogen adsorption in the active centers, as well as the effect of support in metal dispersion and the resistance of the catalyst deactivation along the susceptive uses.

From the results depicted in Table 6, the In_2O_3 seems to be one of the best options as a support for noble metals, achieving CO_2 conversion between 10–20% and selectivity values up to 100% with Pt, Pd, and Ni as metals.

On the other hand, metal sintering, as well as the effect of different synthesis methods in the development of different morphological and/or metal-support interaction effects have also been considered, as well as the Single-Atom Catalysts (SACs) technique, which promotes atomically distributed active metal sites on the support surfaces. In this way, SACs provide great advantages in minimizing the usage of precious metals with a 100% atom-utilization efficiency, which thus results in improved catalytic reactivity [268].

It is noteworthy that bimetallic catalysts are best suited for methanol hydrogenation in comparison to their monometallic counterparts. Herein, a summary regarding the advances of the bimetallic catalysts (Ni, Cu, Pd, Rh, Ru, Zn, and In-based bimetallic systems) for methanol production in recent years, as well as the different strategies to enhance the catalytic activity, including regulating the active species, nanoparticle size, and catalyst support, have been included, Table 7.

3.1.3. CO_2 Hydrogenation to Methanol over Mixed Oxide-Based Catalysts

Despite the fact that catalysts based on the use of supported Cu [269] or noble metals [270] have demonstrated their ability to produce methanol as a product of CO_2 hydrogenation, the investigation of simple metal oxides or diverse metal oxides mixtures (MOs) to obtain heterogeneous systems with enough catalytic activity, selectivity, and durability for the synthesis of methanol from CO_2 hydrogenation is currently an important line of research, collecting a large number of publications in recent years. The most interesting results are summarized in Table 8. In this regard, a rational design of Mos has been proposed, i.e., the general optimization framework followed to fine-tune non-precious metal oxide sites and their surrounding environment through appropriate synthetic and promotional or modification routes, as shown in Figure 11 [271].

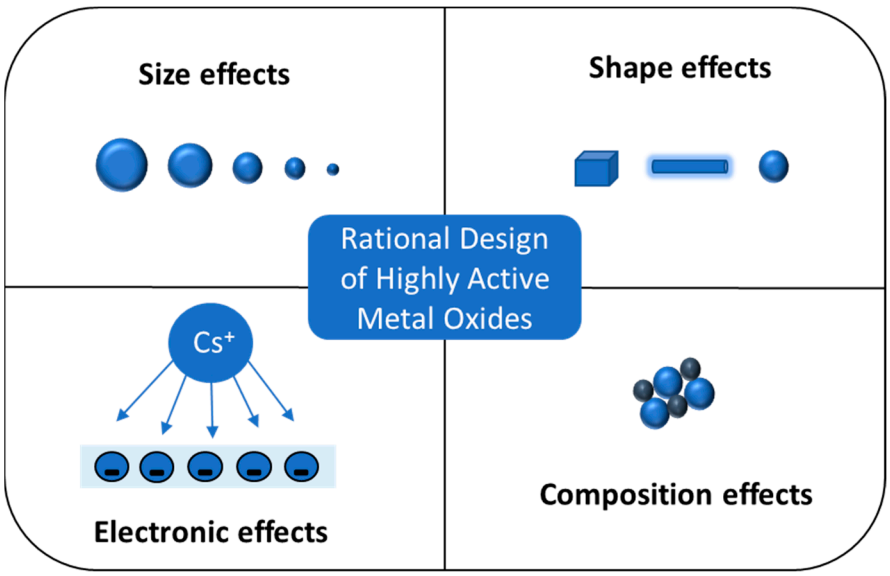

Figure 11. Representative scheme of the parameters affecting the catalytic behavior of metal oxides (MOs) in the CO_2 hydrogenation process: size, shape, composition, and electronic/chemical state. Adapted from ref. [271], open access, Catalysts 2020.

The multiple studies collected in Table 8 show that there are fundamentally two options that meet expectations. On the one hand, results obtained using binary metal

oxides ZnO-ZrO_2 and, and on the other hand, heterogeneous catalysts including In_2O_3, either alone or in various hybrid mixtures. In this sense, some research is currently directed to the optimization of the ZnO-ZrO_2 mixtures, evaluating parameters that implement the highly selective production of CH_3OH [272,273], whereas the other line intends the evaluation of the promoting effect of incorporating Ga or small amounts of Cu into ZnZrOx solid solutions [274,275].

Table 8. A comparative summary of different active metal oxides catalysts studied in the carbon dioxide hydrogenation process to obtain methanol.

Metal Oxides	Conversion (%)	S_{CH3OH} (%)	T (°C)	P (Atm.)	Ref.
NiO/In_2O_3	1–3	50–60	250	30	[276] [a]
In_2O_3	1–10	45–95	240–330	30	[277] [b]
InO_x/ZrO_2	0.5–2.5	70−80	250–300	50	[278] [a]
ZnO/ZrO_2	10	86–91	315–320	50	[279] [c]
ZrO_2/In_2O_3	0.4–5.0	85	220–300	50	[280] [a]
$GaxIn_{2-x}O_3$	7–35	0.5–35	320–400	30	[281] [a]
In_2O_3-ZrO_2	3–11	53–91	255–300	40	[282]
$MaZrO_x$ [d]	4.3–12.4	80	250–300	50	[283]
$GaZnZrO_x$	7.7–8.8	86–88	320	50	[274]
In_2O_3/ZrO_2	[e]	[e]	270–310	30–55	[284]
In_2O_3	17	92.4	300	50	[285]
In_2O_3/Support [f]	0.1–6.0	5–40	220–300	1.0	[286] [a]
In_2O_3/Support [g]	1–20	5–51	260–360	30	[287]
ZnO/ZrO_2	9.2	50–95	320	30	[288]
MnO_x/Co_3O_4	3–57	2–22	250	10	[289]
$GaxIn_{2-x}O_3$	7–38	—	320–400	30	[281]
ZnO/ZrO_2	10	10–85	320	50	[272]
Co_3O_4/In_2O_3	10	30–70	300	40	[290]
$ZnZrO_x$ [h]	1–18	30–90	200–360	45	[291]
In_2O_3/ZrO_2	3–8	65–90	300	50	[292]
Co_xO_y/MgO	7–35	8–30	[i]	1.0	[293]
$InNi_3C_{0.5}/ZrO_2$	25.7	90.2	325	60	[294] [a]
In_2O_3/ZrO_2	5–30	—	320–400	20	[295]
$ZrZnO_x$/zeolite	1–8	5–30	400	30	[273]
In_2O_3/GO [j]	1–14	5–100	200–450	30	[296]
In_2O_3	4–18	20–85	260–360	40	[297]

[a] Special attention is paid to the existence of strong metal support interaction (SMSI) and/or geometric and/or electronic effects. [b] A phase-mixing strategy is used in the synthesis of catalysts. [c] The ability of the catalysts for their reuse is determined. [d] (Ma = Cd, Ga). [e] Results are expressed in terms of methanol space-time yield. [f] Supports ZrO_2 and CeO_2. [g] Supports MnO and MgO. [h] Promoters, small amounts (<2%) of Cu, Pd, or Pt. [i] Non thermal plasma-catalysis DBD reactor. [j] Graphene oxide, GO.

Besides, it has also been verified that several mixed systems with oxides [287,296], including ZrO_2, or transition metals, such as Co, Ni, Sn, Pd [298,299], or CuO [300]. Moreover, PdZn alloy catalysts supported on ZnFe composite oxides [301] or molybdenum phosphide catalysts have also been studied, attaining very promising results [302].

Nevertheless, from the different options covered to date, indium oxide-based catalysts are attracting the highest interest due to their excellent selectivity to methanol and high activity for CO_2 conversion. Therefore, most of the new high-performance catalysts are described over ternary Cu-based catalysts with several promotor compounds, including In, Ce, Zn, or Zr [303,304].

3.1.4. Methanol Reaction Process for CO_2 Hydrogenation to Fuels and Chemicals

By coupling two successive reactions using a bifunctional catalyst, the hydrogenation of CO_2 to methanol can be applied to obtain C2+ compounds, including dimethyl ether (DME), light olefins, and gasoline-type hydrocarbons [59]. Thus, after the conversion of CO_2 and H_2 to CH_3OH on the surface of a suitable catalyst, the methanol is dehydrated or coupled on zeolites, alumina, or some other suitable acid-base catalyst, according to the scheme shown in Figure 12. Consequently, the synthesis of products with two or more

carbons (C2+) from CO_2 hydrogenation can be achieved by first converting of CO_2 to carbon monoxide or methanol and then conducting a C–C or C–O coupling reaction with a bifunctional or hybrid catalyst [305].

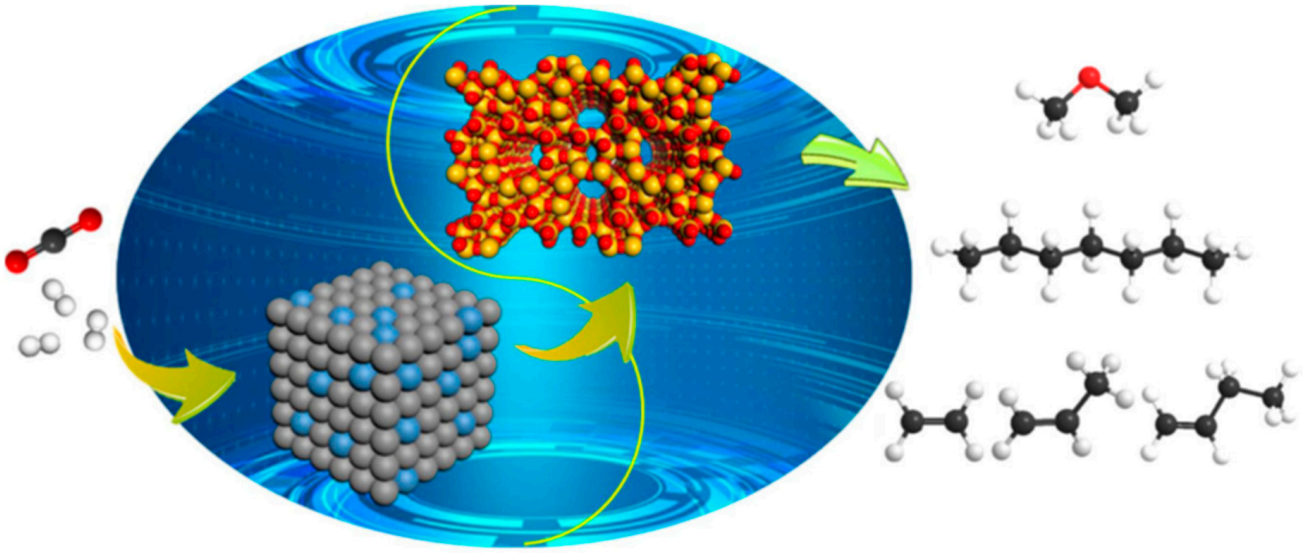

Figure 12. Schematic reaction mechanism of direct CO_2 hydrogenation to C2+ products over bifunctional catalysts. Reproduced with permission from ref. [59], open access Nat. Commun. 2021.

In this respect, dimethyl ether (DME) is a versatile raw material and an interesting alternative fuel that can be produced directly by catalytic hydrogenation of CO_2 [105,306]. Therefore, this process is considered a potential vector to contribute to the CO_2 reduction because of its lower operating costs compared to the classic two-step synthesis of DME, CO, and hydrogen. Figure 13 shows a general scheme of the DME formation. In recent years, a great number of studies have been carried out with the aim of finding a good catalyst for the production of DME from syngas. However, multiple investigations are currently comparing direct CO_2-to-DME to bifunctional/hybrid catalytic systems. Table 9 collects a comparative summary of the different bifunctional/hybrid catalytic systems recently studied in the carbon dioxide hydrogenation process to obtain DME.

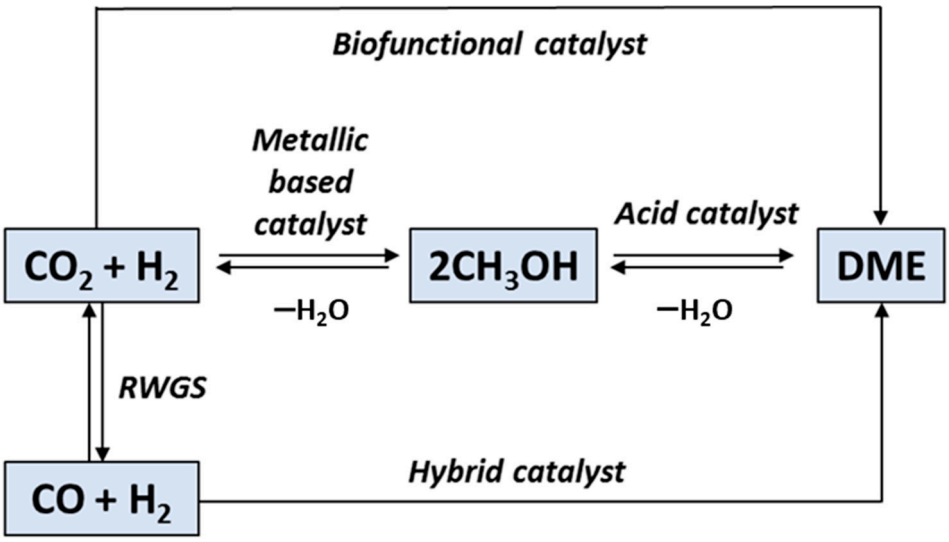

Figure 13. General scheme for the synthesis of DME by direct hydrogenation of CO_2 with hybrid or bifunctional catalysts.

Table 9. Comparative summary of different bifunctional/hybrid catalytic systems for improving the direct conversion of CO_2 to DME.

Metal Catalyst	Acid Catalyst	Conversion (%)	S_{CO} (%)	S_{CH3OH} (%)	S_{DME} (%)	T (°C)	P (Atm.)	Ref.
CZZA [a]	HZSM-5	25–28	20–80	5–7	10–70	220–280	27.6	[185]
$CuO/ZnO/ZrO_2$	Zeolite	2–20	15–20	5–12	1–30	260	30	[192]
$CuO/ZnO/Al_2O_3$	SiO_2-Al_2O_3	5–9	49–65	11–17	22–35	260	30	[307]
Cu-BTC MOF [b]	Al_2O_3	2–26	15–25	5–50	14–90	260	30	[308]
$CuO/ZnO/ZrO_2$	$Zr(SO_4)_2$	14–17	60–80	7–20	14–28	260	20	[309]
CuZnAlZrCe	ZSM-5	13–19	59–63	9–11	26–33	250	30	[310]
In_2O_3	HNT [c]	1–5	0.0	20–80	10–70	200–300	10–40	[311]
CZA/HPW [d]	TiO_2	5–22	14–17	5–99	7–59	250	30	[306]
CuZnAlSi/Sn	——	10	50–60	5–9	80–85	280	40	[312]
$CuO/ZnO/ZrO_2$	SAPO-11	40–50	0.0	10–50	50–90	250–325	10–50	[313]
CZA [e]	HZSM-5	25	25–28	7.0	65–70	220–280	21–42	[314]
CuO/ZnO	HZSM-5	15–35	10–30	5–88	10–80	200–260	15–20	[315]
$CuZnOZrO_2$	WOx/Al_2O_3	10–20	64–69	8–17	15–28	300	20	[316]
$Cu/ZnO/MO_x$ [f]	SAPO-34	5–20	50–90	19–24	25–31	200–260	10	[317]
$Cu/ZnO/ZrO_2$	HZSM-5	1–11	9–90	6–18	5–75	200–330	30	[318]
GaZrOx	——	1–9	10–88	10–100	10–25	240–380	30	[319]
$CuO/ZnO/Al_2O_3$	SAPO-18	1–8	5–8	3–15	85–90	250–350	20–40	[320]
$CuO/ZnO/Al_2O_3$	MCM-41-TPA [g]	2–7	23–65	18–50	18–25	220–250	45	[321]
$Cu/ZnO/ZrO_2$	ZSM5	8–11	15–49	24–26	38–58	240	30	[322]
nano-Pd/In_2O_3	H-ZSM-5	6–11	40–45	17–19	36–42	280–300	30	[323]
Gallium nitride		1–25	40–82	18–42	0–80	300–450	20	[324]

[a] CZZA: $CuO/ZnO/ZrO_2/Al_2O_3$. [b] Cu-BTC MOF: Cu-1,3,5-benzenetricarboxylate metal–organic framework (Cu-BTC MOF). [c] HNT: natural clay halloysite nanotubes, and HNT modified with Al-MCM-41 silica arrays. [d] CZA-HPW: $Cu/ZnO/Al_2O_3$-$H_3PW_{12}O_{40}$. [e] CZA: $CuO/ZnO/Al_2O_3$. [f] MO_x: Al_2O_3, CeO_2, or ZrO_2. [g] TPA: tungstophosphoric acid.

In summary, it can be said that DME is currently considered a firm candidate for its application in the circular process of capturing and using CO_2, not only to carry out an effective mitigation of environmental problems [325], but also to contribute to obtaining chemical products of interest to society [326].

3.2. One-Step Process for the Conversion of CO_2 to Light Olefins

Light olefins such as ethylene, propylene, and butylene are currently among the top petrochemicals and fuels produced. These olefins are used to produce a wide variety of polymers, plastics, solvents, and cosmetics. Moreover, light olefins can be oligomerized into long-chain hydrocarbons that can be used as fuels, making them a desirable product with high potential. Thus, their production from CO_2 hydrogenation can contribute to a great extent to the elimination of CO_2 emissions. Nowadays, there are mainly two methods for the synthesis of light olefins from captured CO_2. The first one is the modified Fischer-Tropsch synthesis (FTS), where carbon monoxide is obtained by the reverse water gas shift (RWGS) reaction in a first step and, in a second step; CO is hydrogenated to lower hydrocarbons (HCs) [327,328]. On the other hand, the production of light olefins can be obtained by a different two-step process, usually called the methanol to olefins process, consisting of the hydrogenation of CO_2 into methanol and subsequently a dehydration-condensation process, as shown in Figure 14. These pathways will be discussed in more detail in the following subsections.

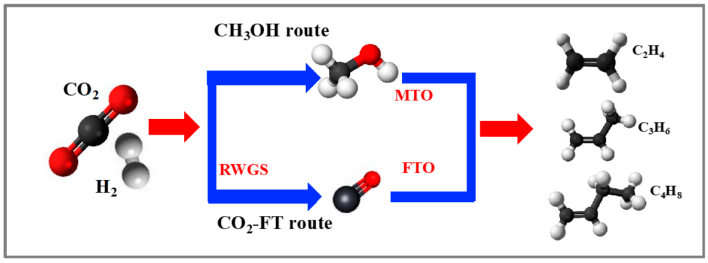

Figure 14. General scheme for the synthesis of DME by direct hydrogenation of CO_2 with hybrid or bifunctional catalysts Reaction scheme for CO_2 hydrogenation to light olefins [328].

3.2.1. CO_2 Hydrogenation in a One-Step Process over Bifunctional or Hybrid Catalysts

At present, the production and marketing of low molecular weight olefins is already being carried out through the MTO process, which has high selectivity values for C2–C4 olefins [329], since this process, along with the methanol-to-gasoline (MTG) process, are technological discoveries in the synfuels arena, first introduced by Mobil Oil Corporation [330]. However, although considerable progress has been made in the hydrogenation of carbon dioxide to various C1 chemicals, it is still a great challenge to synthesize value-added products with two or more carbons directly from CO_2, given the technical and economic interest of the process. In this regard, a great number of investigations have been carried out. Most of these studies aimed at evaluating the experimental conditions and/or the bifunctional catalysts able to couple two successive reactions, the hydrogenation of CO_2 to methanol, followed by its dehydration or coupling on zeolites, alumina, or some other suitable acid-base catalyst. A comparative summary of the different bifunctional/hybrid catalysts recently studied in the MTO process with high selectivity for light olefins is collected in Table 10.

Table 10. Comparative summary of different bifunctional/hybrid catalytic systems for the MTO process for improving the direct conversion of CO_2 to light olefins.

Metal Catalyst	Acid Catalyst	Conversion (%)	S_{CO} (%)	S_{C2-C4} (%)	S_{C5} (%)	T (°C)	P (Atm)	Ref.
In_2O_3	HZSM-5	12–15	45–50	20–25	79	340	30	[331]
Cu/CeO_2	SAPO-34	4–20	30–75	30–65	4–9	300–500	20	[332]
ZnZrOx	Zeolites [a]	18–24	—	1.5–2.8	2–9	325–400	10	[333]
InCo	Zn-zeolite beta	8.0	6	8	85	300	50	[334]
In_2O_3/ZrO_2	SAPO-34	17–26	64–70	65–82	2–5	380	30	[335]
ZnO/ZrO_2	SAPO-34	42–45 [b]	4–22	76–85	2–3	375	15	[336]
ZnGaOx spinel	SAPO-34	7–50	—	15–76	5–7	400	40	[337]
In_2O_3/ZrO_2	SAPO-34	15–21 [c]	—	3–6	—	400	30	[338]
In_2O_3/ZrO_2	SAPO-34	23–25	2–6	2–7	—	400	30	[339]
In-Zr	SAPO-34	35	—	93	—	400	30	[340]
Mn_2O_3-ZnO	SAPO-34	9–30	50–91	86–92	3–13	380	30	[341]
Fe/Co	K-Al_2O_3	37–42	12–16	67	17–21	320	20	[342]
Fe_5C_2	Zeolite [d]	8–56	1–49	12–93 [e]	1–56	300	10	[343]
In_2O_3	SAPO-34	18–35	18–37	16–34	—	340–400	10–25	[344]
ZnZrOx	SAPO-34	9–14	40–43	82–83	—	380	30	[345]
In_2O_3/ZrO_2	SAPO–34	29–38	45–90	68–85	3–5	400	10–30	[331]
ZnZrO	SAPO-34	10–15	—	80.0	1–3	330–380	20	[346]
InCeOx/InCrOx	SAPO-34	5–20	15–60	70–90	3–7	300–350	10–35	[347]
CuZnZr(CZZ)	SAPO-34	10–20	57–86	70–88	0.5–5	400	20	[348]
$NiCu/CeO_2$	SAPO-34	12–20	55–85	62–79	2–4	350–450	20	[349]
ZnO/Y_2O_3	SAPO-34	6–28	75–97	90–94	1–5	390	40	[350]
$ZrS/Fe_2O_3@KO_2$	SAPO-34	46–48	24–27	42–55	25–38	375	30	[351]
$10K_{13}Fe_2Co_{100}Zr$	Polymetallic fibers	10–48	—	70–80	—	400	30	[352]
ZnO/ZrO_2	MnSAPO-34 [f]	15–21	— [g]	90–99	0.4–7.6	380	20	[353]
$GaZrO_x$	SAPO-34	5–12	50–60	92–95	1–3	370–410	30	[354]
$CuO/ZnO/Al_2O_3$	SAPO-34	50–56	4–10	50–56	— [h]	250–450	30	[355]
In_2O_3	SAPO-34 [i]	27–51	3–75	50–92	5–20	360	25	[356]
CuO/ZnO	kaolin/SAPO-34	33–58	7–10	78–81	— [j]	400	30	[357]
Y_2O_3/Fe/Co	SAPO-34	7–18	31–35	75–85	1–3	300–400	10–25	[358]
FeZnK	SAPO-34	42–50	14–20	54–61	8–25	280–360	15	[359]
FeNa	Supports [k]	19–33	10–60	17–73	—	320	20	[360]

[a] Zeolites and silicoaluminophosphates with different topologies, MOR, FER, MFI, BEA, CHA, and ERI. [b] CH_4 selectivity, 2–9%. [c] oxygenates (MeOH and DME): 0.0–0.5%. [d] Containing K, Ce or La. [e] CH_4 Conversion 7–86%. [f] Polymetallic fibers. [g] CH_4: 2.4–8.6. [h] CH_4: 15–18. [i] With Fe-Co/K-Al_2O_3 as composite. [j] CH_4: 11–112. [k] SiO_2, Al_2O_3, ZrO_2 and CNT (multi-walled carbon nanotube).

According to recent research developed, in this tandem catalytic process, methanol is obtained as the product of CO_2 hydrogenation in this tandem catalytic process by using various metal oxides; however, in the second acid-catalyzed C–C coupling reactions, zeolites SAPO-34 are the main catalysts used. In this respect, the acidity and pore structure of the zeolites seem to be decisive factors in obtaining this coupling process among silicoaluminophosphate (SAPO) zeotype materials. Current research seems to show that SAPO-34 is the best acidic catalyst for obtaining C2–C4 olefins and is superior to other catalysts such as ZSM-5 or SSZ-13 [361–363].

On the other hand, they are also being evaluated with promising results, including the use of Fe-based catalysts promoted with K, Na, Mn, Zn, and Ce to increase lower olefin selectivity, owing to their enhanced CO_2 adsorption ability and facilitation of the formation and stability of active species Fe_5C_2. Furthermore, the favorable effect of Fe-Co bimetallic systems on the formation of C2+ hydrocarbons in these supported catalysts has been demonstrated [364]. Thus, the combination of these various factors—the application of Fe catalysts supported on different solids, activated by metals such as Co and alkali metals—constitute promising lines of research for obtaining light olefins from the hydrogenation of CO_2 [365]. Finally, using this tandem technique of hydrogenation of CO_2 in the presence of supports of an acid nature, attempts are also being made to obtain various aromatic compounds. Thus, the use of a series of metal oxides (In_2O_3, Cu-Zn-Al, and $ZnZr_xO$) with different spherical HZSM-5 zeolites has been investigated to obtain the direct conversion of CO_2 to aromatics [366].

3.2.2. Modified Fischer-Tropsch Synthesis Route

The modified Fisher-Tropsch synthesis route has a clear controlling factor, determined by the RWGS reaction, since it exhibits an endothermic and reversible character, which limits the CO_2 conversion to CO at values around 20% [367]. However, the FTS process, on the other hand, is a well known route for the transformation of syngas (CO + H_2) into C2+ hydrocarbons, that proceeds on catalyst surfaces through the following steps: (1) adsorption and dissociation of CO and H_2; (2) formation of CH_x (x = 0–3) species on catalyst surface; (3) C–C bond formation through coupling of CHx species, that leading to chain growth and surface CnHm intermediates or CH_4 by the hydrogenation of CH_x species; (4) dehydrogenation or hydrogenation of C_nH_m into olefins or paraffins compounds [368].

Fe, Co, and Ru metals are conventionally employed as active catalyst components owing to their capabilities in both CO dissociation and C–C coupling or chain growth [369]. However, the C–C coupling is uncontrollable on these metal surfaces, leading to a statistical distribution of products, i.e., the Anderson-Schulz-Flory (ASF) distribution. Consequently, one of the main objectives of the research on these catalytic systems is finding supports, either metal or bimetallic. In this sense, it has been shown that Ni-Fe catalysts improved selectivity towards CO without significantly compromising FTS process activity, coupling the high activity of Ni catalysts with the high CO selectivity of Fe [370]. Similarly, a large number of studies have recently evaluated the behavior of different supports, different metals, and different operating conditions in the CO_2-FT process, as collected in several reviews [328,371,372]. Besides, a comparative summary of the different FTS catalysts recently studied are collected in Table 11. Obviously, this table expresses very summarized values of several selected parameters, obtained from very extensive studies addressing different goals but aiming to carry out an approximate comparison between the different catalysts currently evaluated in FTS reactions.

Table 11. Comparative summary of different catalytic systems for FTS process activity improving the direct conversion of CO_2 to light olefins.

Metal Catalysts	Alkali Metal	Support	Conversion (%)	S_{CO} (%)	S_{CH4} (%)	S_{C2-C5} (%)	T (°C)	P (Atm)	Ref.
Fe	—	Carbon	14–52	5–49	3–8	5–38	300	25	[373]
Co	—	SAPO-34	—	64–74	24–28	65–70	220	20	[374]
Fe_3O_4/Mn	Na	—	22–30	14–32	12–36	64–88	320	5.0	[375]
Co	K	Al_2O_3	15–97	1–34	2–33	2–57	200–350	1–50	[376]
Fe_5C_2	—	—	41–50	3–10	20–46	51–70	320	30	[377]
Fe/Co	K	—	32–58	2–10	8–36	62–82	300	25	[378]
Fe/Mn	K	—	38.2	5.6	10.4	22.3	300	10	[379]
Co/Mn	Na	SiO_2	45–47	18–20	2.0	52–54	260–270	50	[380]
Fe/Co (Ru)	K	—	30–57	2–16	7–30	54–84	450	2.0	[381]
Co_3O_4/MnO_2	—	—	42–48	2–39	4–23	90–96	270	1.0	[382]
Co/Pt	—	ZSM-5	10–28	—	52–100	10–48	200–500	1–30	[383]
Fe	Na	ZSM-5	18–22	28–32	22–41	30–54	450	20	[384]
Fe/C	K	X-ZSM-5 [a]	34–36	18–20	10–15	85–89	320	20	[385]
$CuFeO_2$	—	—	13–18	28–32	1–60	40–95	300	10	[386]
Cu/Fe	—	Al_2O_3	35–42	23–42	28–38	51–91	300–400	30	[387]
Fe		SMC [b]	8–45	16–86	5–11	70–89	260	10	[388]

Table 11. *Cont.*

Metal Catalysts	Alkali Metal	Support	Conversion (%)	S_{CO} (%)	S_{CH4} (%)	S_{C2-C5} (%)	T (°C)	P (Atm)	Ref.
Ru/Ni(NPs) [c]	—-		2–30	0–47	1–100	7–76	150	2–8.5	[389]
Raney-Fe, Fe	—-	SiO_2	4–12	14–27	5–22	22–78	220–265	20	[390]
Fe/Ti [d]	K	—-	30–35	38–85	23–25	72–75	320	20	[391]
FeMn	—	HZSM-5	28–40	64–68	—-	58–69	280	10	[392]
$RuCl_3$/Ru	—	—-	—-	0–85	14–100	17.5	180	50	[393]
Co, CoO, Co_3O_4	—-	$Si_xAl_yO_z$	3–35	0–12	6–31	15–93	220–260	20	[394]
Fe_3O_4	—-	SiO_2	5–7	2–5	57–93	7–43	220	1.0	[395]
Fe_3O_4/Fe_xC_y	Na		36–46	8–11	36–60	16–52	320	20	[396]
Fe_3O_4/FeC_x		Mesop. C	15–54	5–31	13–75	25–87	320	30	[397]
Co/Ce/La	—-	Al_2O_3	13	49–52	15	99–100	230	20	[398]
Co@CoOx/Co_2C-Mn	Na		1–62	1–92	45–70	29–54	230–310	40	[399]
Fe-/Co	—-	SiO_2	4–20	11–13	26–45	43–70	260–280	20	[400]
FeCo X,(X: La, Mn, Zn)	K	Al_2O_3	65–100	30–38	0–58	44–100	300	10	[401]
Co	—-	C/SiO_2 [e]	2–8	6–14	21–32	62–70	250	5	[402]
Co_6/MnOx	—-	——-	15	0–0.7	—-	0–99	200	8	[403]
Fe_2O_3	K	Al_2O_3	40–47	19–33	20–31	40–50	400	30	[404]
Fe-Co	K	Al_2O_3	37–49	9–29	14–23	58–68	320–360	20–30	[405]
Fe-Cu	K	—-	24–41	6–16	5–10	79–88	250–340	20	[406]
X-Fe_5C_2/ZnO	Na	—-	2–28	15–36	10–16	68–89	280–370	25	[407]
Ni		$MgAl_2O_4$	6–70	2–96	3–98	—-	330–400	1.0	[408]
$FeAlO_x$	Na	HZSM-5/SiO_2	29–48	8–18	10–35	47–88 [f]	335–400	35	[409]
Fe-Zn	K	SAPO	43–48	14–18	15–40	36–57	320	15	[359]
Fe-Zn	Na	—-	15–39	14–30	12–48	52–88	340	25	[410]
$ZnCo_xFe_{2-x}O_4$		SiO_2	24–52	6–16	16–21	36.1	260–340	25	[275]
Fe (Cu, Mn, V, Zn, Co)	K	Al_2O_3	29–40	10–20	15–22	65–74	340	20	[411]

[a] X: K^+, Na^+, Cu^{2+}, Mn^{2+}, Mg^{2+}, Ce^{2+}, La^{3+}, or Cs^{2+}. [b] spherical mesoporous carbon: (SMC). [c] nanoparticles (2–3 nm), in a hydrophobic ionic liquid (IL). [d] K–Fe–Ti layered metal oxides (LMO). [e] oxygenates, including alcohols and aldehydes Sel.(%): 2–8. [f] Selectivity to aromatics: 7–30.

As can be seen, the majority of catalysts investigated in the two consecutive processes for CO_2 Fischer-Tropsch synthesis (CO_2–FTS) contain metallic Fe as the active species, enhanced with different inorganic supports, other transition metals, and/or alkali metals. Therefore, these are similar catalysts to those employed in the last few years to obtain olefins from syngas. The main handicap is that these catalysts also work for the water-gas-shift reaction (WGSR), producing large amounts of CO_2 as areaction product [412–414]. Some recent research using different catalysts as well as different kinds of feedstocks (coal, biomass, methane via reforming, and nonconventional energy sources) to obtain the syn-gas (CO and H_2) is shown in Table 12.

Table 12. Comparative summary of different catalytic systems for Fischer-Tropsch (FTS) improving the direct conversion of the water-gas-shift reaction (WGSR) to light olefins.

Metal Catalysts	Alkali Metal	Support	Conversion (%)	S_{CO2} (%)	S_{CH4} (%)	S_{C2-C5} (%)	T (°C)	P (Atm)	Ref.
α-Fe_2O_3		SiO_2, Al_2O_3	18–65	25–36	16–19	81–94	280	10	[415]
Fe-Mn, Cu		SiO_2	75–96	23–45	15–19	80–85	200	20	[416]
$CoMnAlO_x$ [a]	—-	SiO_2	5–14	9–48	2–24	45–85 [b]	260	10	[417]
Co-Re, Pt-ZSM-5	—-	Al_2O_3	5–75	—-	—-	24–43 [c]	225–255	20–30	[418]
Fe	Na	ZSM-5	24–87	26–42	16–41	57–85	300	10	[419]
Co, Re	—-	Al_2O_3, CNT [d]	2–4	—-	42–56	44–58	210	1.9	[420]
Fe-Zn	Na	Zeolites [e]	47–44	88–95	11–16	75–80	360	1.0	[421]
CoO-Co		SiO_2, TiO_2, Al_2O_3	24–75	—-	—-	45–83	210	20	[422]
Fe-Cu	K		65–90	16	19–37	63–81	340	15	[423]
$Fe_1Zn_{1\cdot2}O_x$	Na		38–95	31–37	15–19	85–87	340	20	[424]
Fe, Fe_3C		Carbon	80–90	10–14	7–9	88–90	250–350	34–85	[425]
Fe	K	Al_2O_3	7–90	18–70	7–8	12–74	300–420	20	[426]

[a] Composite oxides. [b] Oxygenates, including alcohols and aldehydes Sel.(%): 6–14. [c] Selectivity C_{10}-C_{20} (%). [d] γ-alumina, α-alumina and carbon nanotube (CNT). [e] Zeolites: HY, NaY, ZSM-5, SAPO-34, Hβ, Liβ, Naβ, Kβ, and Rbβ.

Therefore, from the conventional Fischer-Tropsch reaction, it is possible to access catalytic systems that could be tested in modified Fischer-Tropsch processes capable of

using CO_2 as a raw material to access light olefins (C2-C4) widely used in different fields such as the synthesis of polymers and pharmaceutical intermediates. However, the chain length distributions are given by the Anderson-Flory (ASF) distribution, which limit the C2-C4 range to less than 58% [427]. Finally, it is possible to integrate waste CO_2 in synthesis using Fe-based Fischer-Tropsch with green H_2 as well as olefin oligomerization, thereby increasing the production of value-added liquid hydrocarbons [428].

4. Concluding Remarks, Challenges, and Research Outlook

The use of CO_2 as a raw material for the production of various chemicals via catalytic hydrogenation is currently a necessary eventuality, not only because global warming is a risk, but also, and more importantly, because there is a real possibility of technologically accessing sufficient amounts of green hydrogen at an affordable, economical cost. In this respect, the use of hydrogen as an energy vector, not only in a significant number of heavy industries but also in transportation fuels, is expected to decisively contribute to meeting decarbonization goals to achieve net zero emissions in the next two decades. However, these objectives do not only mean to address efficient hydrogen production but also its trustworthy transportation and storage. For this purpose, it is currently considered that the use of different liquid organic hydrogen carriers (LOHCs) is a valuable solution to making available a reliable and on-demand hydrogen supply. However, green hydrogen can also be stored and transported as a 'green' feedstock for the synthesis of biofuels and several fine chemicals.

Therefore, the production of green hydrogen via electrolysis and its storage and transportation using some hydrogen carriers such as ammonia or methanol must be considered as part of sustainable chemical and biofuel manufacturing. Thus, the power-to-ammonia concept allows producing ammonia by the Haber–Bosch process, the currently second most produced industrial chemical, from air, water, and (renewable) electricity. Besides, methanol synthesis, with a global production capacity of around 85 million metric tons per year, which is expected to rise in the coming years, can be obtained by catalytic CO_2 hydrogenation. In this regard, methanol is one of the most important industrial chemicals, serving as a feedstock for a wide range of chemical products. Besides, it is also being used increasingly as a fuel additive and as a transportation fuel alternative. This assumption is confirmed by the high number of investigations carried out in recent decades. As can be seen in Figure 15, the production of methanol from CO_2 hydrogenation is the option most investigated, followed by CO_2 methanation.

The primary industrial process relevant to the current scenario, developed to reduce global warming, is CO_2 to methanol conversion. However, extensive commercialization of green methanol from CO_2 hydrogenation is still seriously limited by its economic viability due to various factors. These include the difficulty in accessing renewable H_2 and sources of CO_2 recovered from industrial processes, in enough quantity and purity. In addition, it must be added to these factors that the current low price of methanol, due to the low price of natural gas, has been used until now for its industrial production. Despite this, in the last decade there has been widespread industrial interest in the development of technologies in this field, probably encouraged by the increasing implementation of legal regulations on fossil fuels to mitigate climate change and the general introduction of a strict carbon tax.

Furthermore, the actual introduction of Renew Energy technologies in many countries have made solar and wind the cheapest sources of energy in many parts of the world. This has not only caused the rapid decarbonization of the electricity sector but also opened the possibility of obtaining several chemicals by CO_2 hydrogenation via electrolysis.

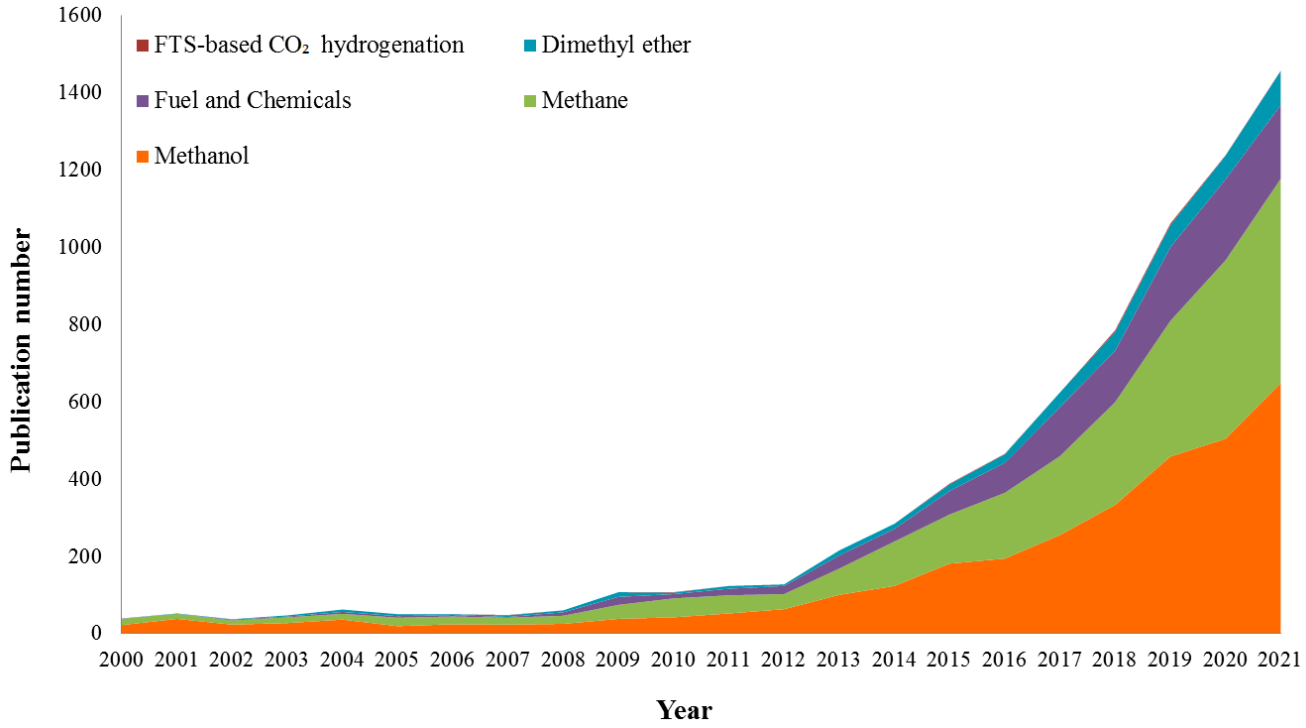

Figure 15. Number of publications found in the Web of Science database using keywords related to CO_2 transformation in various products from 2000 to 2022. Publications include research articles, reviews, patents, books, and letters.

This new scenario allows us to consider that an exemplary carbon capture and utilization cycle based on mature technologies can meet the energy requirements of the "industrial carbon cycle", an emerging paradigm in which industrial CO_2 emissions are captured and reprocessed into chemicals and E-fuels. In this context, methanol would come to occupy a central role as a platform molecule from which most chemical commodities could be obtained (Figure 16), partially replacing the ethanol role granted by the paradigm associated with so-called green chemistry, which is primarily based on biomass feedstocks.

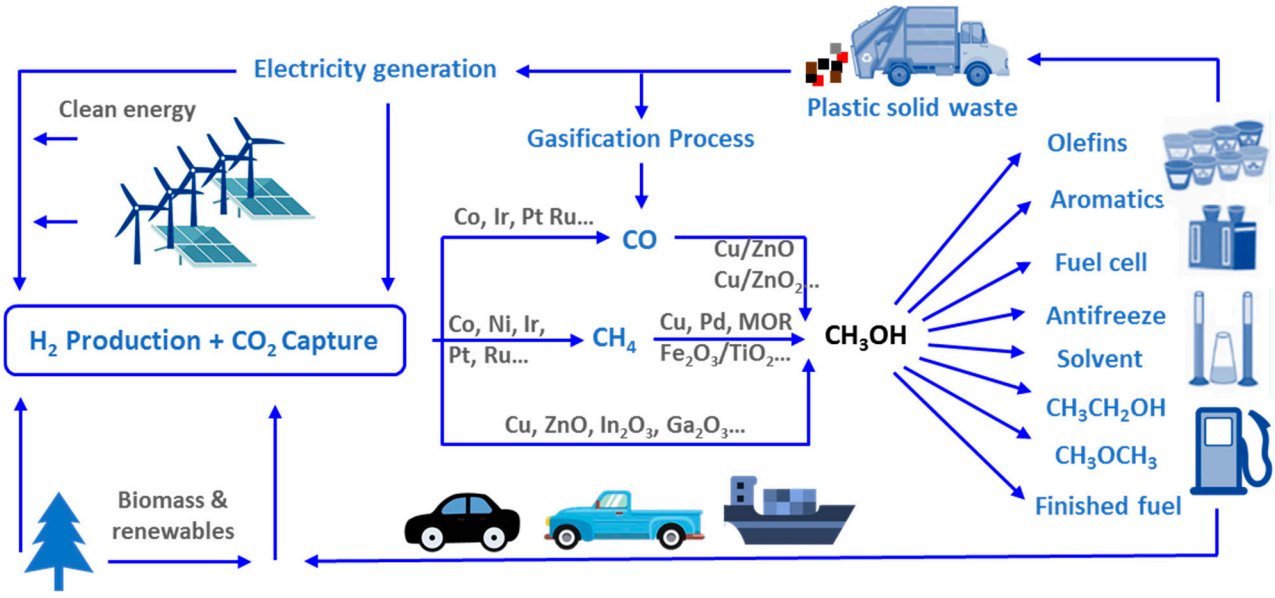

Figure 16. The simplified carbon cycle with green methanol as a platform molecule in the future. Adapted from ref. [429].

At the very least, the massive use of anthropogenic CO_2 would free up huge amounts of agricultural land that, in the paradigm of green chemistry, should be used for crops destined for industrial uses. For this reason, the application of CO_2 as a raw material for obtaining methanol and other chemicals could constitute the main chemical reaction to be developed in the 21st century, similar to what happened in the past 20th century with the catalytic hydrogenation reaction of nitrogen gas for the production of ammonia by the Haber–Bosch process.

Therefore, based on the existing investigations, it can be concluded that there are two priority directions that should be followed in the immediate future. On the one hand, the performance of the electrolysis processes to obtain green hydrogen must be increased as much as possible. On the other hand, implement the processes for catalytic hydrogenation of CO_2 to obtain green methanol. In this sense, it would be necessary to consider the development of more efficient heterogeneous catalysts, both in the yield obtained and in their behavior over successive uses. Likewise, it is a priority to try to obtain catalytic systems that are as economical as possible, through the use of non-noble metals, in order to obtain, in a viable technical and economic way, green methanol, which would be the platform molecule on which, in the present century, the fine chemistry will foreseeably rest.

Author Contributions: Conceptualization, D.L. and R.E.; Methodology, F.M.B. and L.A.-D.; writing—original draft preparation, D.L. and R.E.; writing—review and editing, F.J.L.-T. and R.E.; supervision, A.A.R. and F.M.B. All authors have read and agreed to the published version of the manuscript.

Funding: PID2019–104953RB-I00 Project, the Junta de Andalucía and FEDER funds (P18-RT-4822), and UCO-FEDER (1264113-RMINECO-ENE2016-81013-R (AEI/FEDER, EU).

Acknowledgments: The authors are thankful to the Spanish MICINN through the PID2019–104953RB-I00 Project, the Junta de Andalucía and FEDER funds (P18-RT-4822), and UCO-FEDER (1264113-RMINECO-ENE2016-81013-R (AEI/FEDER, EU)). R. Estevez and L. Aguado-Deblas are indebted to the Junta de Andalucía for the contract associated to the P18-RT-4822 Project. The authors are also thankful to the "Instituto Químico para la Energía y el Medioambiente (IQUEMA)" for technical assistance.

Conflicts of Interest: The authors declare no conflict of interest.

References

1. Zheng, X.; Streimikiene, D.; Balezentis, T.; Mardani, A.; Cavallaro, F.; Liao, H. A review of greenhouse gas emission profiles, dynamics, and climate change mitigation efforts across the key climate change players. *J. Clean. Prod.* **2019**, *234*, 1113–1133. [CrossRef]
2. Teske, S.; Giurco, D.; Morris, T.; Nagrath, K.; Mey, F.; Briggs, C.; Dominish, E.; Florin, N. *Achieving the Paris Climate Agreement Goals: Global and Regional 100% Renewable Energy Scenarios to Achieve the Paris Agreement Goals with Non-Energy GHG Pathways for +1.5 °C and +2 °C*; Springer: Berlin/Heidelberg, Germany, 2019.
3. Hospital-Benito, D.; Lemus, J.; Moya, C.; Santiago, R.; Palomar, J. Process analysis overview of ionic liquids on CO_2 chemical capture. *Chem. Eng. J.* **2020**, *390*, 124509. [CrossRef]
4. Anwar, M.; Fayyaz, A.; Sohail, N.; Khokhar, M.; Baqar, M.; Yasar, A.; Rasool, K.; Nazir, A.; Raja, M.; Rehan, M. CO_2 utilization: Turning greenhouse gas into fuels and valuable products. *J. Environ. Manag.* **2020**, *260*, 110059. [CrossRef] [PubMed]
5. Kleij, A.W.; North, M.; Urakawa, A. *CO_2 Catalysis*; Wiley Online Library: New York, NY, USA, 2017; Volume 10, pp. 1036–1038.
6. Sahoo, P.K.; Zhang, Y.; Das, S. CO_2-promoted reactions: An emerging concept for the synthesis of fine chemicals and pharmaceuticals. *ACS Catal.* **2021**, *11*, 3414–3442. [CrossRef]
7. Zahed, M.A.; Movahed, E.; Khodayari, A.; Zanganeh, S.; Badamaki, M. Biotechnology for carbon capture and fixation: Critical review and future directions. *J. Environ. Manag.* **2021**, *293*, 112830. [CrossRef]
8. Chauvy, R.; Meunier, N.; Thomas, D.; De Weireld, G. Selecting emerging CO_2 utilization products for short-to mid-term deployment. *Appl. Energy* **2019**, *236*, 662–680. [CrossRef]
9. Yan, M.; Kawamata, Y.; Baran, P.S. Synthetic organic electrochemical methods since 2000: On the verge of a renaissance. *Chem. Rev.* **2017**, *117*, 13230–13319. [CrossRef]
10. Roy, S.; Cherevotan, A.; Peter, S. Thermochemical CO_2 hydrogenation to single carbon products: Scientific and technological challenges. *ACS Energy Lett.* **2018**, *3*, 1938–1966. [CrossRef]
11. Alper, E.; Orhan, O.Y. CO_2 utilization: Developments in conversion processes. *Petroleum* **2017**, *3*, 109–126. [CrossRef]
12. Sun, Y.; Lin, Z.; Peng, S.H.; Sage, V.; Sun, Z. A critical perspective on CO_2 conversions into chemicals and fuels. *J. Nanosci. Nanotechnol.* **2019**, *19*, 3097–3109. [CrossRef]

13. Mustafa, A.; Lougou, B.G.; Shuai, Y.; Wang, Z.; Tan, H. Current technology development for CO_2 utilization into solar fuels and chemicals: A review. *J. Energy Chem.* **2020**, *49*, 96–123. [CrossRef]
14. Potrč, S.; Čuček, L.; Martin, M.; Kravanja, Z. Sustainable renewable energy supply networks optimization–The gradual transition to a renewable energy system within the European Union by 2050. *Renew. Sustain. Energy Rev.* **2021**, *146*, 111186. [CrossRef]
15. Southall, E.; Lukashuk, L. Analysis of Liquid Organic Hydrogen Carrier Systems. *Johns. Matthey Technol. Rev.* **2022**, *66*, 271–284. [CrossRef]
16. Safari, A.; Roy, J.; Assadi, M. Petroleum Sector-Driven Roadmap for Future Hydrogen Economy. *Appl. Sci.* **2021**, *11*, 10389. [CrossRef]
17. Gao, R.; Zhang, C.; Jun, K.-W.; Kim, S.K.; Park, H.-G.; Zhao, T.; Wang, L.; Wan, H.; Guan, G. Transformation of CO_2 into liquid fuels and synthetic natural gas using green hydrogen: A comparative analysis. *Fuel* **2021**, *291*, 120111. [CrossRef]
18. Chen, C.-Y.; Yu, J.C.-C.; Nguyen, V.-H.; Wu, J.C.-S.; Wang, W.-H.; Kočí, K. Reactor design for CO_2 photo-hydrogenation toward solar fuels under ambient temperature and pressure. *Catalysts* **2017**, *7*, 63. [CrossRef]
19. Martino, M.; Ruocco, C.; Meloni, E.; Pullumbi, P.; Palma, V. Main hydrogen production processes: An overview. *Catalysts* **2021**, *11*, 547. [CrossRef]
20. Hong, X.; Thaore, V.B.; Karimi, I.A.; Farooq, S.; Wang, X.; Usadi, A.K.; Chapman, B.R.; Johnson, R.A. Techno-enviro-economic analyses of hydrogen supply chains with an ASEAN case study. *Int. J. Hydrogen Energy* **2021**, *46*, 32914–32928. [CrossRef]
21. Cannone, S.F.; Lanzini, A.; Santarelli, M. A review on CO_2 capture technologies with focus on CO_2-enhanced methane recovery from hydrates. *Energies* **2021**, *14*, 387. [CrossRef]
22. Kumar, M.; Sundaram, S.; Gnansounou, E.; Larroche, C.; Thakur, I.S. Carbon dioxide capture, storage and production of biofuel and biomaterials by bacteria: A review. *Bioresour. Technol.* **2018**, *247*, 1059–1068. [CrossRef]
23. Sifat, N.S.; Haseli, Y. A critical review of CO_2 capture technologies and prospects for clean power generation. *Energies* **2019**, *12*, 4143. [CrossRef]
24. Xu, D.; Li, W.; Ren, X.; Shen, W.; Dong, L. Technology selection for sustainable hydrogen production: A multi-criteria assessment framework under uncertainties based on the combined weights and interval best-worst projection method. *Int. J. Hydrogen Energy* **2020**, *45*, 34396–34411. [CrossRef]
25. Catalan, L.J.; Rezaei, E. Coupled hydrodynamic and kinetic model of liquid metal bubble reactor for hydrogen production by noncatalytic thermal decomposition of methane. *Int. J. Hydrogen Energy* **2020**, *45*, 2486–2503. [CrossRef]
26. Wang, L.; Wang, L.; Zhang, J.; Liu, X.; Wang, H.; Zhang, W.; Yang, Q.; Ma, J.; Dong, X.; Yoo, S.J. Selective hydrogenation of CO_2 to ethanol over cobalt catalysts. *Angew. Chem. Int. Ed.* **2018**, *57*, 6104–6108. [CrossRef]
27. Liu, S.; Chen, H.; Zhang, X. Bifunctional {Pb10K2}–Organic Framework for High Catalytic Activity in Cycloaddition of CO_2 with Epoxides and Knoevenagel Condensation. *ACS Catal.* **2022**, *12*, 10373–10383. [CrossRef]
28. Lv, H.; Chen, H.; Fan, L.; Zhang, X. Nanocage-Based Tb3+-Organic Framework for Efficiently Catalyzing the Cycloaddition Reaction of CO_2 with Epoxides and Knoevenagel Condensation. *Inorg. Chem.* **2022**, *61*, 15558–15568. [CrossRef]
29. Ni, Y.; Chen, Z.; Fu, Y.; Liu, Y.; Zhu, W.; Liu, Z. Selective conversion of CO_2 and H2 into aromatics. *Nat. Commun.* **2018**, *9*, 3457. [CrossRef]
30. Wang, Y.; Tan, L.; Tan, M.; Zhang, P.; Fang, Y.; Yoneyama, Y.; Yang, G.; Tsubaki, N. Rationally designing bifunctional catalysts as an efficient strategy to boost CO_2 hydrogenation producing value-added aromatics. *ACS Catal.* **2018**, *9*, 895–901. [CrossRef]
31. Wang, W.; Wang, S.; Ma, X.; Gong, J. Recent advances in catalytic hydrogenation of carbon dioxide. *Chem. Soc. Rev.* **2011**, *40*, 3703–3727. [CrossRef]
32. Lonis, F.; Tola, V.; Cau, G. Renewable methanol production and use through reversible solid oxide cells and recycled CO_2 hydrogenation. *Fuel* **2019**, *246*, 500–515. [CrossRef]
33. Vogt, C.; Monai, M.; Kramer, G.J.; Weckhuysen, B.M. The renaissance of the Sabatier reaction and its applications on Earth and in space. *Nat. Catal.* **2019**, *2*, 188–197. [CrossRef]
34. Alarcón, A.; Guilera, J.; Díaz, J.A.; Andreu, T. Optimization of nickel and ceria catalyst content for synthetic natural gas production through CO_2 methanation. *Fuel Process. Technol.* **2019**, *193*, 114–122. [CrossRef]
35. Lee, W.J.; Li, C.; Prajitno, H.; Yoo, J.; Patel, J.; Yang, Y.; Lim, S. Recent trend in thermal catalytic low temperature CO_2 methanation: A critical review. *Catal. Today* **2021**, *368*, 2–19. [CrossRef]
36. Frontera, P.; Macario, A.; Ferraro, M.; Antonucci, P. Supported catalysts for CO_2 methanation: A review. *Catalysts* **2017**, *7*, 59. [CrossRef]
37. Ashok, J.; Pati, S.; Hongmanorom, P.; Tianxi, Z.; Junmei, C.; Kawi, S. A review of recent catalyst advances in CO_2 methanation processes. *Catal. Today* **2020**, *356*, 471–489. [CrossRef]
38. Fan, W.K.; Tahir, M. Recent trends in developments of active metals and heterogenous materials for catalytic CO_2 hydrogenation to renewable methane: A review. *J. Environ. Chem. Eng.* **2021**, *9*, 105460. [CrossRef]
39. Tada, S.; Nagase, H.; Fujiwara, N.; Kikuchi, R. What are the best active sites for CO_2 methanation over Ni/CeO_2? *Energy Fuels* **2021**, *35*, 5241–5251. [CrossRef]
40. Hu, F.; Ye, R.; Lu, Z.-H.; Zhang, R.; Feng, G. Structure–Activity Relationship of Ni-Based Catalysts toward CO_2 Methanation: Recent Advances and Future Perspectives. *Energy Fuels* **2022**, *36*, 1–156. [CrossRef]
41. Mohd Ridzuan, N.D.; Shaharun, M.S.; Anawar, M.A.; Ud-Din, I. Ni-Based Catalyst for Carbon Dioxide Methanation: A Review on Performance and Progress. *Catalysts* **2022**, *12*, 469. [CrossRef]

42. Italiano, C.; Llorca, J.; Pino, L.; Ferraro, M.; Antonucci, V.; Vita, A. CO and CO_2 methanation over Ni catalysts supported on CeO_2, Al2O3 and Y2O3 oxides. *Appl. Catal. B Environ.* **2020**, *264*, 118494. [CrossRef]
43. Feng, F.; Song, G.; Xiao, J.; Shen, L.; Pisupati, S.V. Carbon deposition on Ni-based catalyst with TiO_2 as additive during the syngas methanation process in a fluidized bed reactor. *Fuel* **2019**, *235*, 85–91. [CrossRef]
44. Alrafei, B.; Polaert, I.; Ledoux, A.; Azzolina-Jury, F. Remarkably stable and efficient Ni and Ni-Co catalysts for CO_2 methanation. *Catal. Today* **2020**, *346*, 23–33. [CrossRef]
45. Champon, I.; Bengaouer, A.; Chaise, A.; Thomas, S.; Roger, A.-C. Carbon dioxide methanation kinetic model on a commercial Ni/Al2O3 catalyst. *J. CO2 Util.* **2019**, *34*, 256–265. [CrossRef]
46. Garbarino, G.; Wang, C.; Cavattoni, T.; Finocchio, E.; Riani, P.; Flytzani-Stephanopoulos, M.; Busca, G. A study of Ni/La-Al2O3 catalysts: A competitive system for CO_2 methanation. *Appl. Catal. B Environ.* **2019**, *248*, 286–297. [CrossRef]
47. Liu, S.-S.; Jin, Y.-Y.; Han, Y.; Zhao, J.; Ren, J. Highly stable and coking resistant Ce promoted Ni/SiC catalyst towards high temperature CO methanation. *Fuel Process. Technol.* **2018**, *177*, 266–274. [CrossRef]
48. Beierlein, D.; Haeussermann, D.; Pfeifer, M.; Schwarz, T.; Stoewe, K.; Traa, Y.; Klemm, E. Is the CO_2 methanation on highly loaded Ni-Al2O3 catalysts really structure-sensitive? *Appl. Catal. B Environ.* **2019**, *247*, 200–219. [CrossRef]
49. Ashok, J.; Ang, M.; Kawi, S. Enhanced activity of CO_2 methanation over Ni/CeO_2-ZrO_2 catalysts: Influence of preparation methods. *Catal. Today* **2017**, *281*, 304–311. [CrossRef]
50. Zhang, T.; Liu, Q. Lanthanum-modified MCF-derived nickel phyllosilicate catalyst for enhanced CO_2 methanation: A comprehensive study. *ACS Appl. Mater. Interfaces* **2020**, *12*, 19587–19600. [CrossRef]
51. Mebrahtu, C.; Abate, S.; Perathoner, S.; Chen, S.; Centi, G. CO_2 methanation over Ni catalysts based on ternary and quaternary mixed oxide: A comparison and analysis of the structure-activity relationships. *Catal. Today* **2018**, *304*, 181–189. [CrossRef]
52. Romero-Sáez, M.D.; Dongil, A.B.; Benito, N.; Espinoza-González, R.; Escalona, N.; Gracia, F. CO_2 methanation over nickel-ZrO_2 catalyst supported on carbon nanotubes: A comparison between two impregnation strategies. *Appl. Catal. B Environ.* **2018**, *237*, 817–825. [CrossRef]
53. Li, L.; Zeng, W.; Song, M.; Wu, X.; Li, G.; Hu, C. Research Progress and Reaction Mechanism of CO_2 Methanation over Ni-Based Catalysts at Low Temperature: A Review. *Catalysts* **2022**, *12*, 244. [CrossRef]
54. Lv, C.; Xu, L.; Chen, M.; Cui, Y.; Wen, X.; Li, Y.; Wu, C.-E.; Yang, B.; Miao, Z.; Hu, X. Recent progresses in constructing the highly efficient Ni based catalysts with advanced low-temperature activity toward CO_2 methanation. *Front. Chem.* **2020**, *8*, 269. [CrossRef] [PubMed]
55. Ho, P.H.; de Luna, G.S.; Angelucci, S.; Canciani, A.; Jones, W.; Decarolis, D.; Ospitali, F.; Aguado, E.R.; Rodríguez-Castellón, E.; Fornasari, G. Understanding structure-activity relationships in highly active La promoted Ni catalysts for CO_2 methanation. *Appl. Catal. B Environ.* **2020**, *278*, 119256. [CrossRef]
56. Liang, C.; Hu, X.; Wei, T.; Jia, P.; Zhang, Z.; Dong, D.; Zhang, S.; Liu, Q.; Hu, G. Methanation of CO_2 over Ni/Al2O3 modified with alkaline earth metals: Impacts of oxygen vacancies on catalytic activity. *Int. J. Hydrogen Energy* **2019**, *44*, 8197–8213. [CrossRef]
57. Lin, J.; Ma, C.; Wang, Q.; Xu, Y.; Ma, G.; Wang, J.; Wang, H.; Dong, C.; Zhang, C.; Ding, M. Enhanced low-temperature performance of CO_2 methanation over mesoporous Ni/Al_2O_3-ZrO_2 catalysts. *Appl. Catal. B Environ.* **2019**, *243*, 262–272. [CrossRef]
58. Sreedhar, I.; Varun, Y.; Singh, S.A.; Venugopal, A.; Reddy, B.M. Developmental trends in CO_2 methanation using various catalysts. *Catal. Sci. Technol.* **2019**, *9*, 4478–4504. [CrossRef]
59. Ye, R.-P.; Ding, J.; Gong, W.; Argyle, M.D.; Zhong, Q.; Wang, Y.; Russell, C.K.; Xu, Z.; Russell, A.G.; Li, Q. CO_2 hydrogenation to high-value products via heterogeneous catalysis. *Nat. Commun.* **2019**, *10*, 5698. [CrossRef]
60. Quindimil, A.; De-La-Torre, U.; Pereda-Ayo, B.; Davó-Quiñonero, A.; Bailón-García, E.; Lozano-Castello, D.; González-Marcos, J.A.; Bueno-López, A.; González-Velasco, J.R. Effect of metal loading on the CO_2 methanation: A comparison between alumina supported Ni and Ru catalysts. *Catal. Today* **2020**, *356*, 419–432. [CrossRef]
61. Chein, R.-Y.; Wang, C.-C. Experimental Study on CO_2 Methanation over Ni/Al_2O_3, Ru/Al_2O_3, and Ru-Ni/Al_2O_3 Catalysts. *Catalysts* **2020**, *10*, 1112. [CrossRef]
62. Tsiotsias, A.I.; Charisiou, N.D.; Yentekakis, I.V.; Goula, M.A. Bimetallic Ni-based catalysts for CO_2 methanation: A review. *Nanomaterials* **2020**, *11*, 28. [CrossRef]
63. Polanski, J.; Lach, D.; Kapkowski, M.; Bartczak, P.; Siudyga, T.; Smolinski, A. Ru and Ni—Privileged Metal Combination for Environmental Nanocatalysis. *Catalysts* **2020**, *10*, 992. [CrossRef]
64. Guilera, J.; del Valle, J.; Alarcón, A.; Díaz, J.A.; Andreu, T. Metal-oxide promoted Ni/Al2O3 as CO_2 methanation micro-size catalysts. *J. CO2 Util.* **2019**, *30*, 11–17. [CrossRef]
65. Baysal, Z.; Kureti, S. CO_2 methanation on Mg-promoted Fe catalysts. *Appl. Catal. B Environ.* **2020**, *262*, 118300. [CrossRef]
66. Abdel-Mageed, A.M.; Wiese, K.; Parlinska-Wojtan, M.; Rabeah, J.; Brückner, A.; Behm, R.J. Encapsulation of Ru nanoparticles: Modifying the reactivity toward CO and CO_2 methanation on highly active Ru/TiO_2 catalysts. *Appl. Catal. B Environ.* **2020**, *270*, 118846. [CrossRef]
67. Dreyer, J.A.; Li, P.; Zhang, L.; Beh, G.K.; Zhang, R.; Sit, P.H.-L.; Teoh, W.Y. Influence of the oxide support reducibility on the CO_2 methanation over Ru-based catalysts. *Appl. Catal. B Environ.* **2017**, *219*, 715–726. [CrossRef]
68. Vrijburg, W.L.; Moioli, E.; Chen, W.; Zhang, M.; Terlingen, B.J.; Zijlstra, B.; Filot, I.A.; Züttel, A.; Pidko, E.A.; Hensen, E.J. Efficient base-metal NiMn/TiO_2 catalyst for CO_2 methanation. *Acs Catal.* **2019**, *9*, 7823–7839. [CrossRef]

69. Jia, X.; Zhang, X.; Rui, N.; Hu, X.; Liu, C.-J. Structural effect of Ni/ZrO_2 catalyst on CO_2 methanation with enhanced activity. *Appl. Catal. B Environ.* **2019**, *244*, 159–169. [CrossRef]
70. Liu, Q.; Wang, S.; Zhao, G.; Yang, H.; Yuan, M.; An, X.; Zhou, H.; Qiao, Y.; Tian, Y. CO_2 methanation over ordered mesoporous NiRu-doped CaO-Al_2O_3 nanocomposites with enhanced catalytic performance. *Int. J. Hydrogen Energy* **2018**, *43*, 239–250. [CrossRef]
71. Ewald, S.; Kolbeck, M.; Kratky, T.; Wolf, M.; Hinrichsen, O. On the deactivation of Ni-Al catalysts in CO_2 methanation. *Appl. Catal. A Gen.* **2019**, *570*, 376–386. [CrossRef]
72. Men, Y.; Fang, X.; Gu, Q.; Singh, R.; Wu, F.; Danaci, D.; Zhao, Q.; Xiao, P.; Webley, P.A. Synthesis of Ni_5Ga_3 catalyst by Hydrotalcite-like compound (HTlc) precursors for CO_2 hydrogenation to methanol. *Appl. Catal. B Environ.* **2020**, *275*, 119067. [CrossRef]
73. Ricca, A.; Truda, L.; Palma, V. Study of the role of chemical support and structured carrier on the CO_2 methanation reaction. *Chem. Eng. J.* **2019**, *377*, 120461. [CrossRef]
74. Vita, A.; Italiano, C.; Pino, L.; Laganà, M.; Ferraro, M.; Antonucci, V. High-temperature CO_2 methanation over structured Ni/GDC catalysts: Performance and scale-up for Power-to-Gas application. *Fuel Process. Technol.* **2020**, *202*, 106365. [CrossRef]
75. Shen, L.; Xu, J.; Zhu, M.; Han, Y.-F. Essential role of the support for nickel-based CO_2 methanation catalysts. *ACS Catal.* **2020**, *10*, 14581–14591. [CrossRef]
76. Gac, W.; Zawadzki, W.; Rotko, M.; Greluk, M.; Słowik, G.; Kolb, G. Effects of support composition on the performance of nickel catalysts in CO_2 methanation reaction. *Catal. Today* **2020**, *357*, 468–482. [CrossRef]
77. Siakavelas, G.I.; Charisiou, N.D.; AlKhoori, S.; AlKhoori, A.A.; Sebastian, V.; Hinder, S.J.; Baker, M.A.; Yentekakis, I.; Polychronopoulou, K.; Goula, M.A. Highly selective and stable nickel catalysts supported on ceria promoted with Sm_2O_3, Pr_2O_3 and MgO for the CO_2 methanation reaction. *Appl. Catal. B Environ.* **2021**, *282*, 119562. [CrossRef]
78. Xie, Y.; Chen, J.; Wu, X.; Wen, J.; Zhao, R.; Li, Z.; Tian, G.; Zhang, Q.; Ning, P.; Hao, J. Frustrated Lewis Pairs Boosting Low-Temperature CO_2 Methanation Performance over Ni/CeO_2 Nanocatalysts. *ACS Catal.* **2022**, *12*, 10587–10602. [CrossRef]
79. Ye, R.-P.; Li, Q.; Gong, W.; Wang, T.; Razink, J.J.; Lin, L.; Qin, Y.-Y.; Zhou, Z.; Adidharma, H.; Tang, J. High-performance of nanostructured Ni/CeO_2 catalyst on CO_2 methanation. *Appl. Catal. B Environ.* **2020**, *268*, 118474. [CrossRef]
80. Cerda-Moreno, C.; Chica, A.; Keller, S.; Rautenberg, C.; Bentrup, U. Ni-sepiolite and Ni-todorokite as efficient CO_2 methanation catalysts: Mechanistic insight by operando DRIFTS. *Appl. Catal. B Environ.* **2020**, *264*, 118546. [CrossRef]
81. Miao, C.; Shang, K.; Liang, L.; Chen, S.; Ouyang, J. Efficient and Stable Ni/ZSM-5@ MCM-41 Catalyst for CO_2 Methanation. *ACS Sustain. Chem. Eng.* **2022**, *10*, 12771–12782. [CrossRef]
82. Zhang, L.; Bian, L.; Zhu, Z.; Li, Z. La-promoted Ni/Mg-Al catalysts with highly enhanced low-temperature CO_2 methanation performance. *Int. J. Hydrogen Energy* **2018**, *43*, 2197–2206. [CrossRef]
83. Cárdenas-Arenas, A.; Quindimil, A.; Davó-Quiñonero, A.; Bailón-García, E.; Lozano-Castello, D.; De-La-Torre, U.; Pereda-Ayo, B.; González-Marcos, J.A.; González-Velasco, J.R.; Bueno-López, A. Isotopic and in situ DRIFTS study of the CO_2 methanation mechanism using Ni/CeO_2 and Ni/Al_2O_3 catalysts. *Appl. Catal. B Environ.* **2020**, *265*, 118538. [CrossRef]
84. Bobadilla, L.; Garcilaso, V.; Centeno, M.; Odriozola, J. CO_2 reforming of methane over Ni-Ru supported catalysts: On the nature of active sites by operando DRIFTS study. *J. CO2 Util.* **2018**, *24*, 509–515.
85. Renda, S.; Ricca, A.; Palma, V. Study of the effect of noble metal promotion in Ni-based catalyst for the Sabatier reaction. *Int. J. Hydrogen Energy* **2021**, *46*, 12117–12127. [CrossRef]
86. Renda, S.; Ricca, A.; Palma, V. Precursor salts influence in Ruthenium catalysts for CO_2 hydrogenation to methane. *Appl. Energy* **2020**, *279*, 115767. [CrossRef]
87. Navarro, J.C.; Centeno, M.A.; Laguna, O.H.; Odriozola, J.A. Ru–Ni/$MgAl_2O_4$ structured catalyst for CO_2 methanation. *Renew. Energy* **2020**, *161*, 120–132. [CrossRef]
88. Salomone, F.; Giglio, E.; Ferrero, D.; Santarelli, M.; Pirone, R.; Bensaid, S. Techno-economic modelling of a Power-to-Gas system based on SOEC electrolysis and CO_2 methanation in a RES-based electric grid. *Chem. Eng. J.* **2019**, *377*, 120233. [CrossRef]
89. Mebrahtu, C.; Nohl, M.; Dittrich, L.; Foit, S.R.; de Haart, L.; Eichel, R.A.; Palkovits, R. Integrated Co-Electrolysis and Syngas Methanation for the Direct Production of Synthetic Natural Gas from CO_2 and H_2O. *ChemSusChem* **2021**, *14*, 2295–2302. [CrossRef]
90. Gorre, J.; Ruoss, F.; Karjunen, H.; Schaffert, J.; Tynjälä, T. Cost benefits of optimizing hydrogen storage and methanation capacities for Power-to-Gas plants in dynamic operation. *Appl. Energy* **2020**, *257*, 113967. [CrossRef]
91. Inkeri, E.; Tynjälä, T.; Karjunen, H. Significance of methanation reactor dynamics on the annual efficiency of power-to-gas-system. *Renew. Energy* **2021**, *163*, 1113–1126. [CrossRef]
92. Park, S.; Choi, K.; Lee, C.; Kim, S.; Yoo, Y.; Chang, D. Techno-economic analysis of adiabatic four-stage CO_2 methanation process for optimization and evaluation of power-to-gas technology. *Int. J. Hydrogen Energy* **2021**, *46*, 21303–21317. [CrossRef]
93. Skorek-Osikowska, A. Thermodynamic and environmental study on synthetic natural gas production in power to gas approaches involving biomass gasification and anaerobic digestion. *Int. J. Hydrogen Energy* **2022**, *47*, 3284–3293. [CrossRef]
94. Straka, P. A comprehensive study of Power-to-Gas technology: Technical implementations overview, economic assessments, methanation plant as auxiliary operation of lignite-fired power station. *J. Clean. Prod.* **2021**, *311*, 127642. [CrossRef]
95. Fuentes, I.; Gracia, F. Fluid dynamic analytical model of CO_2 methanation in a microreactor with potential application in Power-to-Gas technology. *Chem. Eng. Sci.* **2022**, *251*, 117465. [CrossRef]

96. Giglio, E.; Pirone, R.; Bensaid, S. Dynamic modelling of methanation reactors during start-up and regulation in intermittent power-to-gas applications. *Renew. Energy* **2021**, *170*, 1040–1051. [CrossRef]
97. Bailera, M.; Peña, B.; Lisbona, P.; Marín, J.; Romeo, L.M. Lab-scale experimental tests of power to gas-oxycombustion hybridization: System design and preliminary results. *Energy* **2021**, *226*, 120375. [CrossRef]
98. Jensen, M.; Ottosen, L.; Kofoed, M. H_2 gas-liquid mass transfer: A key element in biological Power-to-Gas methanation. *Renew. Sustain. Energy Rev.* **2021**, *147*, 111209. [CrossRef]
99. Hodges, A.; Hoang, A.L.; Tsekouras, G.; Wagner, K.; Lee, C.-Y.; Swiegers, G.F.; Wallace, G.G. A high-performance capillary-fed electrolysis cell promises more cost-competitive renewable hydrogen. *Nat. Commun.* **2022**, *13*, 1304. [CrossRef]
100. Catizzone, E.; Bonura, G.; Migliori, M.; Frusteri, F.; Giordano, G. CO_2 recycling to dimethyl ether: State-of-the-art and perspectives. *Molecules* **2018**, *23*, 31. [CrossRef]
101. Dieterich, V.; Buttler, A.; Hanel, A.; Spliethoff, H.; Fendt, S. Power-to-liquid via synthesis of methanol, DME or Fischer–Tropsch-fuels: A review. *Energy Environ. Sci.* **2020**, *13*, 3207–3252. [CrossRef]
102. Andersson, J.; Grönkvist, S. Large-scale storage of hydrogen. *Int. J. Hydrogen Energy* **2019**, *44*, 11901–11919. [CrossRef]
103. Sarp, S.; Hernandez, S.G.; Chen, C.; Sheehan, S.W. Alcohol production from carbon dioxide: Methanol as a fuel and chemical feedstock. *Joule* **2021**, *5*, 59–76. [CrossRef]
104. Lee, B.; Lee, H.; Lim, D.; Brigljević, B.; Cho, W.; Cho, H.-S.; Kim, C.-H.; Lim, H. Renewable methanol synthesis from renewable H2 and captured CO_2: How can power-to-liquid technology be economically feasible? *Appl. Energy* **2020**, *279*, 115827. [CrossRef]
105. Bowker, M. Methanol synthesis from CO_2 hydrogenation. *ChemCatChem* **2019**, *11*, 4238–4246. [CrossRef]
106. Simon Araya, S.; Liso, V.; Cui, X.; Li, N.; Zhu, J.; Sahlin, S.L.; Jensen, S.H.; Nielsen, M.P.; Kær, S.K. A review of the methanol economy: The fuel cell route. *Energies* **2020**, *13*, 596. [CrossRef]
107. Ren, M.; Zhang, Y.; Wang, X.; Qiu, H. Catalytic Hydrogenation of CO_2 to Methanol: A Review. *Catalysts* **2022**, *12*, 403. [CrossRef]
108. Guil-López, R.; Mota, N.; Llorente, J.; Millán, E.; Pawelec, B.; Fierro, J.L.G.; Navarro, R. Methanol synthesis from CO_2: A review of the latest developments in heterogeneous catalysis. *Materials* **2019**, *12*, 3902. [CrossRef] [PubMed]
109. Laudenschleger, D.; Ruland, H.; Muhler, M. Identifying the nature of the active sites in methanol synthesis over $Cu/ZnO/Al_2O_3$ catalysts. *Nat. Commun.* **2020**, *11*, 3898. [CrossRef] [PubMed]
110. Dang, S.; Yang, H.; Gao, P.; Wang, H.; Li, X.; Wei, W.; Sun, Y. A review of research progress on heterogeneous catalysts for methanol synthesis from carbon dioxide hydrogenation. *Catal. Today* **2019**, *330*, 61–75. [CrossRef]
111. Jiang, X.; Nie, X.; Guo, X.; Song, C.; Chen, J.G. Recent advances in carbon dioxide hydrogenation to methanol via heterogeneous catalysis. *Chem. Rev.* **2020**, *120*, 7984–8034. [CrossRef]
112. Zhong, J.; Yang, X.; Wu, Z.; Liang, B.; Huang, Y.; Zhang, T. State of the art and perspectives in heterogeneous catalysis of CO_2 hydrogenation to methanol. *Chem. Soc. Rev.* **2020**, *49*, 1385–1413. [CrossRef]
113. Marcos, F.C.; Cavalcanti, F.M.; Petrolini, D.D.; Lin, L.; Betancourt, L.E.; Senanayake, S.D.; Rodriguez, J.A.; Assaf, J.M.; Giudici, R.; Assaf, E.M. Effect of operating parameters on H_2/CO_2 conversion to methanol over Cu-Zn oxide supported on ZrO_2 polymorph catalysts: Characterization and kinetics. *Chem. Eng. J.* **2022**, *427*, 130947. [CrossRef]
114. Cui, Z.; Meng, S.; Yi, Y.; Jafarzadeh, A.; Li, S.; Neyts, E.C.; Hao, Y.; Li, L.; Zhang, X.; Wang, X. Plasma-Catalytic Methanol Synthesis from CO_2 Hydrogenation over a Supported Cu Cluster Catalyst: Insights into the Reaction Mechanism. *ACS Catal.* **2022**, *12*, 1326–1337. [CrossRef]
115. Zhang, G.; Liu, M.; Fan, G.; Zheng, L.; Li, F. Efficient Role of Nanosheet-Like Pr_2O_3 Induced Surface-Interface Synergistic Structures over Cu-Based Catalysts for Enhanced Methanol Production from CO_2 Hydrogenation. *ACS Appl. Mater. Interfaces* **2022**, *14*, 2768–2781. [CrossRef] [PubMed]
116. Murthy, P.S.; Liang, W.; Jiang, Y.; Huang, J. Cu-Based Nanocatalysts for CO_2 hydrogenation to methanol. *Energy Fuels* **2021**, *35*, 8558–8584. [CrossRef]
117. Wang, Y.; Kattel, S.; Gao, W.; Li, K.; Liu, P.; Chen, J.G.; Wang, H. Exploring the ternary interactions in $Cu–ZnO–ZrO_2$ catalysts for efficient CO_2 hydrogenation to methanol. *Nat. Commun.* **2019**, *10*, 1166. [CrossRef]
118. Huang, C.; Wen, J.; Sun, Y.; Zhang, M.; Bao, Y.; Zhang, Y.; Liang, L.; Fu, M.; Wu, J.; Ye, D. CO_2 hydrogenation to methanol over Cu/ZnO plate model catalyst: Effects of reducing gas induced Cu nanoparticle morphology. *Chem. Eng. J.* **2019**, *374*, 221–230. [CrossRef]
119. Tada, S.; Otsuka, F.; Fujiwara, K.; Moularas, C.; Deligiannakis, Y.; Kinoshita, Y.; Uchida, S.; Honma, T.; Nishijima, M.; Kikuchi, R. Development of CO_2-to-Methanol Hydrogenation Catalyst by Focusing on the Coordination Structure of the Cu Species in Spinel-Type Oxide $Mg_{1-x}Cu_xAl_2O_4$. *ACS Catal.* **2020**, *10*, 15186–15194. [CrossRef]
120. Wang, H.; Zhang, G.; Fan, G.; Yang, L.; Li, F. Fabrication of Zr–Ce Oxide Solid Solution Surrounded Cu-Based Catalyst Assisted by a Microliquid Film Reactor for Efficient CO_2 Hydrogenation to Produce Methanol. *Ind. Eng. Chem. Res.* **2021**, *60*, 16188–16200. [CrossRef]
121. Yu, J.; Yang, M.; Zhang, J.; Ge, Q.; Zimina, A.; Pruessmann, T.; Zheng, L.; Grunwaldt, J.-D.; Sun, J. Stabilizing Cu+ in Cu/SiO_2 catalysts with a shattuckite-like structure boosts CO_2 hydrogenation into methanol. *ACS Catal.* **2020**, *10*, 14694–14706. [CrossRef]
122. Chen, H.; Cui, H.; Lv, Y.; Liu, P.; Hao, F.; Xiong, W. CO_2 hydrogenation to methanol over $Cu/ZnO/ZrO_2$ catalysts: Effects of ZnO morphology and oxygen vacancy. *Fuel* **2022**, *314*, 123035. [CrossRef]
123. Cui, W.-G.; Li, Y.-T.; Yu, L.; Zhang, H.; Hu, T.-L. Zeolite-Encapsulated Ultrasmall Cu/ZnOx Nanoparticles for the Hydrogenation of CO_2 to Methanol. *ACS Appl. Mater. Interfaces* **2021**, *13*, 18693–18703. [CrossRef] [PubMed]

124. Tada, S.; Fujiwara, K.; Yamamura, T.; Nishijima, M.; Uchida, S.; Kikuchi, R. Flame spray pyrolysis makes highly loaded Cu nanoparticles on ZrO_2 for CO_2-to-methanol hydrogenation. *Chem. Eng. J.* **2020**, *381*, 122750. [CrossRef]
125. Dasireddy, V.D.; Neja, S.Š.; Blaž, L. Correlation between synthesis pH, structure and $Cu/MgO/Al_2O_3$ heterogeneous catalyst activity and selectivity in CO_2 hydrogenation to methanol. *J. CO2 Util.* **2018**, *28*, 189–199. [CrossRef]
126. Dasireddy, V.D.; Likozar, B. The role of copper oxidation state in Cu/ZnO/Al2O3 catalysts in CO_2 hydrogenation and methanol productivity. *Renew. Energy* **2019**, *140*, 452–460. [CrossRef]
127. Noh, G.; Lam, E.; Alfke, J.L.; Larmier, K.; Searles, K.; Wolf, P.; Copéret, C. Selective hydrogenation of CO_2 to CH_3OH on supported Cu nanoparticles promoted by isolated TiIV surface sites on SiO_2. *ChemSusChem* **2019**, *12*, 968–972. [CrossRef] [PubMed]
128. Lam, E.; Noh, G.; Larmier, K.; Safonova, O.V.; Copéret, C. CO_2 hydrogenation on Cu-catalysts generated from ZnII single-sites: Enhanced CH3OH selectivity compared to $Cu/ZnO/Al_2O_3$. *J. Catal.* **2021**, *394*, 266–272. [CrossRef]
129. Fang, X.; Men, Y.; Wu, F.; Zhao, Q.; Singh, R.; Xiao, P.; Du, T.; Webley, P.A. Improved methanol yield and selectivity from CO_2 hydrogenation using a novel Cu-ZnO-ZrO_2 catalyst supported on Mg-Al layered double hydroxide (LDH). *J. CO2 Util.* **2019**, *29*, 57–64. [CrossRef]
130. Koh, M.K.; Khavarian, M.; Chai, S.P.; Mohamed, A.R. The morphological impact of siliceous porous carriers on copper-catalysts for selective direct CO_2 hydrogenation to methanol. *Int. J. Hydrogen Energy* **2018**, *43*, 9334–9342. [CrossRef]
131. Lei, H.; Zheng, R.; Liu, Y.; Gao, J.; Chen, X.; Feng, X. Cylindrical shaped ZnO combined Cu catalysts for the hydrogenation of CO_2 to methanol. *RSC Adv.* **2019**, *9*, 13696–13704. [CrossRef]
132. Chen, K.; Yu, J.; Liu, B.; Si, C.; Ban, H.; Cai, W.; Li, C.; Li, Z.; Fujimoto, K. Simple strategy synthesizing stable CuZnO/SiO_2 methanol synthesis catalyst. *J. Catal.* **2019**, *372*, 163–173. [CrossRef]
133. Tada, S.; Oshima, K.; Noda, Y.; Kikuchi, R.; Sohmiya, M.; Honma, T.; Satokawa, S. Effects of Cu precursor types on the catalytic activity of Cu/ZrO_2 toward methanol synthesis via CO_2 hydrogenation. *Ind. Eng. Chem. Res.* **2019**, *58*, 19434–19445. [CrossRef]
134. Guo, H.; Li, Q.; Zhang, H.; Peng, F.; Xiong, L.; Yao, S.; Huang, C.; Chen, X. CO_2 hydrogenation over acid-activated Attapulgite/$Ce_{0.75}Zr_{0.25}O_2$ nanocomposite supported Cu-ZnO based catalysts. *Mol. Catal.* **2019**, *476*, 110499. [CrossRef]
135. Li, M.M.-J.; Chen, C.; Ayvalı, T.C.E.; Suo, H.; Zheng, J.; Teixeira, I.F.; Ye, L.; Zou, H.; O'Hare, D.; Tsang, S.C.E. CO_2 hydrogenation to methanol over catalysts derived from single cationic layer CuZnGa LDH precursors. *ACS Catal.* **2018**, *8*, 4390–4401. [CrossRef]
136. Prašnikar, A.; Dasireddy, V.D.; Likozar, B. Scalable combustion synthesis of copper-based perovskite catalysts for CO_2 reduction to methanol: Reaction structure-activity relationships, kinetics, and stability. *Chem. Eng. Sci.* **2022**, *250*, 117423. [CrossRef]
137. Li, H.-X.; Yang, L.-Q.-Q.; Chi, Z.-Y.; Zhang, Y.-L.; Li, X.-G.; He, Y.-L.; Reina, T.R.; Xiao, W.-D. CO_2 Hydrogenation to Methanol Over $Cu/ZnO/Al_2O_3$ Catalyst: Kinetic Modeling Based on Either Single-or Dual-Active Site Mechanism. *Catal. Lett.* **2022**, *152*, 1–15. [CrossRef]
138. Liu, T.; Hong, X.; Liu, G. In Situ Generation of the Cu@ 3D-ZrO x Framework Catalyst for Selective Methanol Synthesis from CO_2/H2. *ACS Catal.* **2019**, *10*, 93–102. [CrossRef]
139. Wu, C.; Lin, L.; Liu, J.; Zhang, J.; Zhang, F.; Zhou, T.; Rui, N.; Yao, S.; Deng, Y.; Yang, F. Inverse ZrO_2/Cu as a highly efficient methanol synthesis catalyst from CO_2 hydrogenation. *Nat. Commun.* **2020**, *11*, 5767. [CrossRef]
140. Pori, M.; Arčon, I.; Lašič Jurković, D.; Marinšek, M.; Dražić, G.; Likozar, B.; Crnjak Orel, Z. Synthesis of a Cu/ZnO Nanocomposite by electroless plating for the catalytic conversion of CO_2 to methanol. *Catal. Lett.* **2019**, *149*, 1427–1439. [CrossRef]
141. Zabilskiy, M.; Sushkevich, V.L.; Newton, M.A.; van Bokhoven, J.A. Copper–zinc alloy-free synthesis of methanol from carbon dioxide over Cu/ZnO/faujasite. *ACS Catal.* **2020**, *10*, 14240–14244. [CrossRef]
142. Zhu, J.; Ciolca, D.; Liu, L.; Parastaev, A.; Kosinov, N.; Hensen, E.J. Flame synthesis of Cu/ZnO–CeO_2 catalysts: Synergistic metal–support interactions promote CH_3OH selectivity in CO_2 hydrogenation. *ACS Catal.* **2021**, *11*, 4880–4892. [CrossRef]
143. Din, I.U.; Shaharun, M.S.; Naeem, A.; Tasleem, S.; Ahmad, P. Revalorization of CO_2 for methanol production via ZnO promoted carbon nanofibers based Cu-ZrO_2 catalytic hydrogenation. *J. Energy Chem.* **2019**, *39*, 68–76. [CrossRef]
144. Zhang, C.; Yang, H.; Gao, P.; Zhu, H.; Zhong, L.; Wang, H.; Wei, W.; Sun, Y. Preparation and CO_2 hydrogenation catalytic properties of alumina microsphere supported Cu-based catalyst by deposition-precipitation method. *J. CO2 Util.* **2017**, *17*, 263–272. [CrossRef]
145. Jiang, Y.; Yang, H.; Gao, P.; Li, X.; Zhang, J.; Liu, H.; Wang, H.; Wei, W.; Sun, Y. Slurry methanol synthesis from CO_2 hydrogenation over micro-spherical SiO_2 support Cu/ZnO catalysts. *J. CO2 Util.* **2018**, *26*, 642–651. [CrossRef]
146. Li, S.; Guo, L.; Ishihara, T. Hydrogenation of CO_2 to methanol over Cu/AlCeO catalyst. *Catal. Today* **2020**, *339*, 352–361. [CrossRef]
147. Li, S.; Wang, Y.; Yang, B.; Guo, L. A highly active and selective mesostructured Cu/AlCeO catalyst for CO_2 hydrogenation to methanol. *Appl. Catal. A Gen.* **2019**, *571*, 51–60. [CrossRef]
148. Diez-Ramirez, J.; Dorado, F.; de la Osa, A.R.; Valverde, J.L.; Sánchez, P. Hydrogenation of CO_2 to methanol at atmospheric pressure over Cu/ZnO catalysts: Influence of the calcination, reduction, and metal loading. *Ind. Eng. Chem. Res.* **2017**, *56*, 1979–1987. [CrossRef]
149. Ouyang, B.; Tan, W.; Liu, B. Morphology effect of nanostructure ceria on the Cu/CeO_2 catalysts for synthesis of methanol from CO_2 hydrogenation. *Catal. Commun.* **2017**, *95*, 36–39. [CrossRef]
150. Kim, J.; Jeong, C.; Baik, J.H.; Suh, Y.-W. Phases of Cu/Zn/Al/Zr precursors linked to the property and activity of their final catalysts in CO_2 hydrogenation to methanol. *Catal. Today* **2020**, *347*, 70–78. [CrossRef]
151. L'hospital, V.; Angelo, L.; Zimmermann, Y.; Parkhomenko, K.; Roger, A.-C. Influence of the Zn/Zr ratio in the support of a copper-based catalyst for the synthesis of methanol from CO_2. *Catal. Today* **2021**, *369*, 95–104. [CrossRef]

152. Chen, S.; Zhang, J.; Wang, P.; Wang, X.; Song, F.; Bai, Y.; Zhang, M.; Wu, Y.; Xie, H.; Tan, Y. Effect of Vapor-phase-treatment to CuZnZr Catalyst on the Reaction Behaviors in CO_2 Hydrogenation into Methanol. *ChemCatChem* **2019**, *11*, 1448–1457. [CrossRef]
153. Yao, L.; Shen, X.; Pan, Y.; Peng, Z. Synergy between active sites of Cu-In-Zr-O catalyst in CO_2 hydrogenation to methanol. *J. Catal.* **2019**, *372*, 74–85. [CrossRef]
154. Chen, K.; Fang, H.; Wu, S.; Liu, X.; Zheng, J.; Zhou, S.; Duan, X.; Zhuang, Y.; Tsang, S.C.E.; Yuan, Y. CO_2 hydrogenation to methanol over Cu catalysts supported on La-modified SBA-15: The crucial role of Cu–LaOx interfaces. *Appl. Catal. B Environ.* **2019**, *251*, 119–129. [CrossRef]
155. Yan, Y.; Wong, R.J.; Ma, Z.; Donat, F.; Xi, S.; Saqline, S.; Fan, Q.; Du, Y.; Borgna, A.; He, Q. CO_2 hydrogenation to methanol on tungsten-doped Cu/CeO_2 catalysts. *Appl. Catal. B Environ.* **2022**, *306*, 121098. [CrossRef]
156. Wang, X.; Alabsi, M.H.; Zheng, P.; Mei, J.; Ramirez, A.; Duan, A.; Xu, C.; Huang, K.-W. PdCu supported on dendritic mesoporous $Ce_xZr_{1-x}O_2$ as superior catalysts to boost CO_2 hydrogenation to methanol. *J. Colloid Interface Sci.* **2022**, *611*, 739–751. [CrossRef]
157. Yamamura, T.; Tada, S.; Kikuchi, R.; Fujiwara, K.; Honma, T. Effect of Sm Doping on CO_2-to-Methanol Hydrogenation of Cu/Amorphous-ZrO_2 Catalysts. *J. Phys. Chem. C* **2021**, *125*, 15899–15909. [CrossRef]
158. Guil-López, R.; Mota, N.; Llorente, J.; Millan, E.; Pawelec, B.; García, R.; Fierro, J.; Navarro, R. Structure and activity of Cu/ZnO catalysts co-modified with aluminium and gallium for methanol synthesis. *Catal. Today* **2020**, *355*, 870–881. [CrossRef]
159. Mota, N.; Guil-Lopez, R.; Pawelec, B.; Fierro, J.; Navarro, R. Highly active Cu/ZnO–Al catalyst for methanol synthesis: Effect of aging on its structure and activity. *RSC Adv.* **2018**, *8*, 20619–20629. [CrossRef]
160. Deerattrakul, V.; Yigit, N.; Rupprechter, G.; Kongkachuichay, P. The roles of nitrogen species on graphene aerogel supported Cu-Zn as efficient catalysts for CO_2 hydrogenation to methanol. *Appl. Catal. A Gen.* **2019**, *580*, 46–52. [CrossRef]
161. Fang, X.; Men, Y.; Wu, F.; Zhao, Q.; Singh, R.; Xiao, P.; Du, T.; Webley, P.A. Promoting CO_2 hydrogenation to methanol by incorporating adsorbents into catalysts: Effects of hydrotalcite. *Chem. Eng. J.* **2019**, *378*, 122052. [CrossRef]
162. Fang, X.; Men, Y.; Wu, F.; Zhao, Q.; Singh, R.; Xiao, P.; Du, T.; Webley, P.A. Moderate-pressure conversion of H_2 and CO_2 to methanol via adsorption enhanced hydrogenation. *Int. J. Hydrogen Energy* **2019**, *44*, 21913–21925. [CrossRef]
163. Paris, C.; Karelovic, A.; Manrique, R.; Le Bras, S.; Devred, F.; Vykoukal, V.; Styskalik, A.; Eloy, P.; Debecker, D.P. CO_2 hydrogenation to methanol with Ga-and Zn-doped mesoporous Cu/SiO_2 catalysts prepared by the aerosol-assisted sol-gel process. *ChemSusChem* **2020**, *13*, 6409–6417. [PubMed]
164. Jiang, X.; Jiao, Y.; Moran, C.; Nie, X.; Gong, Y.; Guo, X.; Walton, K.S.; Song, C. CO_2 hydrogenation to methanol on PdCu bimetallic catalysts with lower metal loadings. *Catal. Commun.* **2019**, *118*, 10–14. [CrossRef]
165. Tan, Q.; Shi, Z.; Wu, D. CO_2 hydrogenation to methanol over a highly active Cu–Ni/CeO_2–nanotube catalyst. *Ind. Eng. Chem. Res.* **2018**, *57*, 10148–10158. [CrossRef]
166. Sharma, S.K.; Khan, T.S.; Singha, R.K.; Paul, B.; Poddar, M.K.; Sasaki, T.; Bordoloi, A.; Samanta, C.; Gupta, S.; Bal, R. Design of highly stable MgO promoted Cu/ZnO catalyst for clean methanol production through selective hydrogenation of CO_2. *Appl. Catal. A Gen.* **2021**, *623*, 118239. [CrossRef]
167. Dasireddy, V.D.; Štefančič, N.S.; Huš, M.; Likozar, B. Effect of alkaline earth metal oxide (MO) Cu/MO/Al_2O_3 catalysts on methanol synthesis activity and selectivity via CO_2 reduction. *Fuel* **2018**, *233*, 103–112. [CrossRef]
168. Mureddu, M.; Ferrara, F.; Pettinau, A. Highly efficient CuO/ZnO/ZrO_2@ SBA-15 nanocatalysts for methanol synthesis from the catalytic hydrogenation of CO_2. *Appl. Catal. B Environ.* **2019**, *258*, 117941. [CrossRef]
169. Shi, Z.; Tan, Q.; Tian, C.; Pan, Y.; Sun, X.; Zhang, J.; Wu, D. CO_2 hydrogenation to methanol over Cu-In intermetallic catalysts: Effect of reduction temperature. *J. Catal.* **2019**, *379*, 78–89. [CrossRef]
170. Fujiwara, K.; Tada, S.; Honma, T.; Sasaki, H.; Nishijima, M.; Kikuchi, R. Influences of particle size and crystallinity of highly loaded CuO/ZrO_2 on CO_2 hydrogenation to methanol. *AIChE J.* **2019**, *65*, e16717. [CrossRef]
171. Chang, K.; Wang, T.; Chen, J.G. Hydrogenation of CO_2 to methanol over CuCeTiOx catalysts. *Appl. Catal. B Environ.* **2017**, *206*, 704–711. [CrossRef]
172. Wang, G.; Mao, D.; Guo, X.; Yu, J. Methanol synthesis from CO_2 hydrogenation over CuO-ZnO-ZrO_2-MxOy catalysts (M = Cr, Mo and W). *Int. J. Hydrogen Energy* **2019**, *44*, 4197–4207. [CrossRef]
173. Sadeghinia, M.; Ghaziani, A.N.K.; Rezaei, M. Component ratio dependent Cu/Zn/Al structure sensitive catalyst in CO_2/CO hydrogenation to methanol. *Mol. Catal.* **2018**, *456*, 38–48. [CrossRef]
174. Tada, S.; Watanabe, F.; Kiyota, K.; Shimoda, N.; Hayashi, R.; Takahashi, M.; Nariyuki, A.; Igarashi, A.; Satokawa, S. Ag addition to CuO-ZrO_2 catalysts promotes methanol synthesis via CO_2 hydrogenation. *J. Catal.* **2017**, *351*, 107–118. [CrossRef]
175. Wang, W.; Qu, Z.; Song, L.; Fu, Q. Effect of the nature of copper species on methanol synthesis from CO_2 hydrogenation reaction over CuO/$Ce_{0.4}Zr_{0.6}O_2$ catalyst. *Mol. Catal.* **2020**, *493*, 111105. [CrossRef]
176. Jiang, X.; Chen, X.; Ling, C.; Chen, S.; Wu, Z. High-performance Cu/ZnO catalysts prepared using a three-channel microreactor. *Appl. Catal. A Gen.* **2019**, *570*, 192–199. [CrossRef]
177. Allam, D.; Bennici, S.; Limousy, L.; Hocine, S. Improved Cu-and Zn-based catalysts for CO_2 hydrogenation to methanol. *Comptes Rendus Chim.* **2019**, *22*, 227–237. [CrossRef]
178. Chang, K.; Wang, T.; Chen, J.G. Methanol synthesis from CO_2 hydrogenation over CuZnCeTi mixed oxide catalysts. *Ind. Eng. Chem. Res.* **2019**, *58*, 7922–7928. [CrossRef]

179. Xiao, J.; Mao, D.; Wang, G.; Guo, X.; Yu, J. CO_2 hydrogenation to methanol over $CuOZnOTiO_2ZrO_2$ catalyst prepared by a facile solid-state route: The significant influence of assistant complexing agents. *Int. J. Hydrogen Energy* **2019**, *44*, 14831–14841. [CrossRef]
180. Shi, Z.; Tan, Q.; Wu, D. Enhanced CO_2 hydrogenation to methanol over TiO_2 nanotubes-supported CuO-ZnO-CeO_2 catalyst. *Appl. Catal. A Gen.* **2019**, *581*, 58–66. [CrossRef]
181. Chen, D.; Mao, D.; Wang, G.; Guo, X.; Yu, J. CO_2 hydrogenation to methanol over CuO-ZnO-ZrO_2 catalyst prepared by polymeric precursor method. *J. Sol-Gel Sci. Technol.* **2019**, *89*, 686–699. [CrossRef]
182. Witoon, T.; Numpilai, T.; Phongamwong, T.; Donphai, W.; Boonyuen, C.; Warakulwit, C.; Chareonpanich, M.; Limtrakul, J. Enhanced activity, selectivity and stability of a CuO-ZnO-ZrO_2 catalyst by adding graphene oxide for CO_2 hydrogenation to methanol. *Chem. Eng. J.* **2018**, *334*, 1781–1791. [CrossRef]
183. Ye, H.; Na, W.; Gao, W.; Wang, H. Carbon-Modified CuO/ZnO Catalyst with High Oxygen Vacancy for CO_2 Hydrogenation to Methanol. *Energy Technol.* **2020**, *8*, 2000194. [CrossRef]
184. Wang, G.; Mao, D.; Guo, X.; Yu, J. Enhanced performance of the CuO-ZnO-ZrO_2 catalyst for CO_2 hydrogenation to methanol by WO_3 modification. *Appl. Surf. Sci.* **2018**, *456*, 403–409. [CrossRef]
185. Ren, S.; Fan, X.; Shang, Z.; Shoemaker, W.R.; Ma, L.; Wu, T.; Li, S.; Klinghoffer, N.B.; Yu, M.; Liang, X. Enhanced catalytic performance of Zr modified CuO/ZnO/Al_2O_3 catalyst for methanol and DME synthesis via CO_2 hydrogenation. *J. CO2 Util.* **2020**, *36*, 82–95. [CrossRef]
186. Sadeghinia, M.; Rezaei, M.; Kharat, A.N.; Jorabchi, M.N.; Nematollahi, B.; Zareiekordshouli, F. Effect of In_2O_3 on the structural properties and catalytic performance of the CuO/ZnO/Al_2O_3 catalyst in CO_2 and CO hydrogenation to methanol. *Mol. Catal.* **2020**, *484*, 110776. [CrossRef]
187. Kourtelesis, M.; Kousi, K.; Kondarides, D.I. CO_2 hydrogenation to methanol over La2O3-promoted CuO/ZnO/Al_2O_3 catalysts: A kinetic and mechanistic study. *Catalysts* **2020**, *10*, 183. [CrossRef]
188. Phongamwong, T.; Chantaprasertporn, U.; Witoon, T.; Numpilai, T.; Poo-Arporn, Y.; Limphirat, W.; Donphai, W.; Dittanet, P.; Chareonpanich, M.; Limtrakul, J. CO_2 hydrogenation to methanol over CuO–ZnO–ZrO_2–SiO_2 catalysts: Effects of SiO_2 contents. *Chem. Eng. J.* **2017**, *316*, 692–703. [CrossRef]
189. Liang, Y.; Mao, D.; Guo, X.; Yu, J.; Wu, G.; Ma, Z. Solvothermal preparation of CuO-ZnO-ZrO_2 catalysts for methanol synthesis via CO_2 hydrogenation. *J. Taiwan Inst. Chem. Eng.* **2021**, *121*, 81–91. [CrossRef]
190. Poto, S.; van Berkel, D.V.; Gallucci, F.; d'Angelo, M.F.N. Kinetic modelling of the methanol synthesis from CO_2 and H2 over a CuO/CeO_2/ZrO_2 catalyst: The role of CO_2 and CO hydrogenation. *Chem. Eng. J.* **2022**, *435*, 134946. [CrossRef]
191. Tada, S.; Satokawa, S. Effect of Ag loading on CO_2-to-methanol hydrogenation over Ag/CuO/ZrO_2. *Catal. Commun.* **2018**, *113*, 41–45. [CrossRef]
192. Bonura, G.; Cannilla, C.; Frusteri, L.; Catizzone, E.; Todaro, S.; Migliori, M.; Giordano, G.; Frusteri, F. Interaction effects between CuO-ZnO-ZrO_2 methanol phase and zeolite surface affecting stability of hybrid systems during one-step CO_2 hydrogenation to DME. *Catal. Today* **2020**, *345*, 175–182. [CrossRef]
193. Tursunov, O.; Kustov, L.; Tilyabaev, Z. Methanol synthesis from the catalytic hydrogenation of CO_2 over CuO–ZnO supported on aluminum and silicon oxides. *J. Taiwan Inst. Chem. Eng.* **2017**, *78*, 416–422. [CrossRef]
194. Wang, W.; Qu, Z.; Song, L.; Fu, Q. An investigation of Zr/Ce ratio influencing the catalytic performance of CuO/$Ce_{1-x}Zr_xO_2$ catalyst for CO_2 hydrogenation to CH_3OH. *J. Energy Chem.* **2020**, *47*, 18–28. [CrossRef]
195. Poerjoto, A.J.; Ashok, J.; Dewangan, N.; Kawi, S. The role of lattice oxygen in CO_2 hydrogenation to methanol over La1-xSrxCuO catalysts. *J. CO2 Util.* **2021**, *47*, 101498. [CrossRef]
196. Min, L.; Wei, N.; YE, H.-C.; HUO, H.-H.; GAO, W.-G. Effect of additive on CuO-ZnO/SBA-15 catalytic performance of CO_2 hydrogenation to methanol. *J. Fuel Chem. Technol.* **2019**, *47*, 1214–1225.
197. Liu, X.; Zhan, G.; Wu, J.; Li, W.; Du, Z.; Huang, J.; Sun, D.; Li, Q. Preparation of integrated CuO/ZnO/OS nanocatalysts by using acid-etched oyster shells as a support for CO_2 hydrogenation. *ACS Sustain. Chem. Eng.* **2020**, *8*, 7162–7173. [CrossRef]
198. Trifan, B.; Lasobras, J.; Soler, J.; Herguido, J.; Menéndez, M. Modifications in the composition of CuO/ZnO/Al_2O_3 catalyst for the synthesis of methanol by CO_2 hydrogenation. *Catalysts* **2021**, *11*, 774. [CrossRef]
199. Ortner, N.; Lund, H.; Armbruster, U.; Wohlrab, S.; Kondratenko, E.V. Factors affecting primary and secondary pathways in CO_2 hydrogenation to methanol over CuZnIn/MZrOx (La, Ti or Y). *Catal. Today* **2022**, *387*, 47–53. [CrossRef]
200. Song, H.-T.; Fazeli, A.; Kim, H.D.; Eslami, A.A.; Noh, Y.S.; Saeidabad, N.G.; Moon, D.J. Effect of lanthanum group promoters on Cu/(mixture of ZnO and Zn-Al-spinnel-oxides) catalyst for methanol synthesis by hydrogenation of CO and CO_2 mixtures. *Fuel* **2021**, *283*, 118987. [CrossRef]
201. Yang, B.; Liu, C.; Halder, A.; Tyo, E.C.; Martinson, A.B.; Seifert, S.n.; Zapol, P.; Curtiss, L.A.; Vajda, S. Copper cluster size effect in methanol synthesis from CO_2. *J. Phys. Chem. C* **2017**, *121*, 10406–10412. [CrossRef]
202. Sha, F.; Han, Z.; Tang, S.; Wang, J.; Li, C. Hydrogenation of Carbon Dioxide to Methanol over Non− Cu-based Heterogeneous Catalysts. *ChemSusChem* **2020**, *13*, 6160–6181. [CrossRef]
203. Rui, N.; Zhang, F.; Sun, K.; Liu, Z.; Xu, W.; Stavitski, E.; Senanayake, S.D.; Rodriguez, J.A.; Liu, C.-J. Hydrogenation of CO_2 to methanol on a Auδ+–In_2O_3–x catalyst. *ACS Catal.* **2020**, *10*, 11307–11317. [CrossRef]
204. Shen, C.; Sun, K.; Zhang, Z.; Rui, N.; Jia, X.; Mei, D.; Liu, C.-J. Highly active Ir/In2O3 catalysts for selective hydrogenation of CO_2 to methanol: Experimental and theoretical studies. *ACS Catal.* **2021**, *11*, 4036–4046. [CrossRef]

205. Docherty, S.R.; Phongprueksathat, N.; Lam, E.; Noh, G.; Safonova, O.V.; Urakawa, A.; Copéret, C. Silica-supported PdGa nanoparticles: Metal synergy for highly active and selective CO_2-to-CH_3OH hydrogenation. *JACS Au* **2021**, *1*, 450–458. [CrossRef] [PubMed]
206. Jiang, F.; Wang, S.; Liu, B.; Liu, J.; Wang, L.; Xiao, Y.; Xu, Y.; Liu, X. Insights into the influence of CeO_2 crystal facet on CO_2 hydrogenation to methanol over Pd/CeO_2 catalysts. *ACS Catal.* **2020**, *10*, 11493–11509. [CrossRef]
207. Song, J.; Liu, S.; Yang, C.; Wang, G.; Tian, H.; Zhao, Z.-J.; Mu, R.; Gong, J. The role of Al doping in Pd/ZnO catalyst for CO_2 hydrogenation to methanol. *Appl. Catal. B Environ.* **2020**, *263*, 118367. [CrossRef]
208. Frei, M.S.; Mondelli, C.; García-Muelas, R.; Kley, K.S.; Puértolas, B.; López, N.; Safonova, O.V.; Stewart, J.A.; Curulla Ferré, D.; Pérez-Ramírez, J. Atomic-scale engineering of indium oxide promotion by palladium for methanol production via CO_2 hydrogenation. *Nat. Commun.* **2019**, *10*, 3377. [CrossRef]
209. Men, Y.-L.; Liu, Y.; Wang, Q.; Luo, Z.-H.; Shao, S.; Li, Y.-B.; Pan, Y.-X. Highly dispersed Pt-based catalysts for selective CO_2 hydrogenation to methanol at atmospheric pressure. *Chem. Eng. Sci.* **2019**, *200*, 167–175. [CrossRef]
210. Jiang, H.; Lin, J.; Wu, X.; Wang, W.; Chen, Y.; Zhang, M. Efficient hydrogenation of CO_2 to methanol over Pd/In_2O_3/SBA-15 catalysts. *J. CO2 Util.* **2020**, *36*, 33–39. [CrossRef]
211. Gallo, A.; Snider, J.L.; Sokaras, D.; Nordlund, D.; Kroll, T.; Ogasawara, H.; Kovarik, L.; Duyar, M.S.; Jaramillo, T.F. Ni_5Ga_3 catalysts for CO_2 reduction to methanol: Exploring the role of Ga surface oxidation/reduction on catalytic activity. *Appl. Catal. B Environ.* **2020**, *267*, 118369. [CrossRef]
212. Choi, H.; Oh, S.; Tran, S.B.T.; Park, J.Y. Size-controlled model Ni catalysts on Ga_2O_3 for CO_2 hydrogenation to methanol. *J. Catal.* **2019**, *376*, 68–76. [CrossRef]
213. Ting, K.W.; Toyao, T.; Siddiki, S.H.; Shimizu, K.-I. Low-temperature hydrogenation of CO_2 to methanol over heterogeneous TiO_2-Supported Re catalysts. *ACS Catal.* **2019**, *9*, 3685–3693. [CrossRef]
214. Toyao, T.; Kayamori, S.; Maeno, Z.; Siddiki, S.H.; Shimizu, K.-I. Heterogeneous Pt and MoOx Co-Loaded TiO_2 Catalysts for Low-Temperature CO_2 Hydrogenation To Form CH_3OH. *ACS Catal.* **2019**, *9*, 8187–8196. [CrossRef]
215. Gothe, M.L.; Pérez-Sanz, F.J.; Braga, A.H.; Borges, L.R.; Abreu, T.F.; Bazito, R.C.; Gonçalves, R.V.; Rossi, L.M.; Vidinha, P. Selective CO_2 hydrogenation into methanol in a supercritical flow process. *J. CO2 Util.* **2020**, *40*, 101195. [CrossRef]
216. Wang, L.; Guan, E.; Wang, Y.; Wang, L.; Gong, Z.; Cui, Y.; Meng, X.; Gates, B.C.; Xiao, F.-S. Silica accelerates the selective hydrogenation of CO_2 to methanol on cobalt catalysts. *Nat. Commun.* **2020**, *11*, 1033. [CrossRef]
217. Sun, K.; Zhang, Z.; Shen, C.; Rui, N.; Liu, C.-J. The feasibility study of the indium oxide supported silver catalyst for selective hydrogenation of CO_2 to methanol. *Green Energy Environ.* **2022**, *7*, 807–817. [CrossRef]
218. Wu, C.; Zhang, P.; Zhang, Z.; Zhang, L.; Yang, G.; Han, B. Efficient hydrogenation of CO_2 to methanol over supported subnanometer gold catalysts at low temperature. *ChemCatChem* **2017**, *9*, 3691–3696. [CrossRef]
219. Vourros, A.; Garagounis, I.; Kyriakou, V.; Carabineiro, S.; Maldonado-Hódar, F.; Marnellos, G.; Konsolakis, M. Carbon dioxide hydrogenation over supported Au nanoparticles: Effect of the support. *J. CO2 Util.* **2017**, *19*, 247–256. [CrossRef]
220. Lu, Z.; Sun, K.; Wang, J.; Zhang, Z.; Liu, C. A highly active Au/In_2O_3-ZrO_2 catalyst for selective hydrogenation of CO_2 to methanol. *Catalysts* **2020**, *10*, 1360. [CrossRef]
221. Wang, W.; Tongo, D.W.K.; Song, L.; Qu, Z. Effect of Au Addition on the Catalytic Performance of CuO/CeO_2 Catalysts for CO_2 Hydrogenation to Methanol. *Top. Catal.* **2021**, *64*, 446–455. [CrossRef]
222. Rezvani, A.; Abdel-Mageed, A.M.; Ishida, T.; Murayama, T.; Parlinska-Wojtan, M.; Behm, R.J.r. CO_2 reduction to methanol on Au/CeO_2 catalysts: Mechanistic insights from activation/deactivation and SSITKA measurements. *ACS Catal.* **2020**, *10*, 3580–3594. [CrossRef]
223. Wu, Q.; Shen, C.; Rui, N.; Sun, K.; Liu, C.-J. Experimental and theoretical studies of CO_2 hydrogenation to methanol on Ru/In_2O_3. *J. CO2 Util.* **2021**, *53*, 101720. [CrossRef]
224. Sagar, T.V.; Zavašnik, J.; Finšgar, M.; Novak Tušar, N.; Pintar, A. Evaluation of Au/ZrO_2 Catalysts Prepared via Postsynthesis Methods in CO_2 Hydrogenation to Methanol. *Catalysts* **2022**, *12*, 218. [CrossRef]
225. Han, Z.; Tang, C.; Sha, F.; Tang, S.; Wang, J.; Li, C. CO_2 hydrogenation to methanol on ZnO-ZrO_2 solid solution catalysts with ordered mesoporous structure. *J. Catal.* **2021**, *396*, 242–250. [CrossRef]
226. Wang, J.; Sun, K.; Jia, X.; Liu, C.-J. CO_2 hydrogenation to methanol over Rh/In_2O_3 catalyst. *Catal. Today* **2021**, *365*, 341–347. [CrossRef]
227. Lu, Z.; Wang, J.; Sun, K.; Xiong, S.; Zhang, Z.; Liu, C.-J. CO_2 hydrogenation to methanol over Rh/In_2O_3–ZrO_2 catalyst with improved activity. *Green Chem. Eng.* **2022**, *3*, 165–170. [CrossRef]
228. Sun, K.; Rui, N.; Zhang, Z.; Sun, Z.; Ge, Q.; Liu, C.-J. A highly active Pt/In_2O_3 catalyst for CO_2 hydrogenation to methanol with enhanced stability. *Green Chem.* **2020**, *22*, 5059–5066. [CrossRef]
229. Rui, N.; Wang, Z.; Sun, K.; Ye, J.; Ge, Q.; Liu, C.-J. CO_2 hydrogenation to methanol over Pd/In_2O_3: Effects of Pd and oxygen vacancy. *Appl. Catal. B Environ.* **2017**, *218*, 488–497. [CrossRef]
230. Jia, X.; Sun, K.; Wang, J.; Shen, C.; Liu, C.-J. Selective hydrogenation of CO_2 to methanol over Ni/In_2O_3 catalyst. *J. Energy Chem.* **2020**, *50*, 409–415. [CrossRef]
231. Dostagir, N.H.M.; Thompson, C.; Kobayashi, H.; Karim, A.M.; Fukuoka, A.; Shrotri, A. Rh promoted In_2O_3 as a highly active catalyst for CO 2 hydrogenation to methanol. *Catal. Sci. Technol.* **2020**, *10*, 8196–8202. [CrossRef]

232. Zhang, Z.; Shen, C.; Sun, K.; Liu, C.-J. Improvement in the activity of Ni/In_2O_3 with the addition of ZrO_2 for CO_2 hydrogenation to methanol. *Catal. Commun.* **2022**, *162*, 106386. [CrossRef]
233. Frei, M.S.; Mondelli, C.; García-Muelas, R.; Morales-Vidal, J.; Philipp, M.; Safonova, O.V.; López, N.; Stewart, J.A.; Ferré, D.C.; Pérez-Ramírez, J. Nanostructure of nickel-promoted indium oxide catalysts drives selectivity in CO_2 hydrogenation. *Nat. Commun.* **2021**, *12*, 1960. [CrossRef] [PubMed]
234. Cai, Z.; Dai, J.; Li, W.; Tan, K.B.; Huang, Z.; Zhan, G.; Huang, J.; Li, Q. Pd supported on MIL-68 (In)-derived In_2O_3 nanotubes as superior catalysts to boost CO_2 hydrogenation to methanol. *ACS Catal.* **2020**, *10*, 13275–13289. [CrossRef]
235. Alharthi, A.I.; Din, I.U.; Alotaibi, M.A.; Bagabas, A.; Naeem, A.; Alkhalifa, A. Low temperature green methanol synthesis by CO_2 hydrogenation over Pd/SiO_2 catalysts in slurry reactor. *Inorg. Chem. Commun.* **2022**, *142*, 109688. [CrossRef]
236. Collins, S.E.; Baltanás, M.A.; Delgado, J.J.; Borgna, A.; Bonivardi, A.L. CO_2 hydrogenation to methanol on Ga_2O_3-Pd/SiO_2 catalysts: Dual oxide-metal sites or (bi) metallic surface sites? *Catal. Today* **2021**, *381*, 154–162. [CrossRef]
237. Lee, K.; Anjum, U.; Araújo, T.P.; Mondelli, C.; He, Q.; Furukawa, S.; Pérez-Ramírez, J.; Kozlov, S.M.; Yan, N. Atomic Pd-promoted ZnZrOx solid solution catalyst for CO_2 hydrogenation to methanol. *Appl. Catal. B Environ.* **2022**, *304*, 120994. [CrossRef]
238. Khobragade, R.; Roškarič, M.; Žerjav, G.; Košiček, M.; Zavašnik, J.; Van de Velde, N.; Jerman, I.; Tušar, N.N.; Pintar, A. Exploring the effect of morphology and surface properties of nanoshaped Pd/CeO_2 catalysts on CO_2 hydrogenation to methanol. *Appl. Catal. A Gen.* **2021**, *627*, 118394. [CrossRef]
239. Manrique, R.; Jiménez, R.; Rodríguez-Pereira, J.; Baldovino-Medrano, V.G.; Karelovic, A. Insights into the role of Zn and Ga in the hydrogenation of CO_2 to methanol over Pd. *Int. J. Hydrogen Energy* **2019**, *44*, 16526–16536. [CrossRef]
240. Richard, A.R.; Fan, M. Low-pressure hydrogenation of CO_2 to CH3OH using $Ni\text{-}In\text{-}Al/SiO_2$ catalyst synthesized via a phyllosilicate precursor. *ACS Catal.* **2017**, *7*, 5679–5692. [CrossRef]
241. Cherevotan, A.; Raj, J.; Dheer, L.; Roy, S.; Sarkar, S.; Das, R.; Vinod, C.P.; Xu, S.; Wells, P.; Waghmare, U.V. Operando generated ordered heterogeneous catalyst for the selective conversion of CO_2 to methanol. *ACS Energy Lett.* **2021**, *6*, 509–516. [CrossRef]
242. Bavykina, A.; Yarulina, I.; Al Abdulghani, A.J.; Gevers, L.; Hedhili, M.N.; Miao, X.; Galilea, A.R.; Pustovarenko, A.; Dikhtiarenko, A.; Cadiau, A. Turning a methanation Co catalyst into an In–Co methanol producer. *ACS Catal.* **2019**, *9*, 6910–6918. [CrossRef]
243. Snider, J.L.; Streibel, V.; Hubert, M.A.; Choksi, T.S.; Valle, E.; Upham, D.C.; Schumann, J.; Duyar, M.S.; Gallo, A.; Abild-Pedersen, F. Revealing the synergy between oxide and alloy phases on the performance of bimetallic In–Pd catalysts for CO_2 hydrogenation to methanol. *ACS Catal.* **2019**, *9*, 3399–3412. [CrossRef]
244. Li, M.M.J.; Zou, H.; Zheng, J.; Wu, T.S.; Chan, T.S.; Soo, Y.L.; Wu, X.P.; Gong, X.Q.; Chen, T.; Roy, K. Methanol synthesis at a wide range of H_2/CO_2 ratios over a Rh-In bimetallic catalyst. *Angew. Chem.* **2020**, *132*, 16173–16180. [CrossRef]
245. Ojelade, O.A.; Zaman, S.F.; Daous, M.A.; Al-Zahrani, A.A.; Malik, A.S.; Driss, H.; Shterk, G.; Gascon, J. Optimizing Pd: Zn molar ratio in $PdZn/CeO_2$ for CO_2 hydrogenation to methanol. *Appl. Catal. A Gen.* **2019**, *584*, 117185. [CrossRef]
246. Malik, A.S.; Zaman, S.F.; Al-Zahrani, A.A.; Daous, M.A.; Driss, H.; Petrov, L.A. Selective hydrogenation of CO_2 to CH_3OH and in-depth DRIFT analysis for $PdZn/ZrO_2$ and $CaPdZn/ZrO_2$ catalysts. *Catal. Today* **2020**, *357*, 573–582. [CrossRef]
247. Geng, F.; Zhan, X.; Hicks, J.C. Promoting Methanol Synthesis and Inhibiting CO_2 Methanation with Bimetallic In–Ru Catalysts. *ACS Sustain. Chem. Eng.* **2021**, *9*, 11891–11902. [CrossRef]
248. Rasteiro, L.F.; De Sousa, R.A.; Vieira, L.H.; Ocampo-Restrepo, V.K.; Verga, L.G.; Assaf, J.M.; Da Silva, J.L.; Assaf, E.M. Insights into the alloy-support synergistic effects for the CO_2 hydrogenation towards methanol on oxide-supported Ni_5Ga_3 catalysts: An experimental and DFT study. *Appl. Catal. B Environ.* **2022**, *302*, 120842. [CrossRef]
249. Nie, X.; Jiang, X.; Wang, H.; Luo, W.; Janik, M.J.; Chen, Y.; Guo, X.; Song, C. Mechanistic understanding of alloy effect and water promotion for Pd-Cu bimetallic catalysts in CO_2 hydrogenation to methanol. *ACS Catal.* **2018**, *8*, 4873–4892. [CrossRef]
250. Lin, F.; Jiang, X.; Boreriboon, N.; Wang, Z.; Song, C.; Cen, K. Effects of supports on bimetallic Pd-Cu catalysts for CO_2 hydrogenation to methanol. *Appl. Catal. A Gen.* **2019**, *585*, 117210. [CrossRef]
251. Jiang, X.; Nie, X.; Wang, X.; Wang, H.; Koizumi, N.; Chen, Y.; Guo, X.; Song, C. Origin of Pd-Cu bimetallic effect for synergetic promotion of methanol formation from CO_2 hydrogenation. *J. Catal.* **2019**, *369*, 21–32. [CrossRef]
252. Jiang, X.; Wang, X.; Nie, X.; Koizumi, N.; Guo, X.; Song, C. CO_2 hydrogenation to methanol on Pd-Cu bimetallic catalysts: H_2/CO_2 ratio dependence and surface species. *Catal. Today* **2018**, *316*, 62–70. [CrossRef]
253. Wang, C.; Fang, Y.; Liang, G.; Lv, X.; Duan, H.; Li, Y.; Chen, D.; Long, M. Mechanistic study of Cu-Ni bimetallic catalysts supported by graphene derivatives for hydrogenation of CO_2 to methanol. *J. CO2 Util.* **2021**, *49*, 101542. [CrossRef]
254. Díez-Ramírez, J.; Díaz, J.; Sánchez, P.; Dorado, F. Optimization of the Pd/Cu ratio in Pd-Cu-Zn/SiC catalysts for the CO_2 hydrogenation to methanol at atmospheric pressure. *J. CO2 Util.* **2017**, *22*, 71–80. [CrossRef]
255. Alharthi, A.I.; Din, I.U.; Alotaibi, M.A. Effect of the Cu/Ni Ratio on the Activity of Zeolite Based Cu–Ni Bimetallic Catalysts for CO_2 Hydrogenation to Methanol. *Russ. J. Phys. Chem. A* **2020**, *94*, 2563–2568. [CrossRef]
256. Geng, F.; Bonita, Y.; Jain, V.; Magiera, M.; Rai, N.; Hicks, J.C. Bimetallic Ru–Mo phosphide catalysts for the hydrogenation of CO_2 to methanol. *Ind. Eng. Chem. Res.* **2020**, *59*, 6931–6943. [CrossRef]
257. Zheng, X.; Lin, Y.; Pan, H.; Wu, L.; Zhang, W.; Cao, L.; Zhang, J.; Zheng, L.; Yao, T. Grain boundaries modulating active sites in RhCo porous nanospheres for efficient CO_2 hydrogenation. *Nano Res.* **2018**, *11*, 2357–2365. [CrossRef]
258. Hengne, A.M.; Samal, A.K.; Enakonda, L.R.; Harb, M.; Gevers, L.E.; Anjum, D.H.; Hedhili, M.N.; Saih, Y.; Huang, K.-W.; Basset, J.-M. Ni–Sn-supported ZrO_2 catalysts modified by indium for selective CO_2 hydrogenation to methanol. *ACS Omega* **2018**, *3*, 3688–3701. [CrossRef]

259. Lin, F.; Jiang, X.; Boreriboon, N.; Song, C.; Wang, Z.; Cen, K. CO_2 hydrogenation to methanol over bimetallic Pd-Cu catalysts supported on TiO_2-CeO_2 and TiO_2-ZrO_2. *Catal. Today* **2021**, *371*, 150–161. [CrossRef]
260. Choi, E.J.; Lee, Y.H.; Lee, D.-W.; Moon, D.-J.; Lee, K.-Y. Hydrogenation of CO_2 to methanol over Pd–Cu/CeO_2 catalysts. *Mol. Catal.* **2017**, *434*, 146–153. [CrossRef]
261. Zhang, C.; Liao, P.; Wang, H.; Sun, J.; Gao, P. Preparation of novel bimetallic CuZn-BTC coordination polymer nanorod for methanol synthesis from CO_2 hydrogenation. *Mater. Chem. Phys.* **2018**, *215*, 211–220. [CrossRef]
262. Yu, J.; Chen, G.; Guo, Q.; Guo, X.; Da Costa, P.; Mao, D. Ultrasmall bimetallic Cu/ZnOx nanoparticles encapsulated in UiO-66 by deposition–precipitation method for CO_2 hydrogenation to methanol. *Fuel* **2022**, *324*, 124694. [CrossRef]
263. Qi, T.; Zhao, Y.; Chen, S.; Li, W.; Guo, X.; Zhang, Y.; Song, C. Bimetallic metal organic framework-templated synthesis of a Cu-ZnO/Al_2O_3 catalyst with superior methanol selectivity for CO_2 hydrogenation. *Mol. Catal.* **2021**, *514*, 111870. [CrossRef]
264. Alotaibi, M.A.; Din, I.U.; Alharthi, A.I.; Bakht, M.A.; Centi, G.; Shaharun, M.S.; Naeem, A. Green methanol synthesis by catalytic CO_2 hydrogenation, deciphering the role of metal-metal interaction. *Sustain. Chem. Pharm.* **2021**, *21*, 100420. [CrossRef]
265. Duma, Z.G.; Dyosiba, X.; Moma, J.; Langmi, H.W.; Louis, B.; Parkhomenko, K.; Musyoka, N.M. Thermocatalytic Hydrogenation of CO_2 to Methanol Using Cu-ZnO Bimetallic Catalysts Supported on Metal–Organic Frameworks. *Catalysts* **2022**, *12*, 401. [CrossRef]
266. Qiu, R.; Ding, Z.; Xu, Y.; Yang, Q.; Sun, K.; Hou, R. CuPd bimetallic catalyst with high Cu/Pd ratio and its application in CO_2 hydrogenation. *Appl. Surf. Sci.* **2021**, *544*, 148974. [CrossRef]
267. García-Trenco, A.; Regoutz, A.; White, E.R.; Payne, D.J.; Shaffer, M.S.; Williams, C.K. PdIn intermetallic nanoparticles for the hydrogenation of CO_2 to methanol. *Appl. Catal. B Environ.* **2018**, *220*, 9–18. [CrossRef]
268. Zhang, Z.; Shen, C.; Sun, K.; Jia, X.; Ye, J.; Liu, C.-J. Advances in Studies of Structural Effect of the Supported Ni Catalyst for CO_2 Hydrogenation: From Nanoparticle to Single Atom Catalyst. *J. Mater. Chem. A* **2022**, *10*, 5792–5812. [CrossRef]
269. Niu, J.; Liu, H.; Jin, Y.; Fan, B.; Qi, W.; Ran, J. Comprehensive review of Cu-based CO_2 hydrogenation to CH_3OH: Insights from experimental work and theoretical analysis. *Int. J. Hydrogen Energy* **2022**, *47*, 9183–9200. [CrossRef]
270. Shen, C.; Bao, Q.; Xue, W.; Sun, K.; Zhang, Z.; Jia, X.; Mei, D.; Liu, C.-J. Synergistic effect of the metal-support interaction and interfacial oxygen vacancy for CO_2 hydrogenation to methanol over Ni/In_2O_3 catalyst: A theoretical study. *J. Energy Chem.* **2022**, *65*, 623–629. [CrossRef]
271. Konsolakis, M.; Lykaki, M. Recent advances on the rational design of non-precious metal oxide catalysts exemplified by CuOx/CeO_2 binary system: Implications of size, shape and electronic effects on intrinsic reactivity and metal-support interactions. *Catalysts* **2020**, *10*, 160. [CrossRef]
272. Ding, J.; Li, Z.; Xiong, W.; Zhang, Y.; Ye, A.; Huang, W. Structural evolution and catalytic performance in CO_2 hydrogenation reaction of ZnO-ZrO_2 composite oxides. *Appl. Surf. Sci.* **2022**, *587*, 152884. [CrossRef]
273. Ticali, P.; Salusso, D.; Ahmad, R.; Ahoba-Sam, C.; Ramirez, A.; Shterk, G.; Lomachenko, K.A.; Borfecchia, E.; Morandi, S.; Cavallo, L. CO_2 hydrogenation to methanol and hydrocarbons over bifunctional Zn-doped ZrO_2/zeolite catalysts. *Catal. Sci. Technol.* **2021**, *11*, 1249–1268. [CrossRef]
274. Sha, F.; Tang, C.; Tang, S.; Wang, Q.; Han, Z.; Wang, J.; Li, C. The promoting role of Ga in ZnZrOx solid solution catalyst for CO_2 hydrogenation to methanol. *J. Catal.* **2021**, *404*, 383–392. [CrossRef]
275. Xu, Q.; Xu, X.; Fan, G.; Yang, L.; Li, F. Unveiling the roles of Fe-Co interactions over ternary spinel-type $ZnCoxFe_{2-x}O_4$ catalysts for highly efficient CO_2 hydrogenation to produce light olefins. *J. Catal.* **2021**, *400*, 355–366. [CrossRef]
276. Zhu, J.; Cannizzaro, F.; Liu, L.; Zhang, H.; Kosinov, N.; Filot, I.A.; Rabeah, J.; Bruckner, A.; Hensen, E.J. Ni–In Synergy in CO_2 Hydrogenation to Methanol. *ACS Catal.* **2021**, *11*, 11371–11384. [CrossRef]
277. Shi, Z.; Tan, Q.; Wu, D. Mixed-phase indium oxide as a highly active and stable catalyst for the hydrogenation of CO_2 to CH_3OH. *Ind. Eng. Chem. Res.* **2021**, *60*, 3532–3542. [CrossRef]
278. Chen, T.-Y.; Cao, C.; Chen, T.-B.; Ding, X.; Huang, H.; Shen, L.; Cao, X.; Zhu, M.; Xu, J.; Gao, J. Unraveling highly tunable selectivity in CO_2 hydrogenation over bimetallic In-Zr oxide catalysts. *ACS Catal.* **2019**, *9*, 8785–8797. [CrossRef]
279. Wang, J.; Li, G.; Li, Z.; Tang, C.; Feng, Z.; An, H.; Liu, H.; Liu, T.; Li, C. A highly selective and stable ZnO-ZrO_2 solid solution catalyst for CO_2 hydrogenation to methanol. *Sci. Adv.* **2017**, *3*, e1701290. [CrossRef]
280. Frei, M.S.; Mondelli, C.; Cesarini, A.; Krumeich, F.; Hauert, R.; Stewart, J.A.; Curulla Ferré, D.; Pérez-Ramírez, J. Role of zirconia in indium oxide-catalyzed CO_2 hydrogenation to methanol. *ACS Catal.* **2019**, *10*, 1133–1145. [CrossRef]
281. Akkharaphatthawon, N.; Chanlek, N.; Cheng, C.K.; Chareonpanich, M.; Limtrakul, J.; Witoon, T. Tuning adsorption properties of $GaxIn_2-xO_3$ catalysts for enhancement of methanol synthesis activity from CO_2 hydrogenation at high reaction temperature. *Appl. Surf. Sci.* **2019**, *489*, 278–286. [CrossRef]
282. Chou, C.-Y.; Lobo, R.F. Direct conversion of CO_2 into methanol over promoted indium oxide-based catalysts. *Appl. Catal. A Gen.* **2019**, *583*, 117144. [CrossRef]
283. Wang, J.; Tang, C.; Li, G.; Han, Z.; Li, Z.; Liu, H.; Cheng, F.; Li, C. High-Performance MaZrOx (Ma = Cd, Ga) Solid-Solution Catalysts for CO_2 Hydrogenation to Methanol. *ACS Catal.* **2019**, *9*, 10253–10259. [CrossRef]
284. Araújo, T.P.; Hergesell, A.H.; Faust-Akl, D.; Büchele, S.; Stewart, J.A.; Mondelli, C.; Pérez-Ramírez, J. Methanol Synthesis by Hydrogenation of Hybrid CO_2-CO Feeds. *ChemSusChem* **2021**, *14*, 2914–2923. [CrossRef] [PubMed]
285. Dang, S.; Qin, B.; Yang, Y.; Wang, H.; Cai, J.; Han, Y.; Li, S.; Gao, P.; Sun, Y. Rationally designed indium oxide catalysts for CO_2 hydrogenation to methanol with high activity and selectivity. *Sci. Adv.* **2020**, *6*, eaaz2060. [CrossRef] [PubMed]

286. Vera, C.Y.R.; Manavi, N.; Zhou, Z.; Wang, L.-C.; Diao, W.; Karakalos, S.; Liu, B.; Stowers, K.J.; Zhou, M.; Luo, H. Mechanistic understanding of support effect on the activity and selectivity of indium oxide catalysts for CO_2 hydrogenation. *Chem. Eng. J.* **2021**, *426*, 131767. [CrossRef]
287. Tian, G.; Wu, Y.; Wu, S.; Huang, S.; Gao, J. Influence of Mn and Mg oxides on the performance of In_2O_3 catalysts for CO_2 hydrogenation to methanol. *Chem. Phys. Lett.* **2022**, *786*, 139173. [CrossRef]
288. Wang, X.; Wang, Y.; Yang, C.; Yi, Y.; Wang, X.; Liu, F.; Cao, J.; Pan, H. A novel microreaction strategy to fabricate superior hybrid zirconium and zinc oxides for methanol synthesis from CO_2. *Appl. Catal. A Gen.* **2020**, *595*, 117507. [CrossRef]
289. Stangeland, K.; Kalai, D.Y.; Ding, Y.; Yu, Z. Mesoporous manganese-cobalt oxide spinel catalysts for CO_2 hydrogenation to methanol. *J. CO2 Util.* **2019**, *32*, 146–154. [CrossRef]
290. Li, L.; Yang, B.; Gao, B.; Wang, Y.; Zhang, L.; Ishihara, T.; Qi, W.; Guo, L. CO_2 hydrogenation selectivity shift over In-Co binary oxides catalysts: Catalytic mechanism and structure-property relationship. *Chin. J. Catal.* **2022**, *43*, 862–876. [CrossRef]
291. Xu, D.; Hong, X.; Liu, G. Highly dispersed metal doping to ZnZr oxide catalyst for CO_2 hydrogenation to methanol: Insight into hydrogen spillover. *J. Catal.* **2021**, *393*, 207–214. [CrossRef]
292. Wei, Y.; Liu, F.; Ma, J.; Yang, C.; Wang, X.; Cao, J. Catalytic roles of In_2O_3 in ZrO_2-based binary oxides for CO_2 hydrogenation to methanol. *Mol. Catal.* **2022**, *525*, 112354. [CrossRef]
293. Ronda-Lloret, M.; Wang, Y.; Oulego, P.; Rothenberg, G.; Tu, X.; Shiju, N.R. CO_2 hydrogenation at atmospheric pressure and low temperature using plasma-enhanced catalysis over supported cobalt oxide catalysts. *ACS Sustain. Chem. Eng.* **2020**, *8*, 17397–17407. [CrossRef] [PubMed]
294. Meng, C.; Zhao, G.; Shi, X.-R.; Chen, P.; Liu, Y.; Lu, Y. Oxygen-deficient metal oxides supported nano-intermetallic $InNi_3C_{0.5}$ toward efficient CO_2 hydrogenation to methanol. *Sci. Adv.* **2021**, *7*, eabi6012. [CrossRef]
295. Numpilai, T.; Kidkhunthod, P.; Cheng, C.K.; Wattanakit, C.; Chareonpanich, M.; Limtrakul, J.; Witoon, T. CO_2 hydrogenation to methanol at high reaction temperatures over In_2O_3/ZrO_2 catalysts: Influence of calcination temperatures of ZrO_2 support. *Catal. Today* **2021**, *375*, 298–306. [CrossRef]
296. Shi, Y.; Su, W.; Kong, L.; Wang, J.; Lv, P.; Hao, J.; Gao, X.; Yu, G. The homojunction formed by h-In_2O_3 (110) and c-In_2O_3 (440) promotes carbon dioxide hydrogenation to methanol on graphene oxide modified In_2O_3. *J. Colloid Interface Sci.* **2022**, *623*, 1048–1062. [CrossRef]
297. Yang, B.; Li, L.; Jia, Z.; Liu, X.; Zhang, C.; Guo, L. Comparative study of CO_2 hydrogenation to methanol on cubic bixbyite-type and rhombohedral corundum-type indium oxide. *Chin. Chem. Lett.* **2020**, *31*, 2627–2633. [CrossRef]
298. Tian, G.; Wu, Y.; Wu, S.; Huang, S.; Gao, J. CO_2 hydrogenation to methanol over $Pd/MnO/In_2O_3$ catalyst. *J. Environ. Chem. Eng.* **2022**, *10*, 106965. [CrossRef]
299. Tian, G.; Wu, Y.; Wu, S.; Huang, S.; Gao, J. Solid-State Synthesis of Pd/In_2O_3 Catalysts for CO_2 Hydrogenation to Methanol. *Catal. Lett.* **2022**, 1–8. [CrossRef]
300. Pechenkin, A.; Potemkin, D.; Rubtsova, M.; Snytnikov, P.; Plyusnin, P.; Glotov, A. CuO-In_2O_3 Catalysts Supported on Halloysite Nanotubes for CO_2 Hydrogenation to Dimethyl Ether. *Catalysts* **2021**, *11*, 1151. [CrossRef]
301. Wang, Y.; Wu, D.; Liu, T.; Liu, G.; Hong, X. Fabrication of PdZn alloy catalysts supported on ZnFe composite oxide for CO_2 hydrogenation to methanol. *J. Colloid Interface Sci.* **2021**, *597*, 260–268. [CrossRef]
302. Duyar, M.S.; Gallo, A.; Regli, S.K.; Snider, J.L.; Singh, J.A.; Valle, E.; McEnaney, J.; Bent, S.F.; Rønning, M.; Jaramillo, T.F. Understanding selectivity in CO_2 hydrogenation to methanol for mop nanoparticle catalysts using in situ techniques. *Catalysts* **2021**, *11*, 143. [CrossRef]
303. Zhang, G.; Fan, G.; Yang, L.; Li, F. Tuning surface-interface structures of ZrO_2 supported copper catalysts by in situ introduction of indium to promote CO_2 hydrogenation to methanol. *Appl. Catal. A Gen.* **2020**, *605*, 117805. [CrossRef]
304. Stangeland, K.; Chamssine, F.; Fu, W.; Huang, Z.; Duan, X.; Yu, Z. CO_2 hydrogenation to methanol over partially embedded Cu within Zn-Al oxide and the effect of indium. *J. CO2 Util.* **2021**, *50*, 101609. [CrossRef]
305. Vu, T.T.N.; Desgagnés, A.; Iliuta, M.C. Efficient approaches to overcome challenges in material development for conventional and intensified CO_2 catalytic hydrogenation to CO, methanol, and DME. *Appl. Catal. A Gen.* **2021**, *617*, 118119. [CrossRef]
306. Millán Ordóñez, E.; Mota, N.; Guil-López, R.; Garcia Pawelec, B.; Fierro, J.L.G.; Navarro Yerga, R.M. Direct Synthesis of Dimethyl Ether on Bifunctional Catalysts Based on Cu–ZnO (Al) and Supported $H_3PW_{12}O_{40}$: Effect of Physical Mixing on Bifunctional Interactions and Activity. *Ind. Eng. Chem. Res.* **2021**, *60*, 18853–18869. [CrossRef]
307. Liu, Z.; An, X.; Song, M.; Wang, Z.; Wei, Y.; Mintova, S.; Giordano, G.; Yan, Z. Dry gel assisting crystallization of bifunctional CuO–ZnO–Al_2O_3/SiO_2–Al_2O_3 catalysts for CO_2 hydrogenation. *Biomass Bioenergy* **2022**, *163*, 106525. [CrossRef]
308. Guo, Y.; Feng, L.; Liu, Y.; Zhao, Z. Cu-embedded porous Al_2O_3 bifunctional catalyst derived from metal–organic framework for syngas-to-dimethyl ether. *Chin. Chem. Lett.* **2022**, *33*, 2906–2910. [CrossRef]
309. Temvuttirojn, C.; Chuasomboon, N.; Numpilai, T.; Faungnawakij, K.; Chareonpanich, M.; Limtrakul, J.; Witoon, T. Development of SO_4^{2-}–ZrO_2 acid catalysts admixed with a CuO-ZnO-ZrO_2 catalyst for CO_2 hydrogenation to dimethyl ether. *Fuel* **2019**, *241*, 695–703. [CrossRef]
310. Mureddu, M.; Lai, S.; Atzori, L.; Rombi, E.; Ferrara, F.; Pettinau, A.; Cutrufello, M.G. Ex-LDH-based catalysts for CO_2 conversion to methanol and dimethyl ether. *Catalysts* **2021**, *11*, 615. [CrossRef]

311. Pechenkin, A.; Potemkin, D.; Badmaev, S.; Smirnova, E.; Cherednichenko, K.; Vinokurov, V.; Glotov, A. CO_2 hydrogenation to dimethyl ether over In_2O_3 catalysts supported on aluminosilicate halloysite nanotubes. *Green Process. Synth.* **2021**, *10*, 594–605. [CrossRef]
312. Zhang, L.; Bian, Z.; Sun, K.; Huang, W. Effects of Sn on the catalytic performance for one step syngas to DME in slurry reactor. *New J. Chem.* **2021**, *45*, 3783–3789. [CrossRef]
313. Ateka, A.; Sánchez-Contador, M.; Portillo, A.; Bilbao, J.; Aguayo, A.T. Kinetic modeling of $CO_2{}^+$ CO hydrogenation to DME over a CuO-ZnO-ZrO_2@ SAPO-11 core-shell catalyst. *Fuel Process. Technol.* **2020**, *206*, 106434. [CrossRef]
314. Ren, S.; Shoemaker, W.R.; Wang, X.; Shang, Z.; Klinghoffer, N.; Li, S.; Yu, M.; He, X.; White, T.A.; Liang, X. Highly active and selective Cu-ZnO based catalyst for methanol and dimethyl ether synthesis via CO_2 hydrogenation. *Fuel* **2019**, *239*, 1125–1133. [CrossRef]
315. Godini, H.R.; Kumar, S.R.; Tadikamalla, N.; Gallucci, F. Performance analysis of hybrid catalytic conversion of CO_2 to DiMethyl ether. *Int. J. Hydrogen Energy* **2022**, *47*, 11341–11358. [CrossRef]
316. Suwannapichat, Y.; Numpilai, T.; Chanlek, N.; Faungnawakij, K.; Chareonpanich, M.; Limtrakul, J.; Witoon, T. Direct synthesis of dimethyl ether from CO_2 hydrogenation over novel hybrid catalysts containing a $CuZnOZrO_2$ catalyst admixed with WOx/Al_2O_3 catalysts: Effects of pore size of Al_2O_3 support and W loading content. *Energy Convers. Manag.* **2018**, *159*, 20–29. [CrossRef]
317. Navarro-Jaén, S.; Virginie, M.; Thuriot-Roukos, J.; Wojcieszak, R.; Khodakov, A.Y. Structure–performance correlations in the hybrid oxide-supported copper–zinc SAPO-34 catalysts for direct synthesis of dimethyl ether from CO_2. *J. Mater. Sci.* **2022**, *57*, 3268–3279. [CrossRef]
318. Fang, X.; Jia, H.; Zhang, B.; Li, Y.; Wang, Y.; Song, Y.; Du, T.; Liu, L. A novel in situ grown Cu-ZnO-ZrO_2/HZSM-5 hybrid catalyst for CO_2 hydrogenation to liquid fuels of methanol and DME. *J. Environ. Chem. Eng.* **2021**, *9*, 105299. [CrossRef]
319. Feng, W.-H.; Yu, M.-M.; Wang, L.-J.; Miao, Y.-T.; Shakouri, M.; Ran, J.; Hu, Y.; Li, Z.; Huang, R.; Lu, Y.-L. Insights into bimetallic oxide synergy during carbon dioxide hydrogenation to methanol and dimethyl ether over GaZrO x oxide catalysts. *ACS Catal.* **2021**, *11*, 4704–4711. [CrossRef]
320. Ateka, A.; Ereña, J.; Pérez-Uriarte, P.; Aguayo, A.T.; Bilbao, J. Effect of the content of CO_2 and H_2 in the feed on the conversion of CO_2 in the direct synthesis of dimethyl ether over a $CuOZnOAl_2O_3$/SAPO-18 catalyst. *Int. J. Hydrogen Energy* **2017**, *42*, 27130–27138. [CrossRef]
321. Şeker, B.; Dizaji, A.K.; Balci, V.; Uzun, A. MCM-41-supported tungstophosphoric acid as an acid function for dimethyl ether synthesis from CO_2 hydrogenation. *Renew. Energy* **2021**, *171*, 47–57. [CrossRef]
322. Singh, R.; Tripathi, K.; Pant, K.K.; Parikh, J.K. Unravelling synergetic interaction over tandem Cu-ZnO-ZrO_2/hierarchical ZSM5 catalyst for CO_2 hydrogenation to methanol and DME. *Fuel* **2022**, *318*, 123641. [CrossRef]
323. Tan, K.B.; Tian, P.; Zhang, X.; Tian, J.; Zhan, G.; Huang, J.; Li, Q. Green synthesis of microspherical-confined nano-Pd/In_2O_3 integrated with H-ZSM-5 as bifunctional catalyst for CO_2 hydrogenation into dimethyl ether: A carbonized alginate templating strategy. *Sep. Purif. Technol.* **2022**, *297*, 121559. [CrossRef]
324. Liu, C.; Kang, J.; Huang, Z.-Q.; Song, Y.-H.; Xiao, Y.-S.; Song, J.; He, J.-X.; Chang, C.-R.; Ge, H.-Q.; Wang, Y. Gallium nitride catalyzed the direct hydrogenation of carbon dioxide to dimethyl ether as primary product. *Nat. Commun.* **2021**, *12*, 2305. [CrossRef] [PubMed]
325. Catizzone, E.; Freda, C.; Braccio, G.; Frusteri, F.; Bonura, G. Dimethyl ether as circular hydrogen carrier: Catalytic aspects of hydrogenation/dehydrogenation steps. *J. Energy Chem.* **2021**, *58*, 55–77. [CrossRef]
326. Ateka, A.; Rodriguez-Vega, P.; Ereña, J.; Aguayo, A.; Bilbao, J. A review on the valorization of CO_2. Focusing on the thermodynamics and catalyst design studies of the direct synthesis of dimethyl ether. *Fuel Process. Technol.* **2022**, *233*, 107310. [CrossRef]
327. Weber, D.; He, T.; Wong, M.; Moon, C.; Zhang, A.; Foley, N.; Ramer, N.J.; Zhang, C. Recent Advances in the Mitigation of the Catalyst Deactivation of CO_2 Hydrogenation to Light Olefins. *Catalysts* **2021**, *11*, 1447. [CrossRef]
328. Ma, Z.; Porosoff, M.D. Development of tandem catalysts for CO_2 hydrogenation to olefins. *ACS Catal.* **2019**, *9*, 2639–2656. [CrossRef]
329. Zhao, Z.; Jiang, J.; Wang, F. An economic analysis of twenty light olefin production pathways. *J. Energy Chem.* **2021**, *56*, 193–202. [CrossRef]
330. Gogate, M.R. Methanol-to-olefins process technology: Current status and future prospects. *Pet. Sci. Technol.* **2019**, *37*, 559–565. [CrossRef]
331. Gao, P.; Li, S.; Bu, X.; Dang, S.; Liu, Z.; Wang, H.; Zhong, L.; Qiu, M.; Yang, C.; Cai, J. Direct conversion of CO_2 into liquid fuels with high selectivity over a bifunctional catalyst. *Nat. Chem.* **2017**, *9*, 1019–1024. [CrossRef]
332. Sedighi, M.; Mohammadi, M. CO_2 hydrogenation to light olefins over Cu-CeO_2/SAPO-34 catalysts: Product distribution and optimization. *J. CO2 Util.* **2020**, *35*, 236–244. [CrossRef]
333. Tada, S.; Kinoshita, H.; Ochiai, N.; Chokkalingam, A.; Hu, P.; Yamauchi, N.; Kobayashi, Y.; Iyoki, K. Search for solid acid catalysts aiming at the development of bifunctional tandem catalysts for the one-pass synthesis of lower olefins via CO_2 hydrogenation. *Int. J. Hydrogen Energy* **2021**, *46*, 36721–36730. [CrossRef]
334. Dokania, A.; Ould-Chikh, S.; Ramirez, A.; Cerrillo, J.L.; Aguilar, A.; Russkikh, A.; Alkhalaf, A.; Hita, I.; Bavykina, A.; Shterk, G. Designing a Multifunctional Catalyst for the Direct Production of Gasoline-Range Isoparaffins from CO_2. *JACS Au* **2021**, *1*, 1961–1974. [CrossRef] [PubMed]

335. Dang, S.; Gao, P.; Liu, Z.; Chen, X.; Yang, C.; Wang, H.; Zhong, L.; Li, S.; Sun, Y. Role of zirconium in direct CO_2 hydrogenation to lower olefins on oxide/zeolite bifunctional catalysts. *J. Catal.* **2018**, *364*, 382–393. [CrossRef]
336. Liu, Z.; Ni, Y.; Hu, Z.; Fu, Y.; Fang, X.; Jiang, Q.; Chen, Z.; Zhu, W.; Liu, Z. Insights into effects of ZrO_2 crystal phase on syngas-to-olefin conversion over ZnO/ZrO_2 and SAPO-34 composite catalysts. *Chin. J. Catal.* **2022**, *43*, 877–884. [CrossRef]
337. Li, N.; Zhu, Y.; Jiao, F.; Pan, X.; Jiang, Q.; Cai, J.; Li, Y.; Tong, W.; Xu, C.; Qu, S. Steering the reaction pathway of syngas-to-light olefins with coordination unsaturated sites of ZnGaOx spinel. *Nat. Commun.* **2022**, *13*, 2742. [CrossRef]
338. Portillo, A.; Ateka, A.; Ereña, J.; Bilbao, J.; Aguayo, A. Role of Zr loading into In2O3 catalysts for the direct conversion of CO_2/CO mixtures into light olefins. *J. Environ. Manag.* **2022**, *316*, 115329. [CrossRef]
339. Portillo, A.; Ateka, A.; Ereña, J.; Aguayo, A.T.; Bilbao, J. Conditions for the joint conversion of CO_2 and syngas in the direct synthesis of light olefins using In_2O_3–ZrO_2/SAPO-34 catalyst. *Ind. Eng. Chem. Res.* **2021**, *61*, 10365–10376. [CrossRef]
340. Gao, P.; Dang, S.; Li, S.; Bu, X.; Liu, Z.; Qiu, M.; Yang, C.; Wang, H.; Zhong, L.; Han, Y. Direct production of lower olefins from CO_2 conversion via bifunctional catalysis. *ACS Catal.* **2018**, *8*, 571–578. [CrossRef]
341. Mou, J.; Fan, X.; Liu, F.; Wang, X.; Zhao, T.; Chen, P.; Li, Z.; Yang, C.; Cao, J. CO_2 hydrogenation to lower olefins over Mn_2O_3-ZnO/SAPO-34 tandem catalysts. *Chem. Eng. J.* **2021**, *421*, 129978. [CrossRef]
342. Numpilai, T.; Chanlek, N.; Poo-Arporn, Y.; Wannapaiboon, S.; Cheng, C.K.; Siri-Nguan, N.; Sornchamni, T.; Kongkachuichay, P.; Chareonpanich, M.; Rupprechter, G. Pore size effects on physicochemical properties of Fe-Co/K-Al_2O_3 catalysts and their catalytic activity in CO_2 hydrogenation to light olefins. *Appl. Surf. Sci.* **2019**, *483*, 581–592. [CrossRef]
343. Guo, L.; Cui, Y.; Li, H.; Fang, Y.; Prasert, R.; Wu, J.; Yang, G.; Yoneyama, Y.; Tsubaki, N. Selective formation of linear-alpha olefins (LAOs) by CO_2 hydrogenation over bimetallic Fe/Co-Y catalyst. *Catal. Commun.* **2019**, *130*, 105759. [CrossRef]
344. Numpilai, T.; Wattanakit, C.; Chareonpanich, M.; Limtrakul, J.; Witoon, T. Optimization of synthesis condition for CO_2 hydrogenation to light olefins over In_2O_3 admixed with SAPO-34. *Energy Convers. Manag.* **2019**, *180*, 511–523. [CrossRef]
345. Tian, P.; Zhan, G.; Tian, J.; Tan, K.B.; Guo, M.; Han, Y.; Fu, T.; Huang, J.; Li, Q. Direct CO_2 Hydrogenation to Light Olefins over ZnZrOx Mixed with Hierarchically Hollow SAPO-34 with Rice Husk as Green Silicon Source and Template. *Appl. Catal. B Environ.* **2022**, *315*, 121572. [CrossRef]
346. Li, Z.; Wang, J.; Qu, Y.; Liu, H.; Tang, C.; Miao, S.; Feng, Z.; An, H.; Li, C. Highly selective conversion of carbon dioxide to lower olefins. *ACS Catal.* **2017**, *7*, 8544–8548. [CrossRef]
347. Wang, S.; Wang, P.; Qin, Z.; Yan, W.; Dong, M.; Li, J.; Wang, J.; Fan, W. Enhancement of light olefin production in CO_2 hydrogenation over In_2O_3-based oxide and SAPO-34 composite. *J. Catal.* **2020**, *391*, 459–470. [CrossRef]
348. Chen, J.; Wang, X.; Wu, D.; Zhang, J.; Ma, Q.; Gao, X.; Lai, X.; Xia, H.; Fan, S.; Zhao, T.-S. Hydrogenation of CO_2 to light olefins on CuZnZr@(Zn-) SAPO-34 catalysts: Strategy for product distribution. *Fuel* **2019**, *239*, 44–52. [CrossRef]
349. Ghasemi, M.; Mohammadi, M.; Sedighi, M. Sustainable production of light olefins from greenhouse gas CO_2 over SAPO-34 supported modified cerium oxide. *Microporous Mesoporous Mater.* **2020**, *297*, 110029. [CrossRef]
350. Li, J.; Yu, T.; Miao, D.; Pan, X.; Bao, X. Carbon dioxide hydrogenation to light olefins over ZnO-Y_2O_3 and SAPO-34 bifunctional catalysts. *Catal. Commun.* **2019**, *129*, 105711. [CrossRef]
351. Ramirez, A.; Chowdhury, A.D.; Caglayan, M.; Rodriguez-Gomez, A.; Wehbe, N.; Abou-Hamad, E.; Gevers, L.; Ould-Chikh, S.; Gascon, J. Coated sulfated zirconia/SAPO-34 for the direct conversion of CO_2 to light olefins. *Catal. Sci. Technol.* **2020**, *10*, 1507–1517. [CrossRef]
352. Li, W.; Zhang, A.; Jiang, X.; Janik, M.J.; Qiu, J.; Liu, Z.; Guo, X.; Song, C. The anti-sintering catalysts: Fe–Co–Zr polymetallic fibers for CO_2 hydrogenation to C2=–C4=–rich hydrocarbons. *J. CO2 Util.* **2018**, *23*, 219–225. [CrossRef]
353. Tong, M.; Chizema, L.G.; Chang, X.; Hondo, E.; Dai, L.; Zeng, Y.; Zeng, C.; Ahmad, H.; Yang, R.; Lu, P. Tandem catalysis over tailored ZnO-ZrO_2/MnSAPO-34 composite catalyst for enhanced light olefins selectivity in CO_2 hydrogenation. *Microporous Mesoporous Mater.* **2021**, *320*, 111105. [CrossRef]
354. Zhang, P.; Ma, L.; Meng, F.; Wang, L.; Zhang, R.; Yang, G.; Li, Z. Boosting CO_2 hydrogenation performance for light olefin synthesis over GaZrOx combined with SAPO-34. *Appl. Catal. B Environ.* **2022**, *305*, 121042. [CrossRef]
355. Tian, H.; Yao, J.; Zha, F.; Yao, L.; Chang, Y. Catalytic activity of SAPO-34 molecular sieves prepared by using palygorskite in the synthesis of light olefins via CO_2 hydrogenation. *Appl. Clay Sci.* **2020**, *184*, 105392. [CrossRef]
356. Numpilai, T.; Kahadit, S.; Witoon, T.; Ayodele, B.V.; Cheng, C.K.; Siri-Nguan, N.; Sornchamni, T.; Wattanakit, C.; Chareonpanich, M.; Limtrakul, J. CO_2 hydrogenation to light olefins over In_2O_3/SAPO-34 and Fe-Co/K-Al_2O_3 composite catalyst. *Top. Catal.* **2021**, *64*, 316–327. [CrossRef]
357. Wang, P.; Zha, F.; Yao, L.; Chang, Y. Synthesis of light olefins from CO_2 hydrogenation over (CuO-ZnO)-kaolin/SAPO-34 molecular sieves. *Appl. Clay Sci.* **2018**, *163*, 249–256. [CrossRef]
358. Oni, B.A.; Sanni, S.E.; Ibegbu, A.J. Production of light olefins by catalytic hydrogenation of CO_2 over Y_2O_3/Fe-Co modified with SAPO-34. *Appl. Catal. A Gen.* **2022**, *643*, 118784. [CrossRef]
359. Liu, Q.; Ding, J.; Wang, R.; Zhong, Q. FeZnK/SAPO-34 Catalyst for Efficient Conversion of CO_2 to Light Olefins. *Catal. Lett.* **2022**, 1–8. [CrossRef]
360. Liu, Y.; Chen, B.; Liu, R.; Liu, W.; Gao, X.; Tan, Y.; Zhang, Z.; Tu, W. CO_2 hydrogenation to olefins on supported iron catalysts: Effects of support properties on carbon-containing species and product distribution. *Fuel* **2022**, *324*, 124649. [CrossRef]
361. Rimaz, S.; Kosari, M.; Zarinejad, M.; Ramakrishna, S. A comprehensive review on sustainability-motivated applications of SAPO-34 molecular sieve. *J. Mater. Sci.* **2022**, *57*, 1–39.

362. Dugkhuntod, P.; Wattanakit, C. A comprehensive review of the applications of hierarchical zeolite nanosheets and nanoparticle assemblies in light olefin production. *Catalysts* **2020**, *10*, 245. [CrossRef]
363. Usman, M. Recent Progress of SAPO-34 Zeolite Membranes for CO_2 Separation: A Review. *Membranes* **2022**, *12*, 507. [CrossRef] [PubMed]
364. Yuan, F.; Zhang, G.; Zhu, J.; Ding, F.; Zhang, A.; Song, C.; Guo, X. Boosting light olefin selectivity in CO_2 hydrogenation by adding Co to Fe catalysts within close proximity. *Catal. Today* **2021**, *371*, 142–149. [CrossRef]
365. Goud, D.; Gupta, R.; Maligal-Ganesh, R.; Peter, S.C. Review of catalyst design and mechanistic studies for the production of olefins from anthropogenic CO_2. *ACS Catal.* **2020**, *10*, 14258–14282. [CrossRef]
366. Tian, H.; He, H.; Jiao, J.; Zha, F.; Guo, X.; Tang, X.; Chang, Y. Tandem catalysts composed of different morphology HZSM-5 and metal oxides for CO_2 hydrogenation to aromatics. *Fuel* **2022**, *314*, 123119. [CrossRef]
367. Li, W.; Wang, H.; Jiang, X.; Zhu, J.; Liu, Z.; Guo, X.; Song, C. A short review of recent advances in CO_2 hydrogenation to hydrocarbons over heterogeneous catalysts. *RSC Adv.* **2018**, *8*, 7651–7669. [CrossRef] [PubMed]
368. Zhou, W.; Cheng, K.; Kang, J.; Zhou, C.; Subramanian, V.; Zhang, Q.; Wang, Y. New horizon in C1 chemistry: Breaking the selectivity limitation in transformation of syngas and hydrogenation of CO_2 into hydrocarbon chemicals and fuels. *Chem. Soc. Rev.* **2019**, *48*, 3193–3228. [CrossRef]
369. Cheng, K.; Kang, J.; Zhang, Q.; Wang, Y. Reaction coupling as a promising methodology for selective conversion of syngas into hydrocarbons beyond Fischer-Tropsch synthesis. *Sci. China Chem.* **2017**, *60*, 1382–1385. [CrossRef]
370. Winter, L.R.; Gomez, E.; Yan, B.; Yao, S.; Chen, J.G. Tuning Ni-catalyzed CO_2 hydrogenation selectivity via Ni-ceria support interactions and Ni-Fe bimetallic formation. *Appl. Catal. B Environ.* **2018**, *224*, 442–450. [CrossRef]
371. Azhari, N.J.; Nurdini, N.; Mardiana, S.; Ilmi, T.; Fajar, A.T.; Makertihartha, I.; Kadja, G.T. Zeolite-based catalyst for direct conversion of CO_2 to C2+ hydrocarbon: A review. *J. CO2 Util.* **2022**, *59*, 101969. [CrossRef]
372. Wang, D.; Xie, Z.; Porosoff, M.D.; Chen, J.G. Recent advances in carbon dioxide hydrogenation to produce olefins and aromatics. *Chem* **2021**, *7*, 2277–2311. [CrossRef]
373. Hwang, S.-M.; Zhang, C.; Han, S.J.; Park, H.-G.; Kim, Y.T.; Yang, S.; Jun, K.-W.; Kim, S.K. Mesoporous carbon as an effective support for Fe catalyst for CO_2 hydrogenation to liquid hydrocarbons. *J. CO2 Util.* **2020**, *37*, 65–73. [CrossRef]
374. Kim, H.D.; Song, H.-T.; Fazeli, A.; Eslami, A.A.; Noh, Y.S.; Saeidabad, N.G.; Lee, K.-Y.; Moon, D.J. CO/CO_2 hydrogenation for the production of lighter hydrocarbons over SAPO-34 modified hybrid FTS catalysts. *Catal. Today* **2020**, *388–389*, 410–416. [CrossRef]
375. Liu, B.; Geng, S.; Zheng, J.; Jia, X.; Jiang, F.; Liu, X. Unravelling the New Roles of Na and Mn Promoter in CO_2 Hydrogenation over Fe_3O_4-Based Catalysts for Enhanced Selectivity to Light α-Olefins. *ChemCatChem* **2018**, *10*, 4718–4732. [CrossRef]
376. Khangale, P.R.; Meijboom, R.; Jalama, K. CO_2 hydrogenation to liquid hydrocarbons via modified Fischer–Tropsch over alumina-supported cobalt catalysts: Effect of operating temperature, pressure and potassium loading. *J. CO2 Util.* **2020**, *41*, 101268. [CrossRef]
377. Liu, J.; Zhang, G.; Jiang, X.; Wang, J.; Song, C.; Guo, X. Insight into the role of Fe_5C_2 in CO_2 catalytic hydrogenation to hydrocarbons. *Catal. Today* **2021**, *371*, 162–170. [CrossRef]
378. Hwang, S.-M.; Han, S.J.; Park, H.-G.; Lee, H.; An, K.; Jun, K.-W.; Kim, S.K. Atomically Alloyed Fe–Co Catalyst derived from a N-coordinated Co single-atom structure for CO_2 hydrogenation. *ACS Catal.* **2021**, *11*, 2267–2278. [CrossRef]
379. Yao, B.; Xiao, T.; Makgae, O.A.; Jie, X.; Gonzalez-Cortes, S.; Guan, S.; Kirkland, A.I.; Dilworth, J.R.; Al-Megren, H.A.; Alshihri, S.M. Transforming carbon dioxide into jet fuel using an organic combustion-synthesized Fe-Mn-K catalyst. *Nat. Commun.* **2020**, *11*, 1–12. [CrossRef]
380. Li, L.; Yu, F.; Li, X.; Lin, T.; An, Y.; Zhong, L.; Sun, Y. Fischer-Tropsch to olefins over $C_{O2}C$-based catalysts: Effect of thermal pretreatment of SiO_2 support. *Appl. Catal. A Gen.* **2021**, *623*, 118283. [CrossRef]
381. Jiang, F.; Liu, B.; Geng, S.; Xu, Y.; Liu, X. Hydrogenation of CO_2 into hydrocarbons: Enhanced catalytic activity over Fe-based Fischer–Tropsch catalysts. *Catal. Sci. Technol.* **2018**, *8*, 4097–4107. [CrossRef]
382. Gong, K.; Lin, T.; An, Y.; Wang, X.; Yu, F.; Wu, B.; Li, X.; Li, S.; Lu, Y.; Zhong, L. Fischer-Tropsch to olefins over CoMn-based catalysts: Effect of preparation methods. *Appl. Catal. A Gen.* **2020**, *592*, 117414. [CrossRef]
383. Kwok, K.M.; Chen, L.; Zeng, H.C. Design of hollow spherical Co@ hsZSM5@ metal dual-layer nanocatalysts for tandem CO_2 hydrogenation to increase C^{2+} hydrocarbon selectivity. *J. Mater. Chem. A* **2020**, *8*, 12757–12766. [CrossRef]
384. Liu, R.; Ma, Z.; Sears, J.D.; Juneau, M.; Neidig, M.L.; Porosoff, M.D. Identifying correlations in Fischer-Tropsch synthesis and CO_2 hydrogenation over Fe-based ZSM-5 catalysts. *J. CO2 Util.* **2020**, *41*, 101290. [CrossRef]
385. Guo, L.; Sun, S.; Li, J.; Gao, W.; Zhao, H.; Zhang, B.; He, Y.; Zhang, P.; Yang, G.; Tsubaki, N. Boosting liquid hydrocarbons selectivity from CO_2 hydrogenation by facilely tailoring surface acid properties of zeolite via a modified Fischer-Tropsch synthesis. *Fuel* **2021**, *306*, 121684. [CrossRef]
386. Choi, Y.H.; Jang, Y.J.; Park, H.; Kim, W.Y.; Lee, Y.H.; Choi, S.H.; Lee, J.S. Carbon dioxide Fischer-Tropsch synthesis: A new path to carbon-neutral fuels. *Appl. Catal. B Environ.* **2017**, *202*, 605–610. [CrossRef]
387. Liu, J.; Zhang, A.; Jiang, X.; Liu, M.; Sun, Y.; Song, C.; Guo, X. Selective CO_2 hydrogenation to hydrocarbons on Cu-promoted Fe-based catalysts: Dependence on Cu–Fe interaction. *ACS Sustain. Chem. Eng.* **2018**, *6*, 10182–10190. [CrossRef]
388. Chen, Q.; Liu, G.; Ding, S.; Sheikh, M.C.; Long, D.; Yoneyama, Y.; Tsubaki, N. Design of ultra-active iron-based Fischer-Tropsch synthesis catalysts over spherical mesoporous carbon with developed porosity. *Chem. Eng. J.* **2018**, *334*, 714–724. [CrossRef]

389. Qadir, M.I.; Bernardi, F.; Scholten, J.D.; Baptista, D.L.; Dupont, J. Synergistic CO_2 hydrogenation over bimetallic Ru/Ni nanoparticles in ionic liquids. *Appl. Catal. B Environ.* **2019**, *252*, 10–17. [CrossRef]
390. Wang, P.; Chen, W.; Chiang, F.-K.; Dugulan, A.I.; Song, Y.; Pestman, R.; Zhang, K.; Yao, J.; Feng, B.; Miao, P. Synthesis of stable and low-CO_2 selective ε-iron carbide Fischer-Tropsch catalysts. *Sci. Adv.* **2018**, *4*, eaau2947. [CrossRef]
391. Wang, X.; Wu, D.; Zhang, J.; Gao, X.; Ma, Q.; Fan, S.; Zhao, T.-S. Highly selective conversion of CO_2 to light olefins via Fischer-Tropsch synthesis over stable layered K–Fe–Ti catalysts. *Appl. Catal. A Gen.* **2019**, *573*, 32–40. [CrossRef]
392. Song, F.; Yong, X.; Wu, X.; Zhang, W.; Ma, Q.; Zhao, T.; Tan, M.; Guo, Z.; Zhao, H.; Yang, G. FeMn@ HZSM-5 capsule catalyst for light olefins direct synthesis via Fischer-Tropsch synthesis: Studies on depressing the CO_2 formation. *Appl. Catal. B Environ.* **2022**, *300*, 120713. [CrossRef]
393. Cui, M.; Qian, Q.; Zhang, J.; Wang, Y.; Bediako, B.B.A.; Liu, H.; Han, B. Liquid fuel synthesis via CO_2 hydrogenation by coupling homogeneous and heterogeneous catalysis. *Chem* **2021**, *7*, 726–737. [CrossRef]
394. Straß-Eifert, A.; Sheppard, T.L.; Becker, H.; Friedland, J.; Zimina, A.; Grunwaldt, J.D.; Güttel, R. Cobalt-based Nanoreactors in Combined Fischer-Tropsch Synthesis and Hydroprocessing: Effects on Methane and CO_2 Selectivity. *ChemCatChem* **2021**, *13*, 5216–5227. [CrossRef]
395. Sirikulbodee, P.; Ratana, T.; Sornchamni, T.; Phongaksorn, M.; Tungkamani, S. Catalytic performance of Iron-based catalyst in Fischer–Tropsch synthesis using CO_2 containing syngas. *Energy Procedia* **2017**, *138*, 998–1003. [CrossRef]
396. Zhang, Z.; Liu, Y.; Jia, L.; Sun, C.; Chen, B.; Liu, R.; Tan, Y.; Tu, W. Effects of the reducing gas atmosphere on performance of FeCeNa catalyst for the hydrogenation of CO_2 to olefins. *Chem. Eng. J.* **2022**, *428*, 131388. [CrossRef]
397. Zhang, P.; Han, F.; Yan, J.; Qiao, X.; Guan, Q.; Li, W. N-doped ordered mesoporous carbon (N-OMC) confined Fe_3O_4-FeCx heterojunction for efficient conversion of CO_2 to light olefins. *Appl. Catal. B Environ.* **2021**, *299*, 120639. [CrossRef]
398. Guilera, J.; Díaz-López, J.A.; Berenguer, A.; Biset-Peiró, M.; Andreu, T. Fischer-Tropsch synthesis: Towards a highly-selective catalyst by lanthanide promotion under relevant CO_2 syngas mixtures. *Appl. Catal. A Gen.* **2022**, *629*, 118423. [CrossRef]
399. Jo, H.; Khan, M.K.; Irshad, M.; Arshad, M.W.; Kim, S.K.; Kim, J. Unraveling the role of cobalt in the direct conversion of CO_2 to high-yield liquid fuels and lube base oil. *Appl. Catal. B Environ.* **2022**, *305*, 121041. [CrossRef]
400. Ahmad, E.; Upadhyayula, S.; Pant, K.K. Biomass-derived CO_2 rich syngas conversion to higher hydrocarbon via Fischer-Tropsch process over Fe–Co bimetallic catalyst. *Int. J. Hydrogen Energy* **2019**, *44*, 27741–27748.
401. Bashiri, N.; Omidkhah, M.R.; Godini, H.R. Direct conversion of CO_2 to light olefins over FeCo/XK-ϒAl_2O_3 (X = La, Mn, Zn) catalyst via hydrogenation reaction. *Res. Chem. Intermed.* **2021**, *47*, 5267–5289. [CrossRef]
402. Gong, K.; Wei, Y.; Dai, Y.; Lin, T.; Yu, F.; An, Y.; Wang, X.; Sun, F.; Jiang, Z.; Zhong, L. Carbon-encapsulated metallic Co nanoparticles for Fischer-Tropsch to olefins with low CO_2 selectivity. *Appl. Catal. B Environ.* **2022**, *316*, 121700. [CrossRef]
403. He, Z.; Cui, M.; Qian, Q.; Zhang, J.; Liu, H.; Han, B. Synthesis of liquid fuel via direct hydrogenation of CO_2. *Proc. Natl. Acad. Sci. USA* **2019**, *116*, 12654–12659. [CrossRef] [PubMed]
404. Xie, T.; Wang, J.; Ding, F.; Zhang, A.; Li, W.; Guo, X.; Song, C. CO_2 hydrogenation to hydrocarbons over alumina-supported iron catalyst: Effect of support pore size. *J. CO2 Util.* **2017**, *19*, 202–208. [CrossRef]
405. Numpilai, T.; Witoon, T.; Chanlek, N.; Limphirat, W.; Bonura, G.; Chareonpanich, M.; Limtrakul, J. Structure–activity relationships of Fe-Co/K-Al_2O_3 catalysts calcined at different temperatures for CO_2 hydrogenation to light olefins. *Appl. Catal. A Gen.* **2017**, *547*, 219–229. [CrossRef]
406. Bradley, M.J.; Ananth, R.; Willauer, H.D.; Baldwin, J.W.; Hardy, D.R.; Williams, F.W. The effect of copper addition on the activity and stability of iron-based CO_2 hydrogenation catalysts. *Molecules* **2017**, *22*, 1579. [CrossRef] [PubMed]
407. Zhang, Z.; Yin, H.; Yu, G.; He, S.; Kang, J.; Liu, Z.; Cheng, K.; Zhang, Q.; Wang, Y. Selective hydrogenation of CO_2 and CO into olefins over Sodium-and Zinc-Promoted iron carbide catalysts. *J. Catal.* **2021**, *395*, 350–361. [CrossRef]
408. Feng, K.; Tian, J.; Guo, M.; Wang, Y.; Wang, S.; Wu, Z.; Zhang, J.; He, L.; Yan, B. Experimentally unveiling the origin of tunable selectivity for CO_2 hydrogenation over Ni-based catalysts. *Appl. Catal. B Environ.* **2021**, *292*, 120191. [CrossRef]
409. Sibi, M.G.; Khan, M.K.; Verma, D.; Yoon, W.; Kim, J. High-yield synthesis of BTEX over Na–FeAlOx/Zn–HZSM-5@ SiO_2 by direct CO_2 conversion and identification of surface intermediates. *Appl. Catal. B Environ.* **2022**, *301*, 120813. [CrossRef]
410. Zhang, Z.; Huang, G.; Tang, X.; Yin, H.; Kang, J.; Zhang, Q.; Wang, Y. Zn and Na promoted Fe catalysts for sustainable production of high-valued olefins by CO_2 hydrogenation. *Fuel* **2022**, *309*, 122105. [CrossRef]
411. Chaipraditgul, N.; Numpilai, T.; Cheng, C.K.; Siri-Nguan, N.; Sornchamni, T.; Wattanakit, C.; Limtrakul, J.; Witoon, T. Tuning interaction of surface-adsorbed species over Fe/K-Al_2O_3 modified with transition metals (Cu, Mn, V, Zn or Co) on light olefins production from CO_2 hydrogenation. *Fuel* **2021**, *283*, 119248. [CrossRef]
412. Garona, H.A.; Cavalcanti, F.M.; de Abreu, T.F.; Schmal, M.; Alves, R.M. Evaluation of Fischer-Tropsch synthesis to light olefins over Co-and Fe-based catalysts using artificial neural network. *J. Clean. Prod.* **2021**, *321*, 129003. [CrossRef]
413. Hodala, J.L.; Moon, D.J.; Reddy, K.R.; Reddy, C.V.; Kumar, T.N.; Ahamed, M.I.; Raghu, A.V. Catalyst design for maximizing C5+ yields during Fischer-Tropsch synthesis. *Int. J. Hydrogen Energy* **2021**, *46*, 3289–3301. [CrossRef]
414. Shiba, N.C.; Yao, Y.; Liu, X.; Hildebrandt, D. Recent developments in catalyst pretreatment technologies for cobalt based Fisher–Tropsch synthesis. *Rev. Chem. Eng.* **2021**, *38*, 503–538. [CrossRef]
415. Lu, F.; Chen, X.; Lei, Z.; Wen, L.; Zhang, Y. Revealing the activity of different iron carbides for Fischer-Tropsch synthesis. *Appl. Catal. B Environ.* **2021**, *281*, 119521. [CrossRef]

416. Gong, W.; Ye, R.-P.; Ding, J.; Wang, T.; Shi, X.; Russell, C.K.; Tang, J.; Eddings, E.G.; Zhang, Y.; Fan, M. Effect of copper on highly effective Fe-Mn based catalysts during production of light olefins via Fischer-Tropsch process with low CO_2 emission. *Appl. Catal. B Environ.* **2020**, *278*, 119302. [CrossRef]
417. Lin, T.; Liu, P.; Gong, K.; An, Y.; Yu, F.; Wang, X.; Zhong, L.; Sun, Y. Designing silica-coated CoMn-based catalyst for Fischer-Tropsch synthesis to olefins with low CO_2 emission. *Appl. Catal. B Environ.* **2021**, *299*, 120683. [CrossRef]
418. Kirsch, H.; Lochmahr, N.; Staudt, C.; Pfeifer, P.; Dittmeyer, R. Production of CO_2-neutral liquid fuels by integrating Fischer-Tropsch synthesis and hydrocracking in a single micro-structured reactor: Performance evaluation of different configurations by factorial design experiments. *Chem. Eng. J.* **2020**, *393*, 124553. [CrossRef]
419. Li, M.; Noreen, A.; Fu, Y.; Amoo, C.C.; Jiang, Y.; Sun, X.; Lu, P.; Yang, R.; Xing, C.; Wang, S. Direct conversion of syngas to gasoline ranged olefins over Na impellent Fe@ NaZSM-5 catalyst. *Fuel* **2022**, *308*, 121938. [CrossRef]
420. Yang, J.; Rodriguez, C.L.; Qi, Y.; Ma, H.; Holmen, A.; Chen, D. The effect of co-feeding ethene on Fischer-Tropsch synthesis to olefins over Co-based catalysts. *Appl. Catal. A Gen.* **2020**, *598*, 117564. [CrossRef]
421. Hou, Y.; Li, J.; Qing, M.; Liu, C.-L.; Dong, W.-S. Direct synthesis of lower olefins from syngas via Fischer–Tropsch synthesis catalyzed by a dual-bed catalyst. *Mol. Catal.* **2020**, *485*, 110824. [CrossRef]
422. Shiba, N.C.; Yao, Y.; Forbes, R.P.; Okoye-Chine, C.G.; Liu, X.; Hildebrandt, D. Role of CoO-Co nanoparticles supported on SiO_2 in Fischer-Tropsch synthesis: Evidence for enhanced CO dissociation and olefin hydrogenation. *Fuel Process. Technol.* **2021**, *216*, 106781. [CrossRef]
423. Ghosh, I.K.; Iqbal, Z.; van Heerden, T.; van Steen, E.; Bordoloi, A. Insights into the unusual role of chlorine in product selectivity for direct hydrogenation of CO/CO_2 to short-chain olefins. *Chem. Eng. J.* **2021**, *413*, 127424. [CrossRef]
424. Yang, S.; Lee, S.; Kang, S.C.; Han, S.J.; Jun, K.-W.; Lee, K.-Y.; Kim, Y.T. Linear α-olefin production with Na-promoted Fe–Zn catalysts via Fischer–Tropsch synthesis. *RSC Adv.* **2019**, *9*, 14176–14187. [CrossRef]
425. Lu, Y.; Yan, Q.; Han, J.; Cao, B.; Street, J.; Yu, F. Fischer–Tropsch synthesis of olefin-rich liquid hydrocarbons from biomass-derived syngas over carbon-encapsulated iron carbide/iron nanoparticles catalyst. *Fuel* **2017**, *193*, 369–384. [CrossRef]
426. Liu, Z.; Jia, G.; Zhao, C.; Xing, Y. Efficient Fischer-Tropsch to light olefins over iron-based catalyst with low methane selectivity and high olefin/paraffin ratio. *Fuel* **2021**, *288*, 119572. [CrossRef]
427. Lu, P.; Riswan, M.; Chang, X.; Zhu, K.; Hondo, E.; Nyako, A.; Xing, C.; Du, C.; Chen, S. Hydrogenation of CO_2 to light olefins on ZZ/MnSAPO-34@ Si-2: Effect of silicalite-2 seeds on the acidity and catalytic activity. *Fuel* **2022**, *330*, 125470. [CrossRef]
428. Gao, R.; Zhang, L.; Wang, L.; Zhang, C.; Jun, K.-W.; Kim, S.K.; Park, H.-G.; Gao, Y.; Zhu, Y.; Wan, H. Efficient production of renewable hydrocarbon fuels using waste CO_2 and green H2 by integrating Fe-based Fischer-Tropsch synthesis and olefin oligomerization. *Energy* **2022**, *248*, 123616. [CrossRef]
429. Zhang, X.; Zhang, G.; Song, C.; Guo, X. Catalytic conversion of carbon dioxide to methanol: Current status and future perspective. *Front. Energy Res.* **2021**, *8*, 621119. [CrossRef]